Studies on the regulation of gene expression and immune activation by stimuli responsive artificial nucleic acid

by

ATSUO SHIGENO

Submitted to
Japan Advanced Institute of Science and Technology
In partial fulfillment of the requirements
For the degree of
Doctor of Philosophy

Supervisor: Professor Dr. Kenzo Fujimoto

School of Materials Science

Japan Advanced Institute of Science and Technology

March 2014

Contents

	Pages
General Introduction	1
Introduction	2
Chemical synthesis of oligonucleotide	2
Nucleic acid-based drugs	4
Ribozyme	6
siRNA	7
Aptamer	9
Antisense oligonucleotides	11
Artificial oligonucleotides	12
CpG oligonucleotides	18
Objective of this study	19
References	22
Chapter 1	
Quick regulation of mRNA functions by a few seconds of photoirradiation	31
1.1. Introduction	32
1.2. Materials and Method	34
1.3. Results and Discussion	40
1.4. Conclusion	54
1.5. References	55

Chapter 2

Photochemical regulation of RNA functions in cell by cyanovinyl-carbazole mediated photocrosslinking 59

2.1. Introduction 60

2.2. Materials and Method 62

2.3. Results and Discussion 65

2.4. Conclusion 77

2.5. References 78

Chapter 3

Synthesis of disulfide crosslinking tethered CpG oligonucleotide for immune activation by radiation 80

3.1. Introduction 81

3.2. Materials and Method 85

3.3. Results and Discussion 90

3.4. Conclusion 96

3.5. References 97

General Conclusion 99

Achievements 102

Acknowledgement 106

General Introduction

Introduction

The advances in molecular biology and biotechnology in the recent years have greatly enhanced the understanding of disease pathogenesis and various molecular-targeted drugs have been developed. Many of the currently approved molecular targeted drugs are low-molecular compounds or antibody drugs. In particular, 19 antibody drugs have been approved for the treatment of diseases such as cancer, autoimmune diseases and transplant rejections and there are many more in various stages of clinical trials[1]. However, one problem with antibody drugs is that there are many targets that cannot create an antibody. Therefore, the development of an improved molecular-targeted drug is urgently required. In recent years, tailor-made therapy that provides the optimum treatment for each individual has been attracting attention. Nucleic acids are becoming increasingly important as tailor-made therapeutic molecules mainly for the ease with which specificity for a vast range of targets of these drugs is achieved. Therefore nucleic acid-based drugs are a promising successor to antibody drug.

Chemical synthesis of oligonucleotide

With the development of synthetic oligonucleotides technologies oligonucleotides can now be synthesized easily in bulk using DNA and RNA synthesizers. The presently widely used chemical biology, which was formulated by Robert Letsinger and further developed by Marvin Caruthers, is known as the phosphoramidite method[2-5]. The technique is extremely useful in the synthesis of nucleic acid-based drugs. This reaction sequence adds a single nucleotide to a growing oligonucleotide chain as follows (Scheme 1).

Step 1: Detritylation

The dimethoxytrityl (DMTr) protecting group at the 5’ end of the growing oligonucleotide chain (which is anchored via a linking group at the 5’ end to a solid support) is removed with an acid solution, such as 2% trichloroacetic acid (TCA) in dichloromethane.

Step 2: Coupling

The newly liberated 5’ end of the oligonucleotide is coupled to the 3’-phosphoramidaite derivative of the next deoxynucleoside to be added to the chain. Nucleoside phosphoramidite in acetonitrile is activated by a 0.2–0.7 M solution of an acidic azole catalyst (e.g. 1*H*-tetrazole).

Step 3: Capping

Any unreacted 5’ end is capped by acetylation so as to block its extension in subsequent coupling reactions. This prevents the extension of erroneous oligonucleotides.

Step 4: Oxidation

In the coupling step the next desired base is added to the previous base, which results in an unstable phosphite linkage. To stabilize this linkage a solution of dilute iodine in water, pyridine, and tetrahydrofuran is added to the reaction column. The phosphite trimester group is oxidized to form a much more stable phosphotriester, thereby yielding a chain that has been lengthened by one nucleotide. This reaction sequence, in commercially available automated synthesizers, can be repeated up to ~ 150 times with a cycle time of 20 min or less. Once an oligonucleotide of the desired sequence has been synthesized, it is released from its support and its various blocking groups, including those on the bases, are removed. The product can then be purified by high performance liquid chromatography (HPLC) or gel electrophoresis.

Scheme 1. The reaction cycle in the phosphite-triester method of oligonucleotide synthesis.

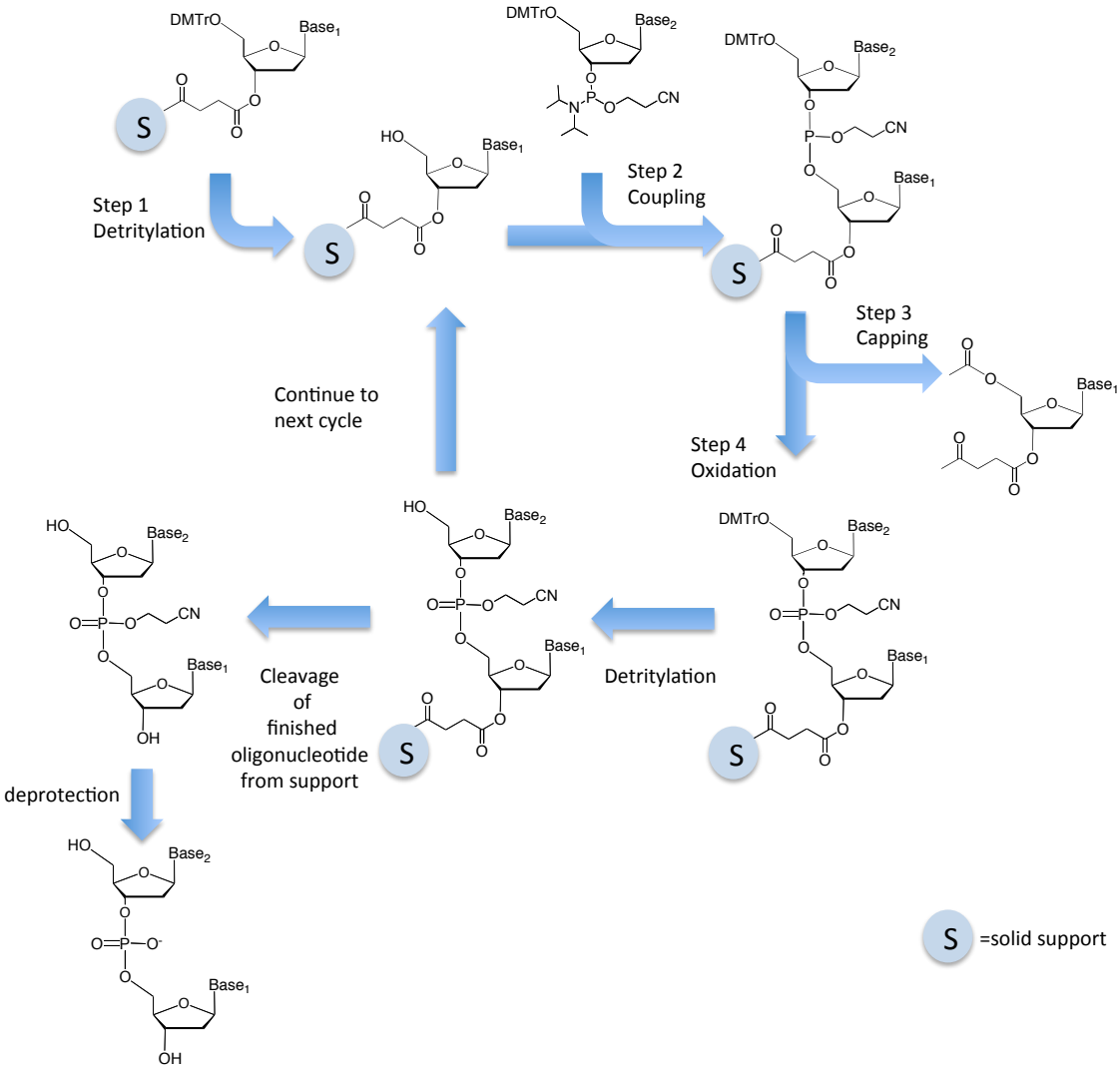

Nucleic acid-based drugs

With the successful sequencing of the human genome by the Human Genome Project[6,7] , a host of candidate genes have emerged with possible roles in the causation, prevention, and/or treatment of human diseases. It is estimated that over 10,000 human diseases have genetic abnormalities as the underlying cause[8]. Furthermore, recent mutations in RNA seem to be responsible for several diseases[9]. For these reasons, it is important to study nucleic acid drugs. Several agents mediate the suppression of mRNA translation. Ribozymes are one of the nucleic acid drugs and are catalytically active oligonucleotides. These enzymes downregulate gene expression by not only binding, but also cleaving, the target RNA[10]. The possibility of designing ribozymes to cleave a specific target RNA has rendered them useful tools in basic studies, however therapeutic applications are only now being found, most likely due to the efficacy results[11]. Small interfering RNAs (siRNAs) are short double-stranded RNA molecules that induce sequence specific gene silencing. siRNA is highly specific and efficient, requiring much smaller doses to achieve effective silencing. Currently there is no approved siRNA-based drug, although there are many compounds in development. On the other hand, aptamers and antisense oligonucleotides have reached the stage of clinical trials and Fomivirsen has been approved by the FDA for use in humans for the treatment of Cytomegalovirus (CMV) retinitis[12]. As some nucleic acid-based drugs have already been put to practical use, many researchers in academia and pharmaceutical companies are studying gene therapy. In this doctoral thesis, the author describes the study of stimuli responsive nucleic acid-based drugs.

Ribozyme

Ribozymes are catalytic RNA molecules capable of cleaving themselves or other RNA molecules[13]. Ribozymes were discovered in 1981 by Cech *et al.* [14] Shortly thereafter, Altman and coworkers discovered the active role of the RNA component of RNase P in the process of tRNA maturation [15]. This was the first characterization of a true RNA enzyme that catalyzes the reaction of a free substrate. The most commonly studied types of ribozymes, hammerhead and hairpin (Fig. 1), are small (<100 nt in the catalytic core) and feature catalytic activities that require the involvement of Mg^{2+} or other divalent ions as cofactors[16]. Using base-pairing and tertiary interactions to help align the cleavage site within the catalytic core, these ribozymes cleave only at a specific location[17-19]. Once the target RNA is cleaved, the ribozymes dissociate and recycle themselves. This makes them very effective gene silencing agents. The therapeutic effectiveness of ribozymes was first shown in experiments in which the mRNA of the oncogenes Ras and Bcr–Abl was cleaved in test tubes and in transfected cells [20,21]. However, ribozyme have low *in vivo* efficacy and improved cellular localization stratified is needed to produce.

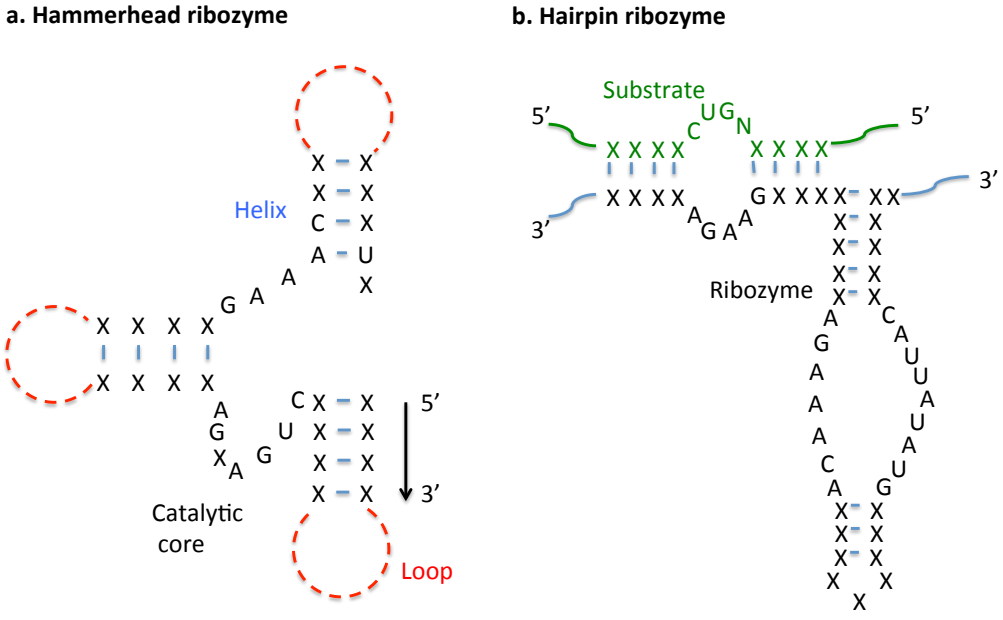

Figure 1. The structures of: a. the hammerhead ribozyme, b. the hairpin ribozyme. X represents any nucleotide.

siRNA

Interference of gene expression by exogenous double-stranded RNA was first discovered in 1998. by Fire et al., and the mechanism of action is called RNA interference (RNAi)[22]. In 1999, silencing in plants was shown to be accompanied by the appearance of ~20–25 nt RNAs that match the sequence of the silencing trigger [23]. Very shortly thereafter, the direct conversion of dsRNAs into~21–23 nt siRNAs was reported. RNA interference is initiated by long double-stranded RNA molecules, which are processed into 21–23 nucleotides long RNAs by the Dicer enzyme (Fig. 2). This RNase III protein is thought to act as a dimer that cleaves both strands of dsRNAs and leaves two-nucleotide, 3’ overhanging ends. These small interfering RNAs (siRNAs) are then incorporated into the RNA-induced silencing complex (RISC), a protein/RNA complex, and guide a nuclease, which degrades the target RNA.

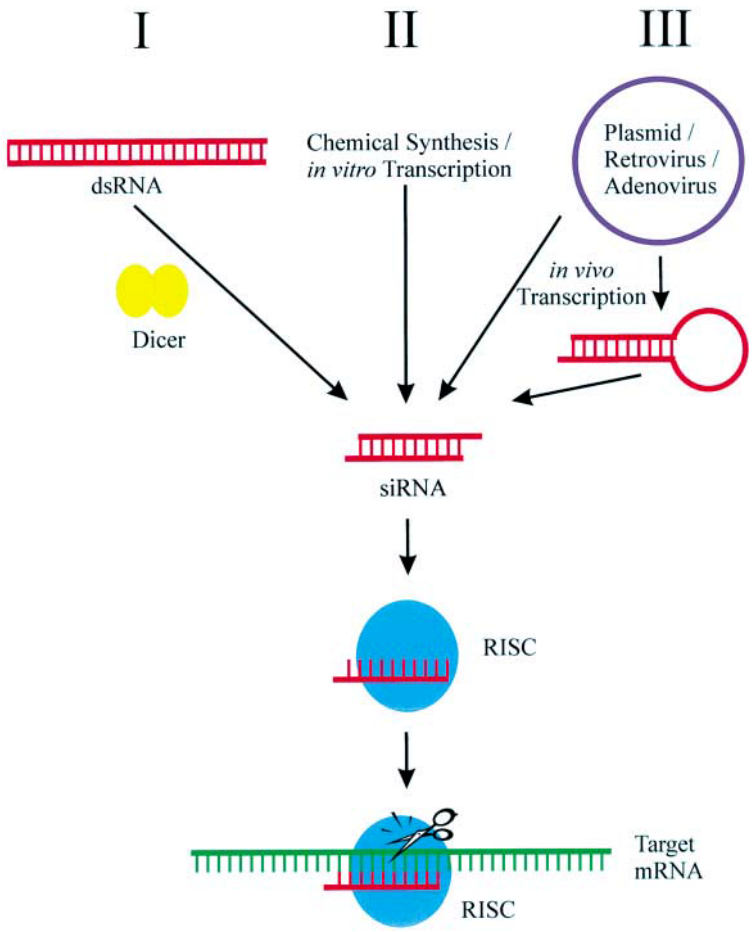

Figure 2. Gene silencing by RNA interference (RNAi). RNAi is triggered by siRNAs,which can by generated in three ways. (I) Long double-stranded RNA molecules are processed into siRNA by the Dicer enzyme; (II) chemically synthesized or in vitro transcribed siRNA duplexes can be transfected into cells; (III) the siRNA molecules can be generated in vivo from plasmids,retroviral vectors or adenoviruses. The siRNA is incorporated into the RISC and guides a nuclease to the target RNA. (Eur. J. Biochem. 2003, 270, 1628−1644.)

This conserved biochemical mechanism could be used to study gene functions in a variety of model organisms, but its application to mammalian cells was hampered by the fact that long double-stranded RNA molecules induce an interferon response. In a revolutionary breakthrough, when Tuschl and coworkers showed that 21 nucleotide-long siRNA duplexes with 3' overhangs could specifically suppress gene expression in mammalian cells [24]. This finding triggered many studies using RNAi in mammalian cells, as it is thought to provide a significantly higher potency.

Aptamer

***Nucleic acid aptamers*:** Nucleic acid aptamers are single-stranded nucleic acids that have been selected from random pools based on their ability to bind target proteins[25]. This selection procedure has been called SELEX (**S**ystematic **E**volution of **L**igands by **EX**ponential Enrichment). The SELEX process normally starts with a large population (10^{13}-10^{16}) of single-stranded nucleic acid molecules and is followed by multiple rounds of processes that utilize PCR to specifically amplify sequences having high binding affinity to a target. Aptamers as therapeutics would most likely bind proteins involved in the regulation and expression of genes. In 2004, the first aptamer based therapeutic drug, Pegaptanib sodium (Macugen; Eyetech Pharmaceuticals/Pfizer) was approved by FDA (Fig. 3). Pegaptanib sodium is an RNA aptamer medicine for the treatment of neovascular (Wet) age-related macular degeneration (AMD)[26]. This aptamer drug is directed against vascular endothelial growth factor (VEGF)-165, the VEGF isoform primarily responsible for pathological ocular neovascularization and vascular permeability. Many other aptamer based drugs are being evaluated in clinical trials.

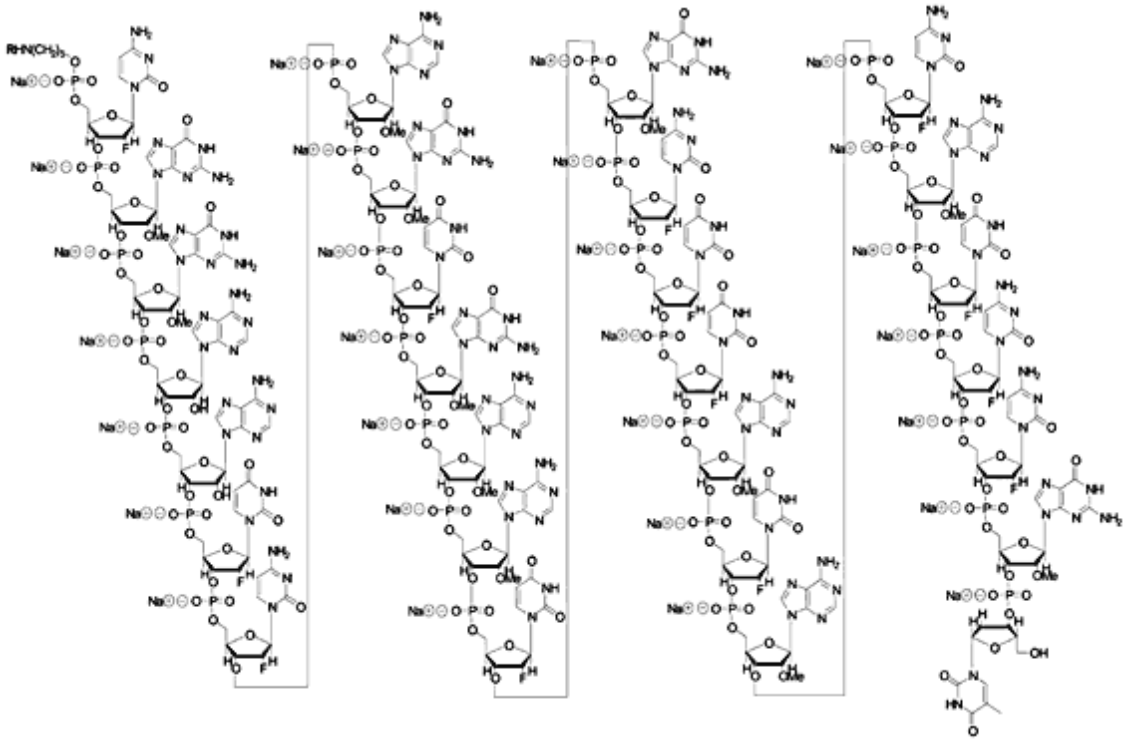

Figure 3. Structure of Pegaptanib sodium
(Fraunfelder, F.W. Pegaptanib for wet macular degeneration Drugs Today 2005, 41(11): 703 ISSN 1699-3993)

Antisense oligonucleotide

Antisense Mechanisms: Antisense oligonucleotides are valuable tools for selectively inhibiting target gene expression. The potential of oligodeoxynucleotides to act as antisense oligonucleotides that inhibit Rous sarcoma viral replication and cell transformation was discovered by Zamecnik and Stephenson in 1978[27]. In general, Antisense oligonucleotides are relatively short (13–25 nucleotides) and hybridize to not only mRNA but also microRNA (miRNA) present in cells. The antisense mechanism to inhibit gene expression can be broadly divided into two distinct categories (Fig. 4). The first category is RNase H-mediated cleavage of the target mRNA after hybridization of the antisense[28]. The second category is the RNase H-independent mechanisms that rely on steric block of translation[29].

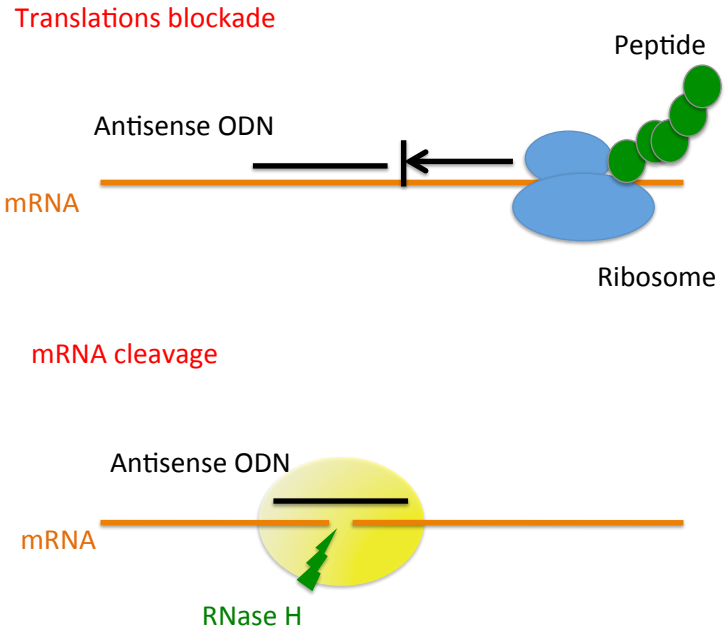

Figure 4. Action mechanism of antisense oligonucleotides

MicroRNA (miRNA): miRNA is an endogenously-encoded, post-transcriptional gene regulator. miRNAs inhibit gene expression by binding in the 3' UTR of target mRNAs with complementarity sequences and preventing protein translation or promoting mRNA degradation[30]. Aberrant miRNA expression leads to developmental abnormalities and diseases, such as cardiovascular disorders and cancer; however, the stimuli and processes regulating miRNA biogenesis are largely unknown[31]. Much of the progress in understanding the miRNA function to date has been from inhibition studies with antisense oligonucleotides.

Artificial Oligonucleotide

Although it is easy to synthesize phosphodiester antisense oligonucleotides, they are rapidly degraded by intracellular endonucleases and exonucleases[32-34]. In addition, the products of enzymatic degradation of the phosphodiester oligonucleotides, deoxyribonucleoside-5'-phosphate (dNMP) mononucleotides, may be cytotoxic and also exert antiproliferative effects[35]. Therefore, many chemical modifications (Fig. 5) have been developed to overcome these problems.

Methylphosphonate modified oligonucleotides:

Methylphosphonate modified oligonucleotides are nuclease resistance oligomers, in which a non-bridging oxygen atom is replaced by a methyl group at each phosphorus in the oligonucleotide chain[36]. These compounds are not negatively charged, which facilitates their cellular uptake[37,38]. However, the absence of a negative charge also reduces their low solubility in water. Besides, stereoisomers of methylphosphonate linkages destabilize the hybrids between methylphosphonate-modified oligonucleotides and

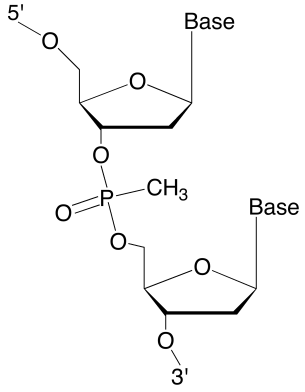

Methylphosphonate Oligonucleotide

the target RNA. Moreover, methylphosphonate modified oligonucleotides cannot invoke RNase H activity[39]. These features severely restrict their use as antisense molecules.

Phosphorothioates oligonucleotides:

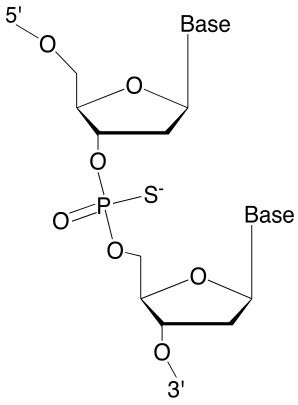

Phosphorothioate Oligonucleotide

Phosphorothioates oligonucleotides were first synthesized in the 1960s by De Clercq *et al*[40]. In these oligonucleotide analogs, one of the non-bridging oxygen atoms in the phophodiester bond is replaced by sulfur. The phosphorothioate oligonucleotides have a good solubility in water, highly nuclease stability and RNase H activity. As phosphorothioate modification is relatively easy to synthesize, these compounds are one of the most widely studied oligonucleotides. Although phosphorothioate oligonucleotides have many attractive features as antisense oligonucleotides, there are potential limitations do exist with these compounds. The major problems with commonly used phosphorothioates oligonucleotides are the toxicity at high concentration and their low affinity towards target RNA due to their diastereomer formation[41].

2'-O-methyl (or 2'-O-methoxy-ethyl) Oligonucleotides:

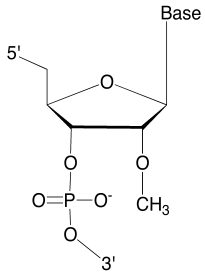

2'-O-methyl Oligoribonucleotides

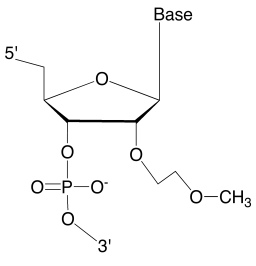

2'-O-methoxy-ethyl Oligoribonucleotides

The disadvantage of phosphorothioate oligonucleotides has been solved to some extent by modifying the alkyl group at the 2' position of the ribose (2'-O-methyl or 2'-O-methoxy-ethyl). These oligonucleotides bind to RNA targets with high melting temperatures[42] and induce an antisense effect. In addition,

they have lower toxicity than phosphorothioates oligonucleotides. On the other hand, owing to the conformational changes induced by the modifications, they do not recruit RNase H and for this reason their antisense effect is limited to a steric block of translation[43-44]. In 1997, Brenda F *et al*. first reported that the expression of the intercellular adhesion molecule 1 (ICAM-1) could be inhibited efficiently with an RNase H-independent 2'-O-methoxy-ethyl-modified antisense oligonucleotide that was targeted against the 5'-cap region[45].

Peptide nucleic acids (PNAs):

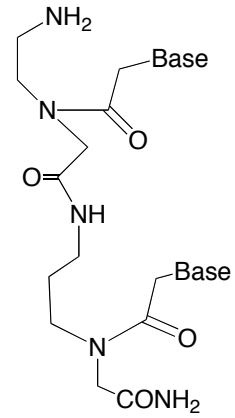

Peptide nucleic acid

Peptide nucleic acid (PNA) is a DNA analog with nucleobases attached to an uncharged pseudopeptide backbone [46-48]. PNA was first introduced by Nielsen et al. in 1991[49]. PNA is resistant to both nucleases and proteases. Furthermore, PNA oligonucleotides can form very stable PNA/RNA hetero duplexes[50]. Because PNAs are not elicit target RNA cleavage by RNase H., the antisense mechanism of PNAs depends on steric hindrance. PNAs can bind mRNA and inhibit splicing [51] or translation initiation[52].

Bridged nucleic acids (BNAs)/ Locked Nucleic Acids (LNAs):

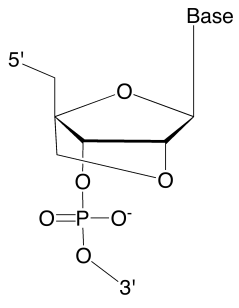

Bridged nucleic acid

In 1997, Obika *et al*. (in Imanishi's group) reported the first synthesis of bridged nucleic acids[53] (BNA, also known as Locked Nucleic Acids (LNAs)[54]). BNA nucleotides contain a methylene bridge that connects the 2' -oxygen with the 4' -carbon of the ribose ring. LNA modified antisense oligonucleotides induce a conformational change of the DNA/RNA hetero duplex towards the A-type helix[55] and therefore prevents RNase H cleavage of the target RNA.

Morpholino oligonucleotides:

Morpholino oligonucleotides were devised by Summerton *et al*. in 1985. Morpholino oligonucleotides are uncharged DNA analogs, in which the ribose sugar is replaced by a morpholino moiety and ribose backbone linked by phosphoroamidate intersubunit bonds instead of phosphodiester bonds[56-58]. These oligonucleotides are completely stable to nucleases[59] and exhibit efficient antisense activity in a few cultured animal cell lines[60, 61].

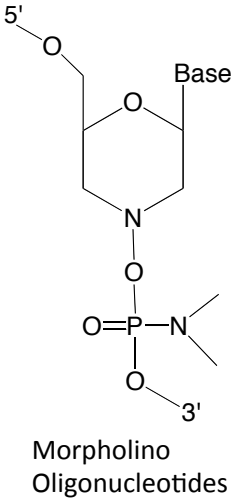

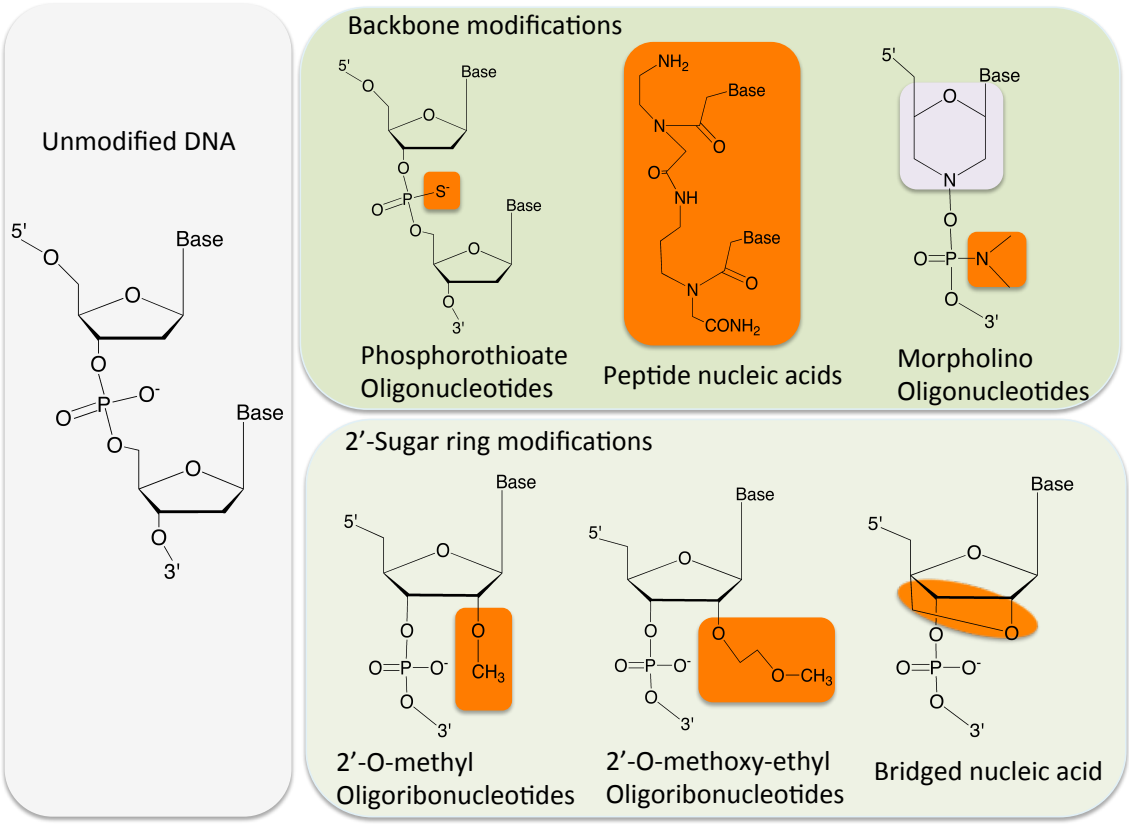

Figure 5. Nucleic acid analogs chemical structures. Schematic of unmodified DNA base pair (left). Different backbone modifications that can be applied (top row) and different 2'-sugar modifications that can be used (bottom row) to increase nuclease resistance and RNA binding affinity of the antisense oligonucleotides. Deviations from the original unmodified Nucleic acid are highlighted by circles.

Stimuli responsive Antisense oligonucleotides

In more recent years, a variety of stimuli responsive antisense nucleotides have been developed (Fig 6). For example, photo caged AS-ODNs that hybridized with complementary caging oligonucleotides having a photocleavable linker[62] (Fig. 6a) or an azobenzene[63,64] moiety (Fig. 6b) that can control the stability of the AS-ODN/RNA duplex by photoirradiation. Moreover, photocrosslinkable antisense oligonucleotide containing psoralen (Fig. 6c) were reported by Higuchi *et al*[65]. Because of the specific and irreversible complexation between psoralen-conjugated oligodeoxy nucleotides and the target mRNA, the regulation of gene expression was achieved with a low concentration of AS-ODN (IC_{50} = 50 nM) and UV irradiation.

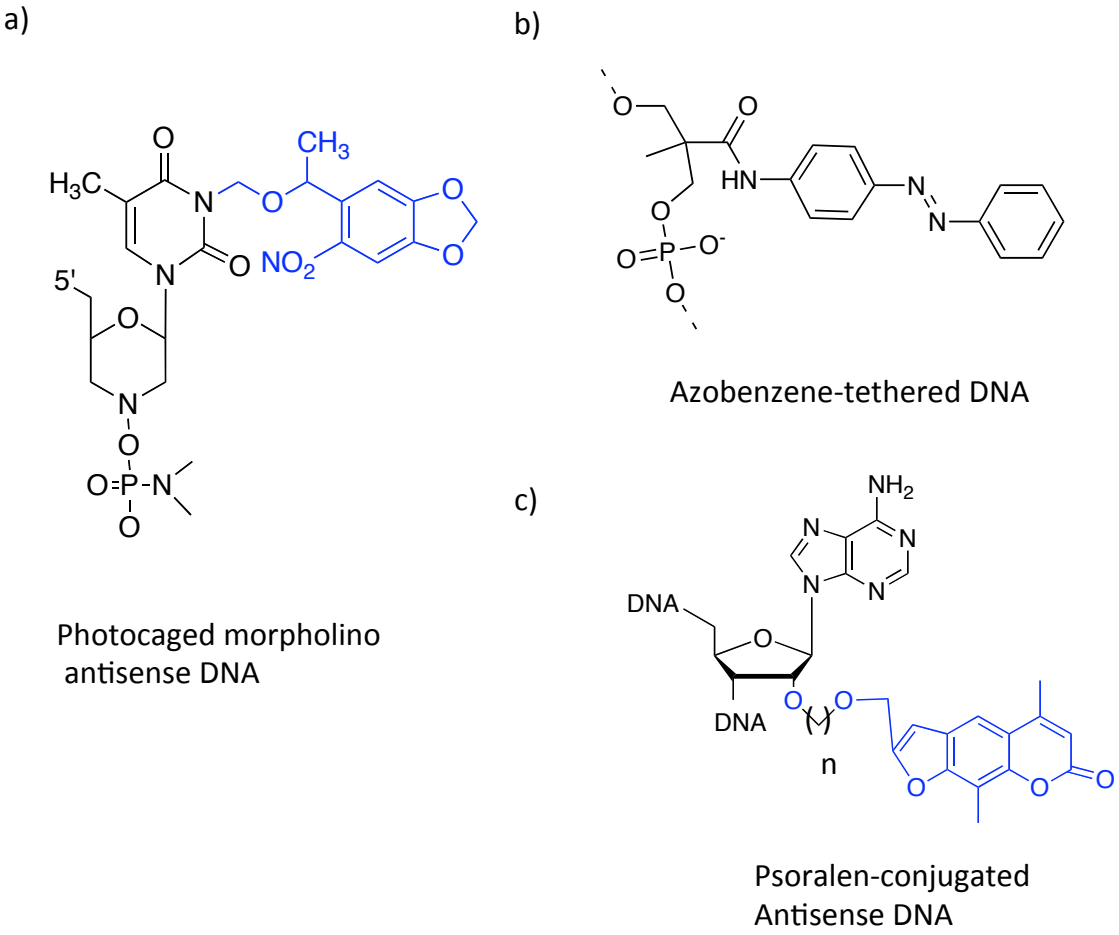

Figure 6. Stimuli responsive antisense oligonucleotides

In 2008, Yoshimura and Fujimoto reported on photoresponsive synthetic oligonucleotides containing 3-Cyanovinylcarbazole nucleoside (^{cnv}K) that can photocrosslink to complementary DNA or RNA strand via [2+2] photocycloaddition between ^{cnv}K and pyrimidine base in complementary strand with a few second of 366 nm irradiation[66] (Fig. 7). This ultra fast photo-crosslinking reaction is applicable for selection of miRNAs[67], construction and/or stabilization of nanostructured DNA[68–70] , single nucleotide polymorphism (SNP) typing of DNA[71] and antisense strategy. The quantum yield of the photo-cross-linking reaction of ^{CNV}K is ca. 10-fold larger than that of psoralen moiety, which is the representative photo-crosslinker used for antisense strategy and that requires some minutes of 365 nm irradiation for the cross-linking reaction[65,71].

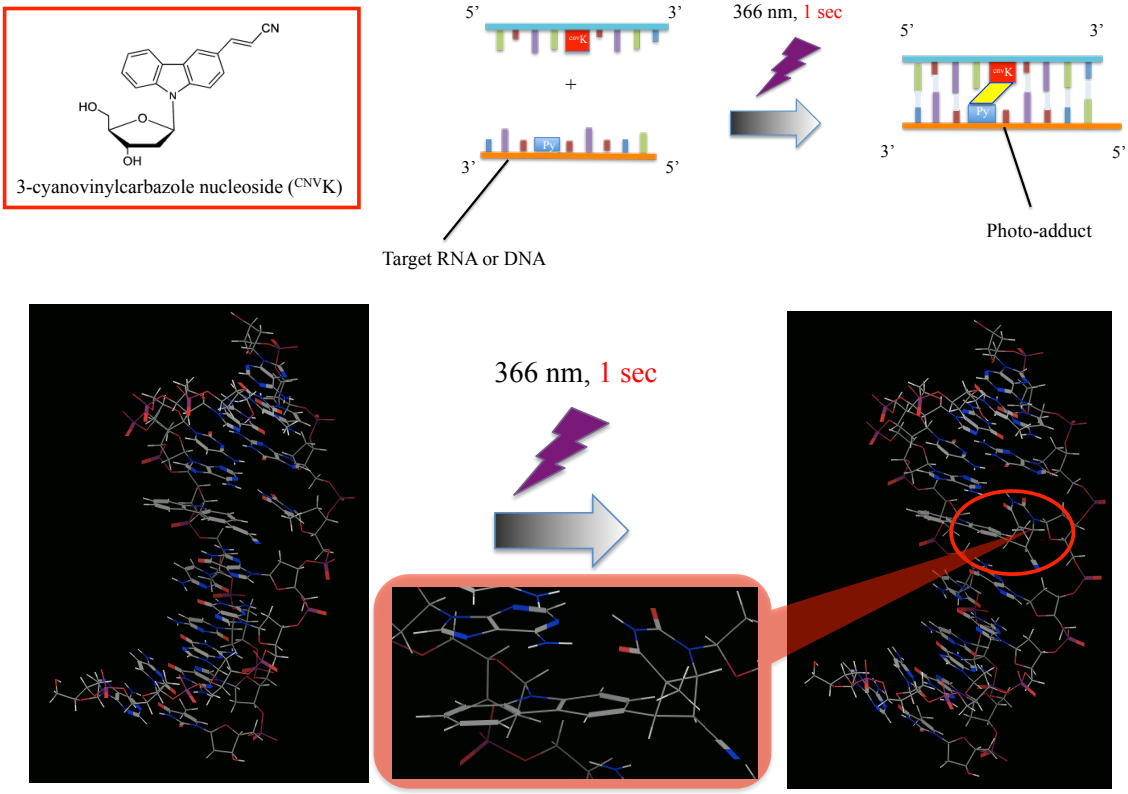

Figure 7. Photo-reactive antisense oligonucleotide containing ^{cnv}K

CpG oligonucleotide

CpG oligonucleotide is one of the activators of the innate immune system via interaction with the pattern-recognition receptor Toll-like receptor 9 (TLR9)[72-74]. Oligonucleotides contain unmethylated CpG (Cytosine – phosphate - Guanine) sequences similar to those commonly found in bacterial DNA (CpG DNA)[75.76]. TLR9 recognizes bacterial and viral components, but the direct interaction between the receptor and ligand is unclear. In humans, TLR9 is expressed predominantly on B cells and plasmacytoid dendritic cells (pDCs). TLR9 activation in cells induces proinflammatory cytokines and interferons through the signal-transduction pathways (Fig. 8) CpG oligonucleotide has important properties that can be applied to infectious diseases, allergy treatments and cancer therapy[77-79].

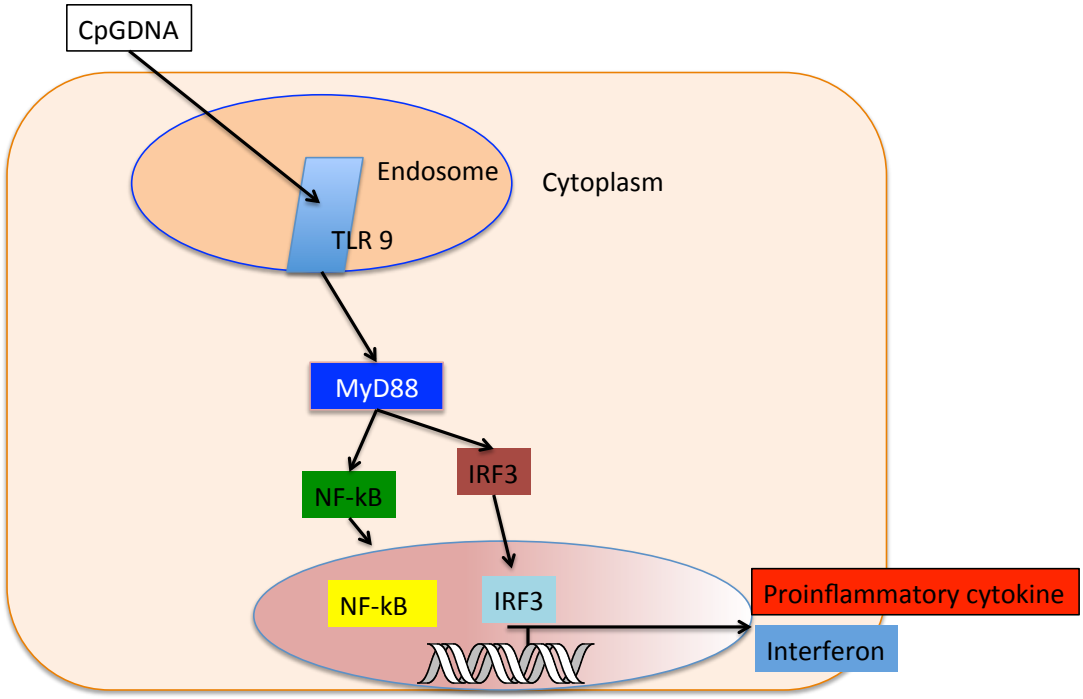

Figure 8. TLR9 signal pathway

Objective of this study

Nucleic acids are becoming increasingly important as tailor-made therapeutic molecules mainly for the ease with which specificity for a vast range of targets of these drugs is achieved. Therefore, many researchers in academia and pharmaceutical companies are paying attention to the development of nucleic acid based drugs. In particular, stimuli responsible nucleic acid drugs have a great potential for organ specific therapy. In this thesis, the author suggests the high photo-responsible antisense oligonucleotide and radiation trigger of artificial CpG oligonucleotides.

In Chapter 1, I describe the development of new photoresponsive AS-ODNs using a photoresponsive nucleoside analogue, 3-cyanovinylcarbazole nucleoside (^{CNV}K.), which can quickly photocrosslink to the pyrimidine base in complementary RNA strands with only a few seconds of photoirradiation. The photoreactivity and the sequence selectivity of the AS-ODNs containing ^{CNV}K with the target oligoribonucleotides (ORNs) were evaluated, and the photoinduced antisense effect was evaluated by an in vitro translation technique.

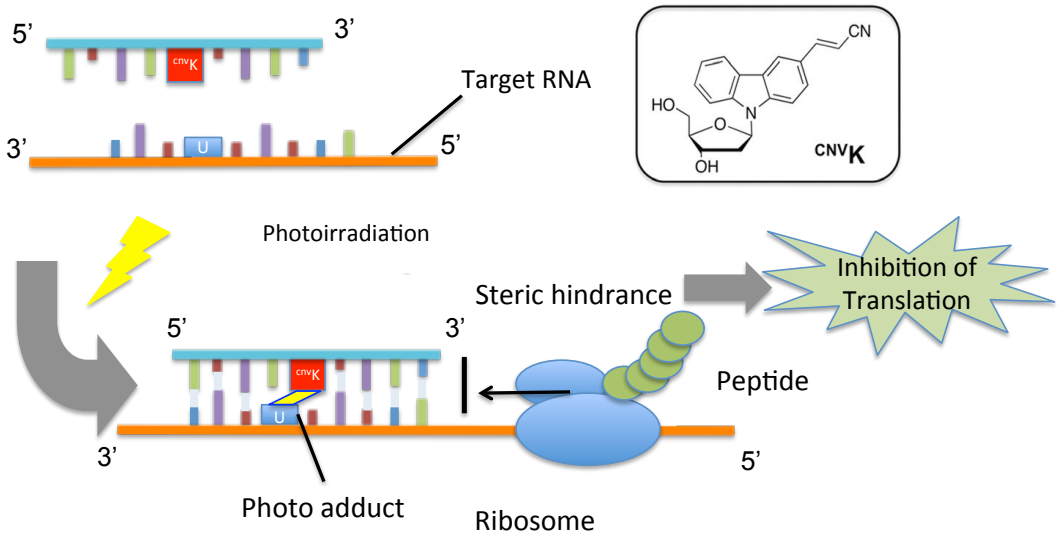

Figure 9. Schematic drawing of the regulation of gene expression by photoresponsive AS-ODN containing ^{CNV}K.

In Chapter 2, I describe the photoresponsive gene silencing activity of ^{CNV}K-AS for the regulation of endogenous GFP expression in a GFP stable cell line (GFP-HeLa). This study clearly demonstrated that photoreactive AS-ODNs having ^{CNV}K act as an effective photo-regulator for endogenous GFP gene expression in living cells with only 10 seconds of 366 nm irradiation, and that the antisense effect is temporally controllable by the photoirradiation.

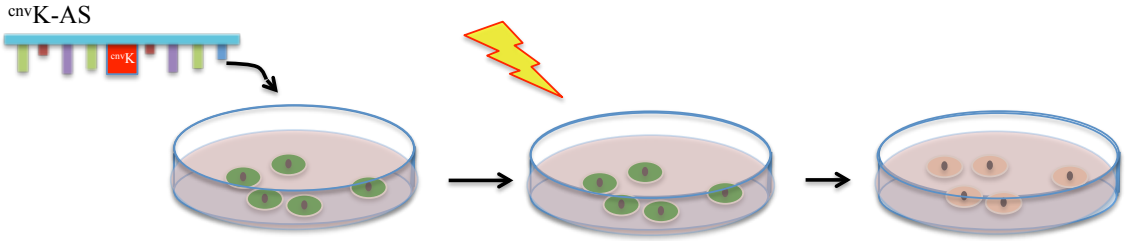

Figure 10. Schematic drawing of the regulation of gene expression by photoresponsive AS-ODN containing ^{CNV}K.

In Chapter 3, I describe the synthesis of disulfide crosslinking tethered CpG oligonucleotide (S-S CpG) as radiation-trigger immune activator. The S-S CpG had an alkyl chain and two CpG DNA units were connected by an X-ray-sensitive disulfide bond. X-irradiation of Raw cells, to which S-S CpG were administered, resulted in an induced Ifnb mRNA expression because of the reductively-cleaved CpG immune activation.

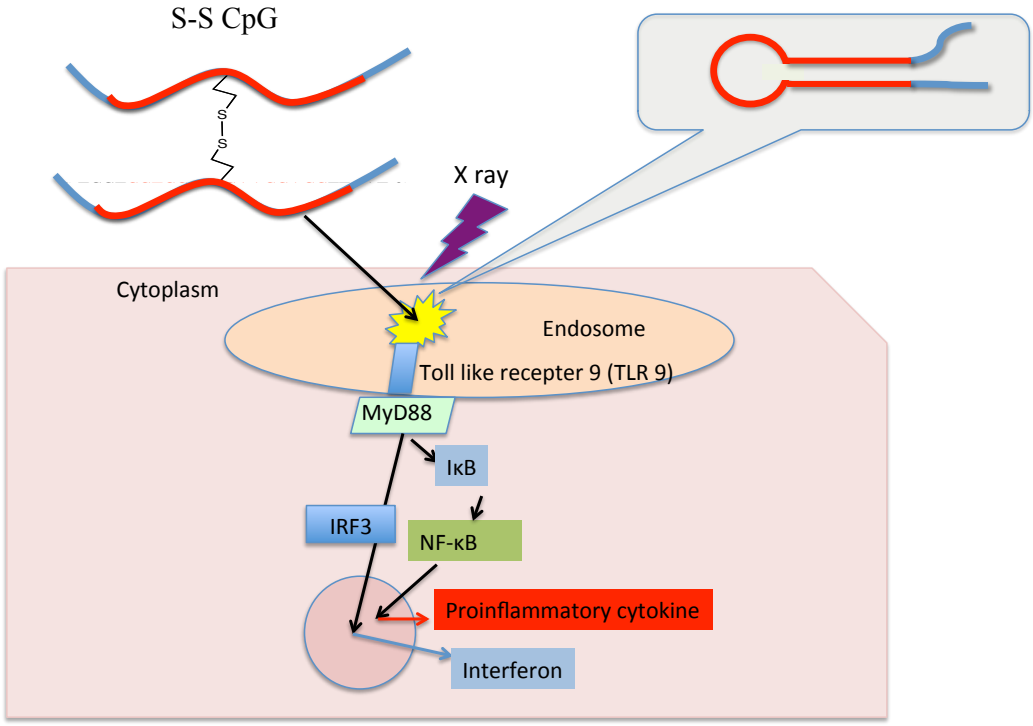

Figure 11. Schematic drawing of the immune activation by disulfide crosslinking tethered CpG oligonucleotide (S-S CpG).

References

1. Carter, P.J. Potent antibody therapeutics by design. *Nat. Rev*. **2006**, 6, 343–357.
2. Letsinger, R. L., and Mahadevan, V. Oligonucleotide synthesis on a polymer support. *J. Am. Chem.* Soc. **1965**, 87, 3526-3527.
3. Letsinger, R. L., and Mahadevan, V. Stepwise synthesis of oligodeoxyribonucleotides on an insoluble polymer support. *J. Am. Chem. Soc*. **1966**, 88, 5319-5324.
4. Matteucci, M.D., and Caruthers, M.H. The synthesis of oligodeoxyprimidines on a polymer support. Tetrahedron Lett. **1980**, 21, 719–722.
5. Matteucci, M.D., and Caruthers, M.H. Studies on nucleotide chemistry iv: Synthesis of deoxyoligonucleotides on a polymer support. *J. Am. Chem. Soc.* **1981**, 103, 3185–3191.
6. McPherson, J.D. *et al*., A physical map of the human genome. *Nature.* **2001,** 409, 934-941.
7. Venter, J.C. *et al*., The sequence of the human genome. *Science*. **2001**, 291, 1304-1351.
8. Leachman, S.A., Hickerson R.P., Hull P.R., Smith F.J., Milstone L.M., LaneE.B., Bale S.J., Roop D.R., McLean W.H., and Kaspar R.L. Therapeutic siRNAs for dominant genetic skin disorders including pachyonychia congenita. *J Dermatol Sci.* **2008**, 51, 151-157.
9. Cooper, T.A., Wan L., and Dreyfuss G. RNA and disease. *Cell.* **2009**, 136, 777-793.
10. Schlosser, K., and Li, Y. Biologically inspired synthetic enzymes made from DNA. *Chem Biol.* **2009**, 16, 311–322.
11. Schubert, S., and Kurreck, J. Ribozyme and deoxyribozymestrategies for medical applications. *Curr Drug Targets*. **2004**, 5, 667-681.
12. Jabs, D.A., and Griffiths, P.D. Fomivirsen for the treatment of cytomegalovirus

retinitis. *Am J Ophthalmol.* **2002**, 133, 552–556

13. Cech, T.R. The chemistry of self-splicing RNA and RNA enzymes. *Science.* **1987**, 236, 1532-1539.
14. Cech, T.R., Zaug, A.J., and Grabowski, P.J. In vitro splicing of the ribosomal RNA precursor of Tetrahymena: involvement of a guanosine nucleotide in the excision of the intervening sequence. *Cell.* **1981**, 27, 487-496.
15. Guerrier-Takada, C., Ga rdiner, K., Marsh, T., Pace, N. and Altman, S. The RNA moiety of ribonuclease P is the catalytic subunit of the enzyme. *Cell.* **1983**, 35, 849–857.
16. Bevilacqua, P., and Yajima, R. Nucleobase catalysis in ribozyme mechanism, *Curr. Opin. Chem. Biol.* **2006**, 10, 455-464.
17. Martick, M., and Scott, W.G. Tertiary contacts distant from the active site prime a ribozyme for catalysis. *Cell.* **2006**, 126, 309–320.
18. Doherty, E.A., and Doudna, J.A. Ribozyme structures and mechanisms. *Annu. Rev. Biochem*. **2000**, 69, 597-615.
19. Jimenez, R.M., Delwart, E., and Luptak, A. Structure-based search reveals hammerhead ribozymes in the human microbiome. *J. Biol. Chem.* **2011**, 286 7737-7743.
20. Kijima, H., and Scanlon, K.J. Ribozyme as an approach for growth suppression of human pancreatic cancer. *Mol. Biotechnol*. **2000**, 14, 59-72.
21. Kuwabara, T., Warashina, M., Tanabe, T., Tani, K., Asano, S., and Taira, K. A novel allosterically trans-activated ribozyme, the maxizyme, with exceptional specificity in vitro and in vivo. *Mol. Cell.* **1998**, 2, 617-627.
22. Fire, A., Xu, S.Q., Montgomery, M.K., Kostas, S.A., Driver, S.E., and Mello, C.C. Potent and specific genetic interference by double-stranded RNA in Caenorhabditis elegans. *Nature*. **1998**, 391, 806–811.
23. Tomari, Y., Zamore, P.D. Perspective: machines for RNAi. *Genes Dev.* **2005**, 19, 517-529.

24. Elbashir, S .M., Harborth, J ., Lendeckel, W., Yalcin, A.,Weber, K., and Tuschl, T. Duplexes of 21-nucleotide RNAs mediate RNA interference in culturedmammalian cells. *Nature.* **2001**, 411, 494-498.
25. Tuerk, C., and Gold, L. Systematic evolution of ligands by exponential enrichment: RNA ligands to bacteriophage T4 DNA polymerase. *Science*. **1990**, 249, 505-510.
26. Ng, E.W., Shima, D.T., Calias, P., Cunningham, E.T., Jr, Guyer, D.R., and Adamis, A.P. Pegaptanib, a targeted anti-VEGF aptamer for ocular vascular disease. *Nat Rev Drug Discov.* **2006**, 5, 123-132.
27. Silverman, S.K. In vitro selection, characterization, and application of deoxyribozymes that cleave RNA, *Nucleic Acids Res.* **2005**, 33, 6151–6163.
28. Lorenz, P., Baker, B.F., Bennett, C.F., and Spector, D.L. Phosphorothioate antisense oligonucleotides induce the formation of nuclear bodies. *Mol Biol Cell.* **1998**, 9, 1007-1023.
29. Sharp, P.A. The centrality of RNA. *Cell.* **2009**, 136, 577-580.
30. Esau, C. C. Inhibition of microRNA with antisense oligonucleotides. *Methods.* **2008**, 44, 55-60.
31. Davis, B.N., Hilyard, A.C., Lagna, G., and Hata, A. SMAD proteins control DROSHA-mediated microRNA maturation. *Nature*, **2008**, 454, 56-61.
32. Wickstrom, E. Oligodeoxynucleotide stability in subcellular extracts and culture media. *J. Biochem. Biophys. Methods.* **1986**, 13, 97-102.
33. Akhtar, S., Kole, R., and Juliano, R. L. Stability of antisense DNA oligodeoxynucleotide analogs in cellular extracts and sera. *Life Sci*. **1991**, 49, 1793-1801.
34. Eder, P. S., DeVine, R. J., Dagle, J. M., and Walder, J. A. Substrate specificity and kinetics of degradation of antisense oligonucleotides by a 3- exonuclease in plasma. *Antisense Res. Dev.* **1991**, 1, 141-151.
35. Vaerman, J. L., Moureau, P., Deldime, F., Lewalle, P., Lammineur, C.,

Morschhauser, F., and Martiat, P. Antisense oligodeoxyribonucleotides suppress hematologic cell growth through stepwise release of deoxyribonucleotides. *Blood.* **1997**, 90, 331-339.

36. Miller, P. S., Yano, J., Yano, E., Carroll, C., Jayaraman, K., and Ts'o, P. O. Nonionic nucleic acid analogues. Synthesis and characterization of dideoxyribonucleoside methylphosphonates. *Biochemistry,* **1979**, 18, 5134-5143.
37. Miller, P. S., McParland, K. B., Jayaraman, K., and Ts'o, P. O. Biochemical and biological effects of nonionic nucleic acid methylphosphonates. *Biochemistry.* **1981**, 20, 1874-1880.
38. Blake, K. R., Murakami, A., Spitz, S. A., Glave, S. A., Reddy, M. P., Ts'o, P. O., and Miller, P. S. Hybridization arrest of globin synthesis in rabbit reticulocyte lysates and cells by oligodeoxyribonucleoside methylphosphonates. *Biochemistry*. **1985**, 24, 6139-6145.
39. Walder, J. Antisense DNA and RNA: progress and prospects. *Genes Dev.* **1988**, 2, 502-504.
40. De Clercq, E., Eckstein, F., and Merigan, T.C. Interferoninduction increased through chemical modification of a synthetic polyribonucleotide. *Science.* **1969**, 165, 1137-1139.
41. Cosstick, R., and Eckstein, F. Synthesis of d(GC) and d(CG) octamers containing alternating phosphorothioate linkages: Effect of the phosphorothioate group on the B-Z transition. *Biochemistry.* **1985**, 24, 3630-3638.
42. Monia, B. P., Lesnik, E. A., Gonzalez, C., Lima, W. F., McGee, D.,Guinosso, C. J., Kawasaki, A. M., Cook, P. D., and Freier, S. M. Evaluation of 2'-modified oligonucleotides containing 2'-deoxy gaps as antisense inhibitors of gene expression. *J. Biol. Chem.* **1993**, 268, 14514-14522.
43. Manoharan, M. 2'-carbohydrate modifications in antisense oligonucleotidetherapy: importance of conformation, configuration and conjugation. *Biochim. Biophys. Acta.* **1999**, 1489, 117-130.

44. Zamaratski, E., Pradeepkumar, P.I., and Chattopadhyaya, J. A critical survey of the structure-function of the antisense oligo/RNA heteroduplex as substrate for RNase H. *J. Biochem.Biophys. Methods.* **2001**, 48, 189–208.
45. Baker, B.F., Lot, S.S., Condon, T.P., Cheng-Flournoy, S., Lesnik, E.A., S asmor, H.M., and Bennett, C.F. 2'-O-(2-methoxy) ethyl-modified anti-intercellular adhesion molecule 1 (ICAM-1) oligonucleotides selectively increase the ICAM-1 mRNA level and inhibit formation of the ICAM-1 translation initiation complex in human umbilical vein endothelial cells. *J. Biol. Chem.* **1997**, 272, 11994-12000.
46. Good, L., and Nielsen, P.E., Progress in developing PNA as a gene-targeted drug. *Antisense Nucleic Acid Drug Dev.* **1997**, 7(4), 431–437.
47. Ray, A., and Norden, B. Peptide nucleic acid (PNA): its medical and biotechnical applications and promise for the future. *Faseb J.* **2000**, 14(9), 1041–1060.
48. Tian, X., Aruva, M.R., Qin, W., Zhu, W., Duffy, K.T., Sauter, E.R., Thakur, M.L., and Wickstrom, E. External imaging of CCND1 cancer gene activity in experimental human breast cancer xenografts with 99mTcpeptide-peptide nucleic acid-peptide chimeras. *J Nucl Med.* **2004**, 45(12), 2070–2082.
49. Nielsen, P.E. Antisense properties of peptide nucleic acid. *Methods Enzymol*. **1999**, 313,156 –164.
50. Jensen, K.K., Orum, H., Nielsen, P.E., and Norden, B. Kinetics for hybridization of peptide nucleic acids (PNA) with DNA and RNA studied with the BIAcore technique. *Biochemistry.* **1997**, 36, 5072–5077.
51. Karras, J. G., Maier, M. A., Lu, T., Watt, A., and Manoharan, M. Peptide nucleic acids are potent modulators of endogenous pre-mRNA splicing of the murine interleukin-5 receptor-chain. Biochemistry. **2001**, 40, 7853–7859.
52. Mologni, L., Marchesi, E., Nielsen, P. E., and Gambacorti-Passerini, C. Inhibition of promyelocytic leukemia (PML)/retinoic acid receptor-alpha and

PML expression in acute promyelocytic leukemia cells by anti-PML peptidenucleic acid. *Cancer Res*. **2001**, 61, 5468-5473.

53. Obika, S., Nanbu, D., Hari, Y., Morio, K., In, Y., Ishida, T., and Imanishi, T. Synthesis of 2'-O,4'-C-Methyleneuridine and -cytidine. Novel Bicyclic Nucleosides Having a Fixed C3'-endo Sugar Puckering. *Tetrahedron Lett.*, **1997**, 38, 8735-8738.
54. Koshkin, A.A., Singh, S.K., Nielsen, P., Rajwanshi, V.K., Kumar, R., Meldgaard, M., Olsen, C. E., and Wengel, J. *Tetrahedron.* **1998**, 54, 3607-3630.
55. Bondensgaard, K., Petersen, M., Singh, S.K., Rajwanshi, V.K., Kumar, R., Wengel, J., and Jacobsen, J.P. Structural studies of LNA: RNA duplexes by NMR: Conformations and implications for RNase H activity. *Chem. Eur. J.* **2000**, 6, 2687-2695.
56. Summerton, J., and Weller, D.D. Uncharged Morpholino-based polymers having phosphorous linked chiral intersubunit linkages. *U.S. Patent.* **1993**,5,185,444.
57. Partridge, M., Vincent, A., Matthews, P., Puma, J., Stein, D., and Summerton, J. A simple method for delivering Morpholino antisense oligos into the cytoplasm of cells. *Antisense Nucleic Acid Drug Dev*. **1996**, 6, 169-175.
58. Hudziak, R., Barofsky, E., Barofsky, D., Weller, D.L., Huang, S., and Weller, D.D. Resistance of Morpholino phosphorodiamidate oligomers to enzymatic degradation. *Antisense Nucleic Acid Drug Dev.* **1996**, 6, 267-272.
59. Hudziak, R.M., Barofsky, E., Barofsky, D.F., Weller, D.L., Huang, S.B., and Weller, D.D. Resistance of morpholino phosphorodiamidate oligomers to enzymatic degradation. *Antisense Nucleic Acid Drug Dev*. **1996**, 6, 267–272.
60. Taylor, M.F., Weller, D.D., and Kobzik, L. Effect of TNF-alpha antisense oligomers on cytokine production by primary murine alveolar macrophages. *Antisense Nucleic Acid Drug Dev.* **1998**, 8, 199–205.

61. Summerton, J., Stein, D., Huang, S.B., Matthews, P., Weller, D., and Partridge, M. Morpholino and phosphorothioate antisense oligomers compared in cell-free and in-cell systems. *Antisense Nucleic Acid Drug Dev.* **1997**, 7, 63–70.
62. Deiters, A., Garner, R.A., Lusic, H., Govan, J.M., Dush, M., Nascone-Yoder, N.M. and Yoder, J.A. Photocaged morpholino oligomers for the lightregulation of gene function in zebrafish and Xenopus embryos. *J. Am. Chem.Soc.* **2010**, 132, 15644-15650.
63. Asanuma, H., Liang, X., Yoshida, T., and Komiyama, M. Photocontrol of DNA Duplex Formation by Using Azobenzene-Bearing Oligonucleotides. *ChemBioChem*. **2001**, 2, 39-44.
64. Asanuma, H., Matsunaga, D., and Komiyama, M. Clear-cut photo-regulation of the formation and dissociation of the DNA duplex by modified oligonucleotide involving multiple azobenzenes. *Nucleic Acids Symp. Ser.* **2005**, 49, 35-36.
65. Higuchi, M., Yamayoshi, A., Kato, K., Kobori, A., Wake, N., and Murakami, A., Specific Regulation of Point-Mutated K-ras-Immortalized Cell Proliferation by a Photodynamic Antisense Strategy. *Oligonucleotides*, **2010**, 20, 37-44.
66. Yoshimura, Y., and Fujimoto, K. Ultrafast Reversible Photo-Cross-Linking Reaction: Toward in Situ DNA Manipulation. *Org. Lett*. **2008**, 10, 3227-3230.
67. Yoshimura, Y., Ohtake, T., Okada, H., and Fujimoto, K. A New Approach for Reversible RNA Photocrosslinking Reaction: Application to Sequence-Specific RNA Selection. *ChemBioChem.* **2009**, 10, 1473-1476.
68. Tagawa, M., Shohda, K., Fujimoto, K., and Suyama, A. Stabilization of DNA nanostructures by photo-cross-linking. *Soft Matter.* **2011**, 7, 10931-10934.
69. Gerrard, S.R., Hardiman, C., Shelbourne, M., Nandhakumar, I., Nordén, B., and Brown, T. A new modular approach to nanoassembly: stable and addressable DNA nanoconstructs via orthogonal click chemistries. *ACS Nano.* **2012**, 6, 9221-9228.

70. Fujimoto, K., Konishi-Hiratsuka, K., Sakamoto, T., Ohtake, T., Shinohara, K., Yoshimura, Y., Specific and reversible photochemical labeling of plasmid DNA using photoresponsive oligonucleotides containing 3-cyanovinylcarbazole. *Mol. BioSyst.* **2012**, 8, 491−494.
71. Fujimoto, K., Yamada, A., Yoshimura, Y., Tsukaguchi, T., and Sakamoto, T. Details of the ultra-fast DNA photocrosslinking reaction of 3-cyanovinylcarbazole nucleoside; Cis-trans isomeric effect and the application for SNP based genotyping. *J. Am. Chem. Soc.* **2013**, 135 (43), 16161–16167.
72. Higuchi M., Kobori A., Yamayoshi A., Murakami A. Synthesis of antisense oligonucleotides containing 2'-O-psoralenylmethoxyalkyladenosine for photodynamic regulation of point mutations in RNA. *Bioorganic & Medicinal Chemistry*. **2009**, 17, 475-483.
73. Takeshita, F. *et al.* Cutting edge: Role of Toll-like receptor 9 in CpG DNA-induced activation of human cells. *J. Immunol.* 2001, 167, 3555–3558.
74. Krieg, A. M. CpG motifs in bacterial DNA and their immune effects. Annu. Rev. Immunol. **2002**, 20, 709–760.
75. Krieg, A. M. Therapeutic potential of Toll-like receptor 9 activation. *Nat. Rev.* **2006**, 5, 471–484.
76. Wilson, K.D. *et al.* "Effects of intravenous and subcutaneous administration on the pharmacokinetics, biodistribution, cellular uptake and immunostimulatory activity of CpG ODN encapsulated in liposomal nanoparticles", *Int Immunopharmacology*. **2007**, 7, 1064-1075.
77. Hemmi, H. *et al.* A Toll-like receptor recognizes bacterial DNA. *Nature.* **2000**, 408, 740–745.
78. Jahrsdorfer, B. and Weiner, G. J. CpG oligodeoxynucleotides for immune stimulation in cancer immunotherapy. *Curr. Opin. Investig. Drugs*. **2003**, 4, 686-690.

79. Fonseca, D. E., and Kline, J. N. Use of CpG oligonucleotides in treatment of asthma and allergic disease. *Adv. Drug Deliv. Rev.* **2009**, 61, 256–262.
80. Klinman, D. M., Klaschik, S., Sato, T., and Tross, D. CpG oligonucleotides as adjuvants for vaccines targeting infectious diseases. *Adv. DrugDeliv. Rev.* **2009**, 61, 248–255.

Chapter 1

Quick regulation of mRNA functions by a few seconds of photoirradiation

1.1 Introduction

It is important to understand the regulation of the mRNA function for the development of genome-based drugs. An antisense strategy that can regulate specifically the mRNA function with the specific binding property of a short oligonucleotide, i.e. an antisense oligonucleotide (AS-ODN), and its complementary target mRNA is a promising technology in this field. Since the pioneering work in the late 70s,[1,2] many researchers have made efforts to further develop this method, and drugs based on this strategy have been applied to clinical usage and/or ongoing phase I/II clinical trials, and also have been applied in the basic study of mRNA function. In this strategy, chemically modified AS-ODNs, such as phosphorothioates,[3,4] peptide nucleic acids[5-7] and locked (bridged) nucleic acids,[8-12] have been used to avoid the degradation by nucleases in blood or cells, or to stabilize the hetero-duplex of AS-ODN and its target mRNA, and these AS-ODNs successfully regulate the gene expression in vivo.[13-15] Other stimuli responsive AS-ODNs have been reported: for example, caged AS-ODNs that hybridized with complementary caging ODN (ccODN) having a photocleavable linker[16] or an azobenzene[17, 18] moiety that can control the stability of the AS-ODN/ccODN duplex by photoirradiation. Recently, Higuchi et al. reported that the photocrosslinkable oligonucleotide containing psoralen moiety at the 2′ position of adenosine effectively and specifically inhibits the expression of the codon 12 point-mutated K-ras (G12V) gene in living cells.[19-21] Because of the specific and irreversible complexation between photoreactive AS-ODN and the target mRNA, the regulation of gene expression was achieved with a low concentration of AS-ODN (IC_{50} = 50 nM) and UV irradiation. This method has the potential to provide a location-specific drug that can regulate gene expression by photoirradiation at the desired location in the body, however, the requirement of relatively long photoirradiation because of the low photoreactivity of AS-ODN may cause undesired toxicity to healthy cells. In

this study, we tried to develop other photoresponsive AS-ODNs using a photoresponsive nucleoside analogue, 3-cyanovinylcarbazole nucleoside[22-24] (^{CNV}K, Fig. 1), which can quickly photocrosslink to the pyrimidine base in complementary RNA strands with only a few seconds of photoirradiation.[25-26] The photoreactivity and the sequence selectivity of the AS-ODNs containing ^{CNV}K with the target oligoribonucleotides (ORNs) were evaluated, and the photoinduced antisense effect was evaluated by an in vitro translation technique. As a target mRNA, point mutated K-ras mRNA that causes irregular cell growth with the perturbation of the EGFR/Ras signaling pathway[27] was adopted.

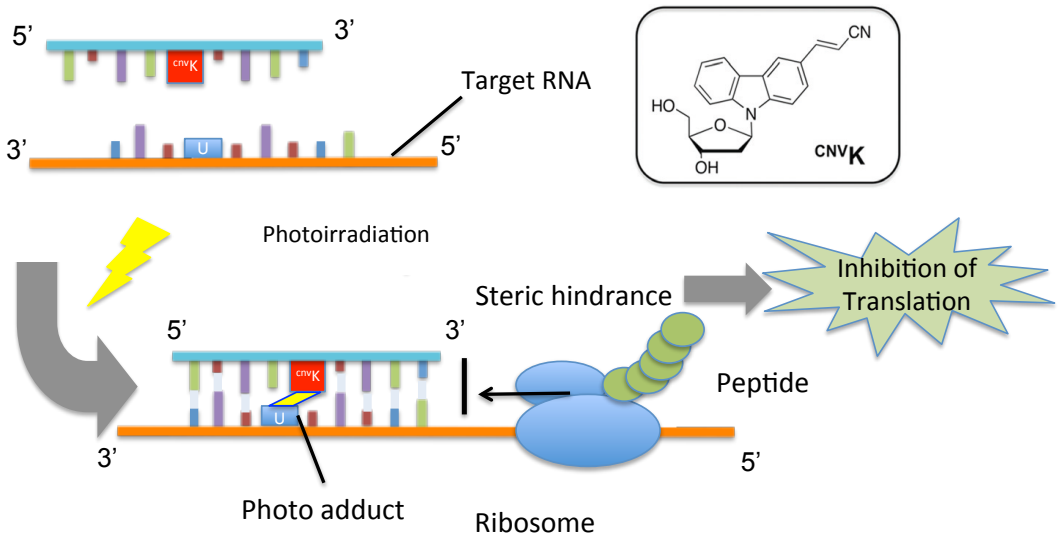

Figure 1. Schematic drawing of the regulation of gene expression by photoresponsive AS-ODN containing ^{cnv}K.

1.3. Materials and Method

General

Mass spectra were recorded on a Voyager-DE PRO-SF, Applied Biosystems. Irradiation was performed by UV-LED (366 nm, 1600 mW cm−2; ZUV, OMRON, Japan). HPLC was performed on a Chemcobond 5-ODS-H column (10 x 150 mm, 4.6 x150 mm) or a Chemcosorb 5-ODS-H column (4.6 x 150 mm) with a JASCO PU-980, HG-980-31, DG-980-50 system equipped with a JASCO UV 970 detector at 260 nm. Reagents for the DNA synthesizer such as A, G, C, T-β-cyanoethyl phosphoramidite, and CPG support were purchased from Glen Research. OligoRNAs were purchased from Fasmac (Japan) and used without further purification.

3-Iodocarbazole

To an ethanol solution (500 mL) of carbazole (2.50 g, 15.0 mmol), $NaIO_4$ (0.80 g, 3.75 mmol) and I_2 (1.89 g, 7.45 mmol) were sequentially added, and then an ethanol solution (100 mL) of H_2SO_4 (1.60 mL, 30.0 mmol) was added. The reaction solution was refluxed for one hour at 65° C. The loss of raw materials was confirmed by TLC (HexH:AcOEt=4:1), and an ethanol solution (100 mL) of NaOH (1.4 g) was added thereto to neutralize the system. Ethanol was removed, and then the reaction solution was extracted two times with chloroform. The extract was washed two times with water. The organic phase was dried over Na_2SO_4, and the solvent was removed. The residue was purified by column chromatography (HexH:AcOEt=4:1), and thus 3-Iodocarbazole (1.83 g, 42%) was obtained as a white powder. 3-Iodocarbazole: ^{1}H NMR (DMSO-d_6) δ 11.4 (s, 1H), 8.49 (d, 1H, J=1.7 Hz), 8.14 (d, 1H, J=8.0 Hz), 7.62 (dd, 1H, J=8.4, 1.7 Hz), 7.48 (d, 1H, J=8.0 Hz), 7.40 (m, 1H), 7.33 (d, 2H, J=8.4 Hz), 7.16 (m, 1H).

3-Cyanovinylcarbazole

In an 8.0 mL glass vessel was placed palladium acetate (88 mg, 0.39 mmol), DMF (0.74 mL), 3-Iodocarbazole (1.15 g, 3.92 mmol), tributylamine (0.93 mL, 3.92 mmol), acrylonitrile (0.65 mL, 9.8 mmol), and H_2O (1.8 mL). The vessel was sealed and placed into the microwave cavity. Initial microwave irradiation of 60 W was used, the temperature being ramped from room temperature to the desired temperature of 160 °C. Once this was reached, the reaction mixture was held at this temperature for 10 min. After allowing the mixture to cool to room temperature, the reaction mixture was monitored by TLC (hexane/AcOEt, 4:1), which showed the absence of starting material. After the reaction mixture was evaporated, the residue was chromatographed on a silica gel using hexane/AcOEt (3:1, v/v) as eluent to give 3-Cyanovinylcarbazole (1.97 g, 67%) as a white powder. ^{1}H NMR (300 MHz, DMSO-d6) δ 11.6 (s, 1H), 8.44 (s, 1H), 8.11 (d, 1H, J = 8.0 Hz), 7.75 (d, 1H, J = 16.7 Hz), 7.69-7.72 (m, 1H), 7.40-7.52 (m, 3H), 7.19-7.24 (m, 1H), 6.36 (d, 1H, J = 16.7 Hz).

3-Cyanovinylcarbazole-1'-β-deoxyriboside-3',5'-di-(p-toluoyl)ester

To a solution of potassium hydroxide (1.31 g, 25.7 mmol) and Tris[2-(2-methoxyethoxy)ethyl]amine (56.0 mg, 0.18 mmol) in CH_3CN (220 mL) was added 3-cyanovinylcarbazole (1.90 g, 8.76 mmol) at room temperature and the reaction mixture was stirred at room temperature for 30 min. To this reaction mixture was added chlorosugar (2.80 g, 6.59 mmol) at room temperature and the reaction mixture was stirred at room temperature for 60 min. The reaction mixture was monitored by TLC (hexane/AcOEt, 4:1), which showed the absence of starting material. After the reaction mixture was evaporated, the residue was chromatographed on a silica gel using $CHCl_3$ as eluent to give 3-cyanovinylcarbazole-1'-β-deoxyriboside-3',5'-di-(p-toluoyl)ester (3.20 g, 62%) as a yellow powder. ^{1}H NMR (300 MHz, $CDCl_3$) δ 8.09 (s, 1H), 8.02 (d, 2H, J = 8.4 Hz), 7.98 (d, 2H, J = 8.4 Hz), 7.62-7.65 (m, 1H), 7.62 (d, 1H, J = 8.8 Hz), 7.49 (d, 1H, J = 16.5 Hz), 7.25-7.31 (m, 7H), 7.17-7.20 (m, 1H), 6.68 (dd, 1H, J = 9.3, 5.8 Hz), 5.78 (m, 1H), 5.76 (d, 1H, J = 16.5 Hz), 4.91 (dd, 1H, J = 12.4, 2.7 Hz), 4.78 (dd, 1H, J = 12.4, 3.3 Hz), 4.55-4.57 (m, 1H), 3.09-3.20 (m, 1H), 2.45-2.52 (m, 1H), 2.45 (s, 3H), 2.44 (s, 3H).

3-Cyanovinylcarbazole-1'-β-deoxyriboside.

To a solution of 3-Cyanovinylcarbazole-1'-β-deoxyriboside-3',5'-di-(p-toluoyl)ester (3.17 g, 16.7 mmol) in CH_3OH (185 mL) was added 0.5 M methanolic $NaOCH_3$ (33.0 mL, 16.7 mmol) and $CHCl_3$ (20 mL) at room temperature and the reaction mixture was stirred at room temperature for 1 h. The reaction mixture was monitored by TLC ($CHCl_3/CH_3OH$, 9:1), which showed the absence of starting material. After the reaction mixture was evaporated, the residue was chromatographed on a silica gel using $CHCl_3/CH_3OH$ (9:1, v/v) as eluent to give 3-Cyanovinylcarbazole-1'-β-deoxyriboside (1.67 g, 90%) as a white powder. ^1H NMR (300 MHz, $CDCl_3$) δ 8.12 (d, 1H, J = 1.7 Hz), 8.06 (d, 1H, J = 7.7 Hz), 7.59 (d, 1H, J = 9.1 Hz), 7.43-7.57 (m, 4H), 7.26-7.31 (m, 1H), 6.64 (dd, 1H, J = 8.2, 6.9 Hz), 5.87 (d, 1H, J = 16.5 Hz), 4.77-4.82 (m, 1H), 3.95-4.06 (m, 3H), 2.95 (dt, 1H, J = 14.0, 8.2 Hz), 2.30 (ddd, 1H, J = 14.0, 6.9, 3.3 Hz).

5'-O -(4,4'-dimethoxytrityl)-3-Cyanovinylcarbazole -1'-β –deoxyri boside-3'-O -(cyanoethoxy-N,N –diis opropylamino)phosphoramidite .

To a solution of 3-Cyanovinylcarbazole-1'-β-deoxyriboside (0.83 g, 2.51 mmol) in pyridine (5 mL) was added a solution of 4,4'-dimethoxytrityl chloride (3.45 g, 10.2 mmol) and 4-(dimethylamino)pyridine (0.21 g, 1.70 mmol) in pyridine (24 mL) at 3-Cyanovinylcarbazole-1'-β-deoxyriboside room temperature and the reaction mixture was stirred at room temperature for 23 h. After the reaction mixture was evaporated, the residue was chromatographed on a silica gel using CHCl3/CH3OH (99:1, v/v) as eluent to give 5'-protected 4 (4.20 g, 78%) as a yellow powder. ^1H NMR (300 MHz, $CDCl_3$) **δ** 8.07 (d, 1H, J = 1.7 Hz), 8.02-8.05 (m, 1H), 7.71 (d, 1H, J = 8.5 Hz), 7.62-7.65 (m, 1H), 7.45-7.52 (m, 3H), 7.33-7.37 (m, 4H), 7.25-7.28 (m, 4H), 7.12 (dd, 1H, J = 8.8, 1.7 Hz), 6.81 (dd, 4H, J = 8.8, 1.7 Hz), 6.61 (dd, 1H, J = 8.2, 6.3 Hz), 5.77 (d, 1H, J = 16.7 Hz), 4.80-4.82 (m, 1H), 4.05-4.07 (m, 1H), 3.77 (s, 3H), 3.76 (s, 3H), 3.56-3.58 (m, 2H), 2.89 (dt, 1H, J = 13.8, 8.2 Hz), 2.23 (ddd, 1H, J = 13.8, 6.3, 2.7 Hz), 1.98 (d, 1H, J = 3.6 Hz). 5'-protected 4 (0.32 g, 0.50 mmol) in a sealed bottle was dissolved in CH_3CN and coevaporated three times in vacuo. After substituted with argon, 2-cyanoethyl N,N,N',N'-tetraisopropylphosphorodiami dite (160 μL, 0.50 mmol) in CH_3CN (2.2 mL) and 0.45 M 1H-tetrazole in CH_3CN (1.18 μL, 0.50 mmol) were added, and the reaction mixture was stirred at room

temperature for 2 h. Then the reaction mixture was extracted with AcOEt, which was washed with a saturated aqueous solution of $NaHCO_3$, and water. The organic layer was collected, dried over anhydrous sodium sulfate, filtered, and evaporated to dryness under reduced pressure. Then, the crude product 5'-O -(4,4'-dimethoxytrityl)-3-Cyanovinylcarbazole -1'-β -deoxyriboside-3'-O -(cyanoethoxy-N,N –diis opropylamino)phosphoramidite (0.42 g, quant.) in a sealed bottle was dissolved in CH_3CN and coevaporated three times, and was used for automated DNA synthesizer without further purification.

Preparation of ODNs

ODN sequences were synthesized by the conventional phosphoramidite method using an automated DNA synthesizer (3400 DNA synthesizer, Applied Biosystems, CA). The coupling efficiency was monitored with a trityl monitor. The coupling efficiency of a crude mixture of ^{CNV}K showed a 97% yield. The coupling time of a crude mixture of ^{CNV}K was 999 s. They were deprotected by incubation with 28% ammonia for 4 h at 65 °C and purified on a Chemcobond 5-ODS-H column (10 x150 mm) by reverse phase HPLC; elution was with 0.05 M ammonium formate containing 3–25% CH_3CN, linear gradient (30 min) at a flow rate of 2.5 mL min−1. Preparation of ODNs was confirmed by MALDI-TOF-MS analysis. MALDI-TOF-MS: calcd 4547.83 for ODN-1 [(M + H)+], found 4548.95; calcd 4563.83 for ODN-2 [(M + H)+], found 4565.43; calcd 4538.82 for ODN-3 [(M + H)+], found 4538.64; calcd 4538.82 for ODN-4 [(M + H)+], found 4538.57; calcd 4563.83 for ODN-5 [(M + H)+], found 4564.31; calcd 4547.83 for ODN-6 [(M + H)+], found 4546.42; calcd 4587.84 for ODN-7 [(M + H)+], found 4587.58; calcd 6112.09 for ODN-8 [(M + H)+], found 6112.69; calcd 7331.30 for ODN-9 [(M + H)+], found 7333.39; calcd 8511.49 for ODN-10 [(M + H)+], found 8510.55; calcd 6046.05 for ODN-11 [(M + H)+], found 6047.26.

Cell culture and RNA extraction

Pancreatic adenocarcinoma cell lines (BxPC-3 and Capan-1) were purchased from ATCC (VA, US). Cells were cultured with an appropriate medium (RPMI1640) containing 10% FBS, 100 U ml^{-1} penicillin and 100 μg ml^{-1} according to the protocol of ATCC. Total RNAwas extracted from each cell line using the High Pure RNA Isolation Kit (Roche, Switzerland) and subjected to the following experiments.

Real-time RT-PCR

Reverse transcription was performed by the PrimeScript® RT reagent Kit (Takara, Japan) with 0.2 μg of total RNA from cells. Resulting cDNA was subjected to Real-time PCR using an automated real-time PCR system (Smart Cycler®, Takara, Japan) with SYBR Premix Ex Taq II perfect real time (Takara, Japan) and 0.4 μM of primers (K-ras, forward; CTGAATATAAACTTGTGGTAGTTGG, reverse; TGACCTGCTGTGTCGAGAAT, GAPDH, forward; CATGCCAGTGAGCTTCCC GTT, reverse; GTGGAGTCTACTGGCGTCTTC). Inhibition efficiency was estimated from the change in CT values with the normalization using the amounts of GAPDH mRNA estimated from RT-PCR with a GAPDH primer set.

In vitro translation and ELISA

In vitro translation was performed with a rabbit reticulocyte lysate system (Promega, WI, US) with 18 μg of total RNA. The reaction solution was subjected to the Ras GTPase Activation ELISA Kit (Millipore, MA, US) and the chemiluminescence was measured by a microplate reader (Varioskan, Thermo, MA, US).

Cell treatment with ^{cnv}K-AS

Pancreatic adenocarcinoma cell lines (BxPC-3 and Capan-1) were grown in RPMI-1640 (Wako) containing 10% fetal bovine serum (FBS), 100 U/ml penicillin, and 100 μg/ml streptomycin at 37 ºC, 5%CO_2 in a moist atmosphere. Cells were trypsinized and resuspended in Opti-MEM medium without antibiotics and transferred to 96-well plate at a density of 2×10^4 cells per well in a volume of 100 μl and incubate for 24 h (37 ºC, 5%CO_2). Transfection of AS-ODNs containing ^{CNV}K was carried our using Lipofectamine 2000 (Invitrogen) according to the manufacture's protocol. Irradiation was performed by transilluminator (366 nm, Funakoshi).

1.3. Results and Discussion

In this study, I have used the photoresponsive nucleoside analogue, ^{CNV}K. The synthesis of the phosphoramidite of ^{CNV}K is outlined in Scheme X. The various modified ODNs, were prepared, according to standard phosphoramidite chemistry, on a DNA synthesizer using phosphoramidite ^{cnv}K . ODNs containing ^{CNV}K were characterized by MALDI-TOF-MS.

Scheme 1. Synthesis of the Phosphoramidite of 3-Cyanovinylcarbazole Nucleoside.

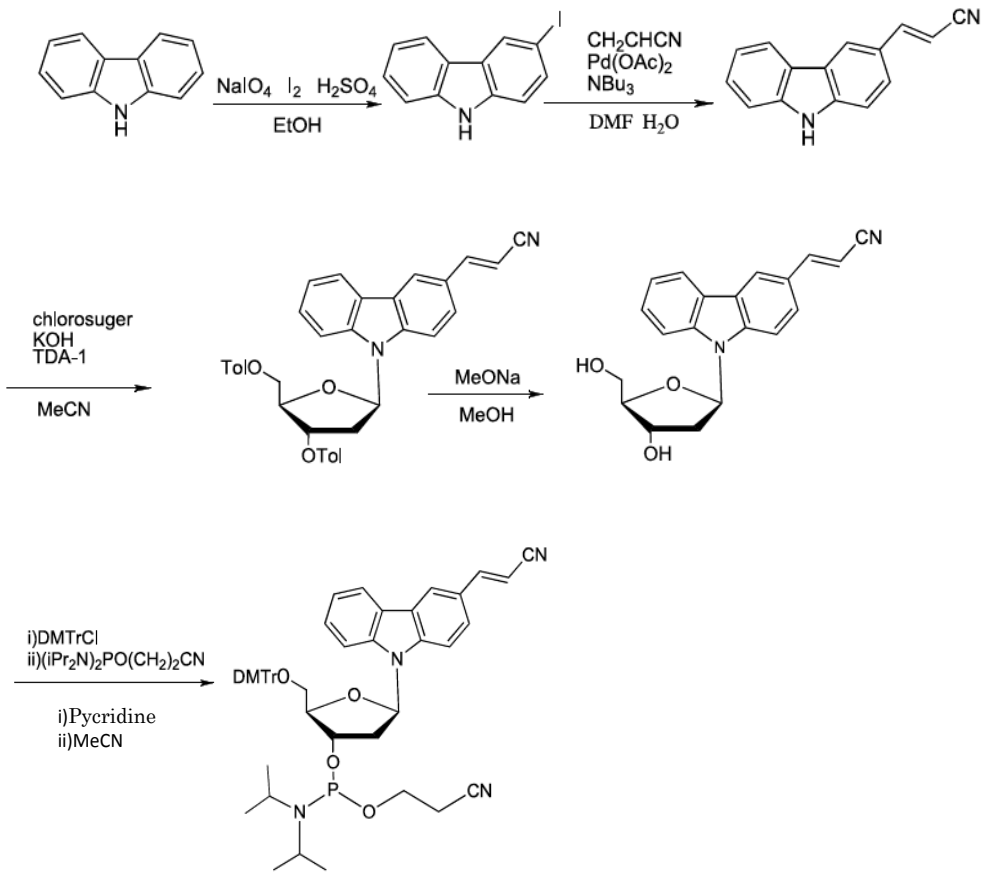

Photocrosslinking property of the AS-ODNs containing ^{CNV}K with synthetic oligoRNAsTo evaluate the selectivity and photoreactivity of ODNs containing ^{CNV}K, ^{CNV}K modified ODNs that have complementary sequences for 6 potential variations of K-ras codon 12 point mutated mRNAs[27] were prepared (Table 1).

Table 1. Oligonucleotides used in this study

Name	Sequence[a]	Target	Mutation variant	Hazard ratio[b]
ORN-wt	GGAGCUGGUGGCGUA		Wild type	—
ORN-1	GGAGCUGUUGGCGUA		G12V	2.56
ORN-2	GGAGCUGC̄UGGCGUA		G12A	—
ORN-3	GGAGCUGĀUGGCGUA		G12D	0.16
ORN-4	GGAGCUAḠUGGCGUA		G12S	0.99
ORN-5	GGAGCUC̄GUGGCGUA		G12R	—
ORN-6	GGAGCUŪGUGGCGUA		G12C	0.98
ODN-1	TACGCCAĀCAXCTCC	ORN-1		
ODN-2	TACGCCAGCAXCTCC	ORN-2		
ODN-3	TACGCCATCAXCTCC	ORN-3		
ODN-4	TACGCCACTAXCTCC	ORN-4		
ODN-5	TACGCCACGAXCTCC	ORN-5		
ODN-6	TACGCCACAAXCTCC	ORN-6		
ODN-7	TACGCCAAXAGCTCC	ORN-1		
ODN-8	TGCCTACGCCAAXAGCTCCA	K-ras mRNA	G12V	
ODN-9	TGCCTACGCCAAXAGCTCCAACTA	K-ras mRNA	G12V	
ODN-10	TGCCTACGCCAAXAGCTCCAACTACCAC	K-ras mRNA	G12V	
ODN-11	CCTTCCTCCTGXCCGGCTCA	VEGFR mRNA		

[a] The under bars indicate the position of mutation and X indicates ^{CNV}K. [b] The values of hazard ratio were reported in ref. 12.

First, I performed UPLC analysis of the 1 : 1 mixture of ODNs and ORNs before and after the 2 s irradiation of UV light (366 nm). As shown in Fig. 2a, peaks identical to the ODN-1 (5.9 min) and ORN-1 (2.8 min) were clearly decreased and a new peak identical to the photo dimer consisting of ODN-1 and ORN-1 (3.2 min) appeared after the UV irradiation. The peaks identical to the ODN-1 and ORN-1 were 75% decreased within 2 s irradiation and a moderate undesired reaction was observed in the case of ORN-wt (Fig. 2b), indicating that the photocrosslinking reaction was selective to the target sequences. This suggests that ODN having ^{CNV}K can crosslink to the complementary RNA with only 2 s photoirradiation and also can discriminate a single base mismatched sequence. The generality of the quick and selective photoreaction to the other ORNs having a potential mutation site of K-ras was evaluated. As shown in Fig. 2c, in the case of most ODNs, photocrosslinking

efficiency was highest in the case of ORNs having full match sequences, although an unspecific reaction was observed.

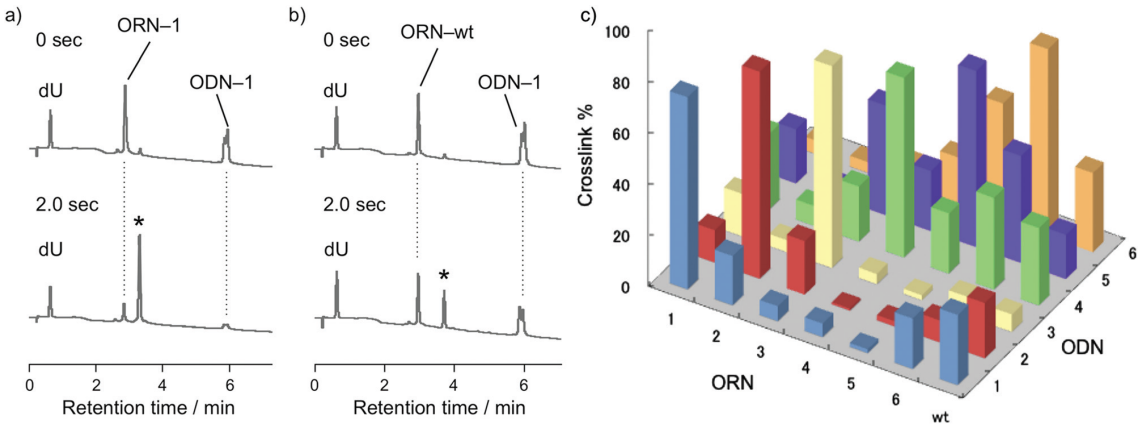

Figure 2. Selective photocrosslinking between the ODNs containing ^{CNV}K and its complementary ORNs. UPLC chromatograms of the mixture of ODN-1 and ORN-1 (a) or ORN-wt (b) before (top) and after (bottom) the 2 s photoirradiation. (c) Crosslinking yields of the ODNs containing ^{CNV}K toward the ORNs after the 2 s photoirradiation. Photoreactions were performed with a 1 : 1 mixture of ODN containing ^{CNV}K and ORN ([ODN] = [ORN] = 2 μM in 50 mM sodium cacodylate buffer (pH 7.4) containing 10 μM 2′-deoxyuridine, 37 °C).

This indicates that the selectivity of the photoreaction is moderate. As shown in Table 2, there was no significant correlation between the selectivity and the difference in thermal stability of the ODN/ORN duplexes or the position of the mismatched site, suggesting that a novel approach is required for clear discrimination of 1 base mismatched RNA sequences.

Improvement of the selectivity of antisense ODN for the G12V variant of K-ras mRNA

As the G12V variant has the highest hazard ratio among all mutation variants at codon 12 of K-ras mRNA (Table 1),[27] it is important that the highly selective crosslinking property of AS-ODN for G12V mutated mRNA is required to avoid the undesired side effect in healthy cells. Therefore, I designed the sequence of ODN to improve the selectivity of antisense ODN for G12V mutated RNA, i.e. ODN-7. ODN-7 has crosslinking ability to the mutated uridine base at the center of codon 12 and the base is guanine in the case of unmutated RNA. To evaluate the selective photocrosslinking property of ODN-7 for mutated K-ras RNA, UPLC (Fig. 3) and PAGE (Fig. 4) analysis were performed.

As shown in Fig. 3a, peaks identical to ODN-7 and ORN-1 clearly disappeared and a new peak (*) having the mass of a photodimer consisting of ODN-7 and ORN-1 (calcd [$(M + K)^+$], 9433.42; found 9433.92) appeared with 1 s irradiation of UV light. These phenomena were not observed in the case of ORN-wt (Fig. 3b and 4), indicating that the ^{CNV}K in the ODN-7 photocrosslinked to the mutated uracil base in ORN-1.

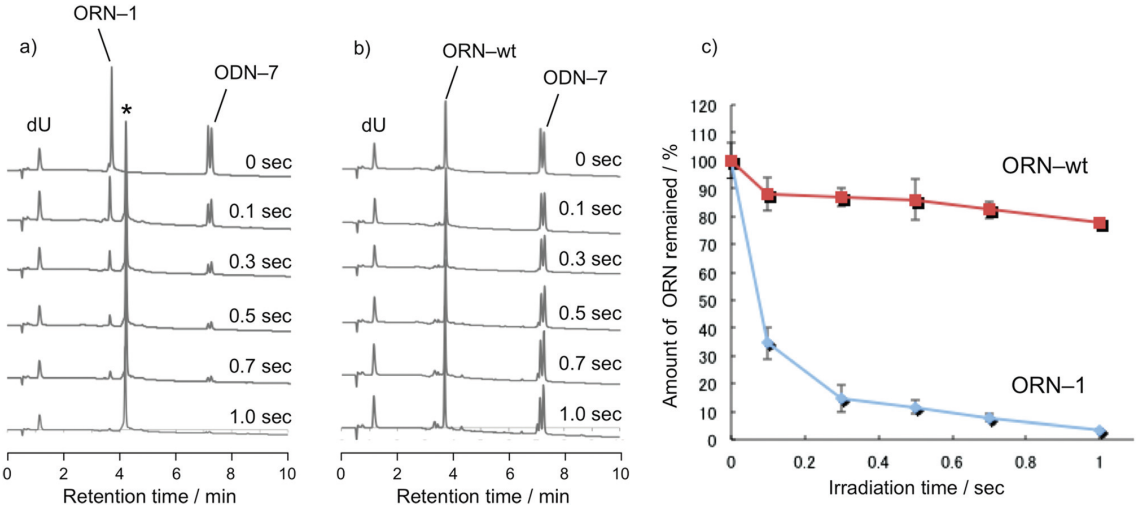

Figure 3. UPLC chromatograms of the mixture of ODN-7 and ORN-1 (a) or ORN-wt (b) at the various photoirradiation time periods. (c) Time course of the remaining ORNs during the photocrosslinking reaction between ODN-7 and ORN-1 (blue) or ORN-wt (red). [ODN-7] = [ORN] = 2 μM in sodium cacodylate buffer (pH 7.4) containing 100 mM NaCl and 10 μM 2′-deoxyuridine (dU) as an internal standard.

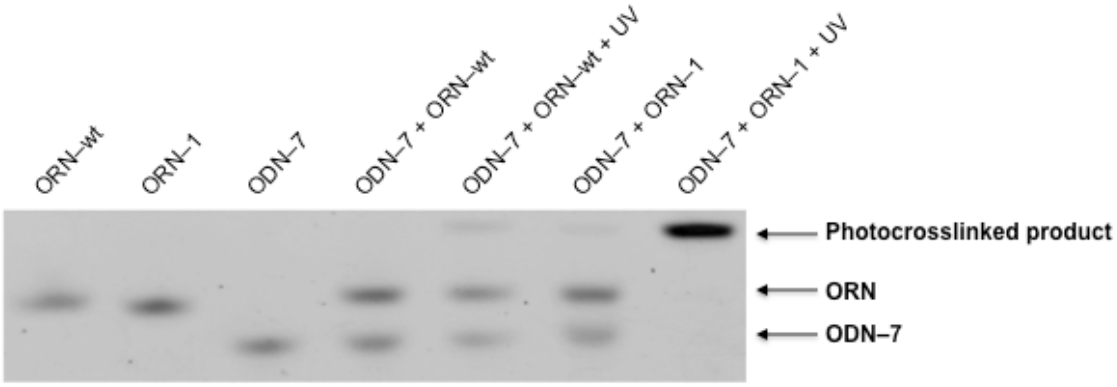

Figure 4. Denatured polyacrylamide gel electrophoresis of the mixture of ODN-7 and ORN-1 before and after the 1 sec photoirradiation. [ODN–7] = [ORN–1] = 1 μM in sodium cacodylate buffer (pH 7.4) containing 100 mM NaCl.

The same point-mutation selective photocrosslinking property was also observed in the case of ODN-8 (Fig. 5), and the photoadduct consists of rU and ^{CNV}K was observed in the enzyme digested products of the photodimer (Fig. 6), suggesting that the photocrosslinked duplex was generated by photoreaction between ^{CNV}K and the mutated uracil base.

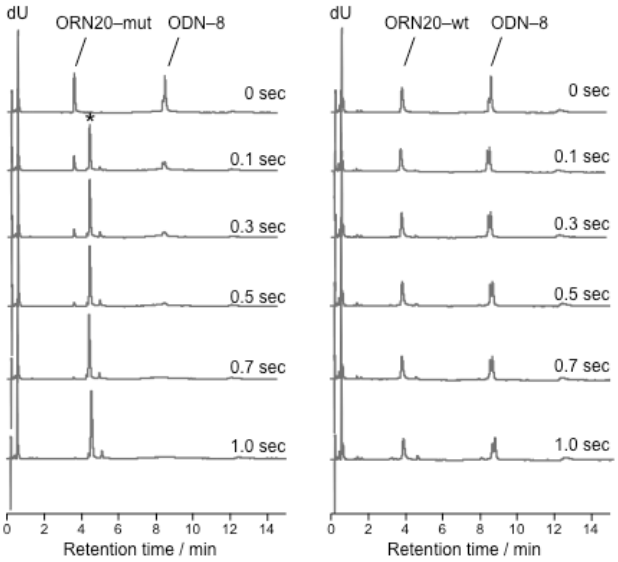

Figure 5. UPLC analysis of the photocrosslinking reaction between ODN–8 and ORN having G12V mutated sequence. [ODN–8] = [ORN] = 2 μM in sodium cacodylate buffer (pH 7.4) containing 100 mM NaCl and 30 μM 2'-deoxyuridine as an internal standard. ORN20–mut, UGGAGCUGUUGGCGUA GGCA; ORN20–wt, UGGAGCUGGUGGCGUAGGCA. Photoirradiation time was indicated on the each chromatograms.

a)

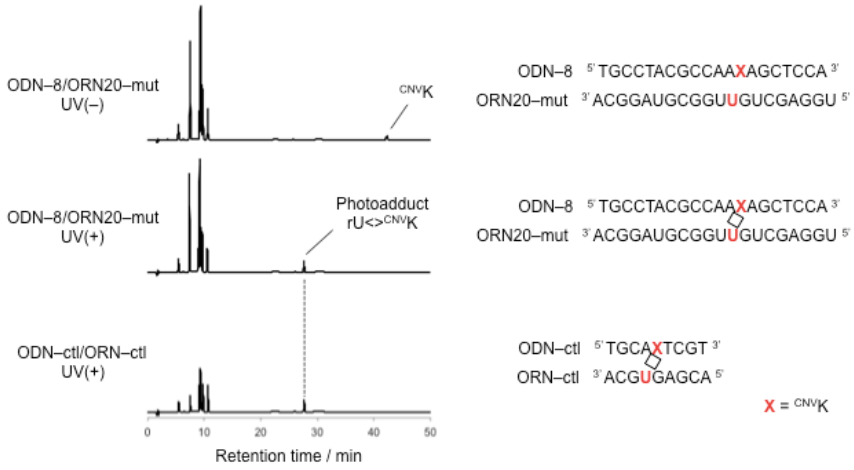

b)

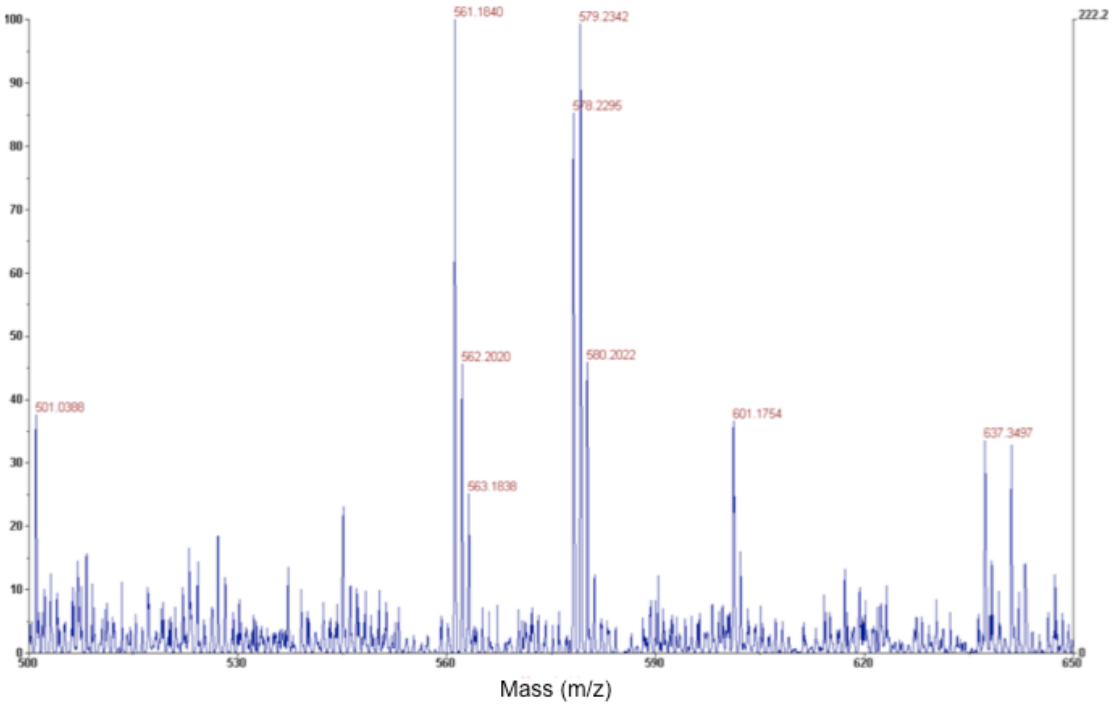

Figure 6. Reversed-phase HPLC analysis of enzyme digested duplexes (a) and MALDI-TOF-MS analysis of the photoadduct (b). ODN/ORN duplexes were treated with P1 nuclease, snake venom phosphodiesterase and calf intestinal alkaline phosphatase, and then subjected to HPLC analysis. ODN-ctl/ORN-ctl was reported that the duplex generate rU<>CNVK photoadduct (Y. Yoshimura et al., ChemBioChem 2009, 10, 1473). Peak generated with the photoirradiation (27 min) was collected and analyzed by MALDI-TOF-MS. rU<>CNVK photoadduct; Calcd. for [(M+H)]+, 579.2085; Found, 579.2342.

Based on this strategy, the selectivity of the photocrosslinking reaction was significantly improved (Table 2).

ODN	T_M with cORN (°C)	T_M with ORN-wt (°C)	% Crosslink With cORN	% Crosslink With ORN-wt	Selectivity[a]
ODN-1	48.5 ± 0.6	41.8 ± 1.2	75	27	2.7
ODN-2	53.8 ± 0.1	39.4 ± 0.8	81	7	11.9
ODN-3	50.6 ± 0.5	48.8 ± 0.6	79	17	4.6
ODN-4	49.5 ± 2.2	46.5 ± 0.6	70	22	3.2
ODN-5	55.5 ± 0.8	41.0 ± 0.2	69	30	2.3
ODN-6	49.8 ± 0.7	42.4 ± 2.2	73	31	2.4
ODN-7	54.0 ± 2.2	52.1 ± 1.6	97	22	4.4

[a] Selectivity was calculated with the following equation: Selectivity = (% crosslink with cORN)/(% crosslink with ORN-wt).

Table 2. T_M, photoreaction yield, and selectivity of ODNs containing ^{CNV}K with complementary ORN (cORN) or ORN-wt

Quick and selective photo-regulation of reverse-transcription activity of G12V point mutated K-ras mRNA extracted from pancreatic cancer cell lines

To prepare the endogenous target mRNA, pancreatic cancer cell lines, BxPC-3 and Capan-1, which have wild type (GGU) and G12V (GUU) mutated sequences at codon 12 of K-ras mRNA, respectively (Fig. 7), were cultured and total RNAs were extracted from each cell line. To evaluate the photoreactivity of ODNs having ^{CNV}K to K-ras mRNAs, the total RNAs were mixed with ODN-8, -9, -10, photoirradiated, and then the mixtures were subjected to real-time reverse transcription polymerase chain reaction (RT-PCR). If the photocrosslinking reaction occurred, the reverse transcription was completely inhibited by the steric hindrance caused by the formation of an irreversible photoadduct.

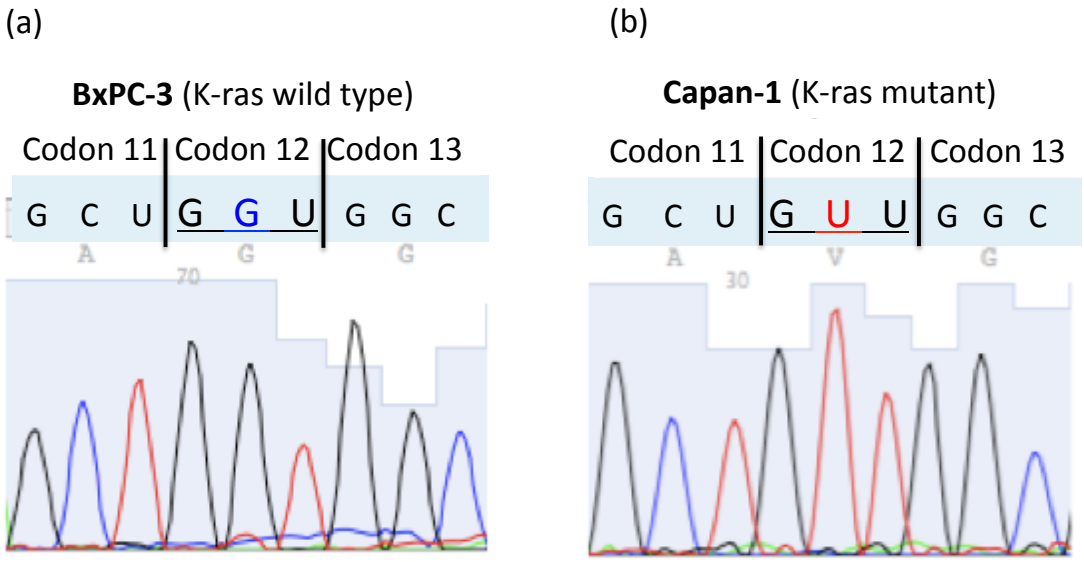

Figure 7. Sequence of K-ras mRNA from BxPC–3 (a) and Capan–1 (b) around codon 12.

As shown in Fig. 8a,c,e, 2 μM ODN-8, -9 or -10 and 1 s UV irradiation caused 38%, 96% or 92% inhibition of reverse transcription, respectively, indicating that the ODN-8, -9 and -10 photocrosslinked to target K-ras mRNA having a point mutated sequence (GUU).

Such inhibition was not observed in the case of total RNA from BxPC-3 having an unmutated K-ras sequence (Fig. 8b,d,f), suggesting that the photocrosslinking reaction is quite selective to GGU to GUU point mutation. The efficient and photoirradiation dependent inhibition was observed in the case of ODN-9 and -10 whose oligonucleotide length was 4 or 8 nucleotides longer than that of ODN-8, respectively, suggesting that the binding affinity of the AS-ODNs to the target mRNA is quite important to the inhibition of the reverse transcription. The photo-induced inhibition was also observed in the presence of 10 μM of the ODNs, although the moderate inhibition was observed in the case without photoirradiation. This indicates that the antisense effect was not dependent on the photoreaction that occurred in such a high concentration of ODN

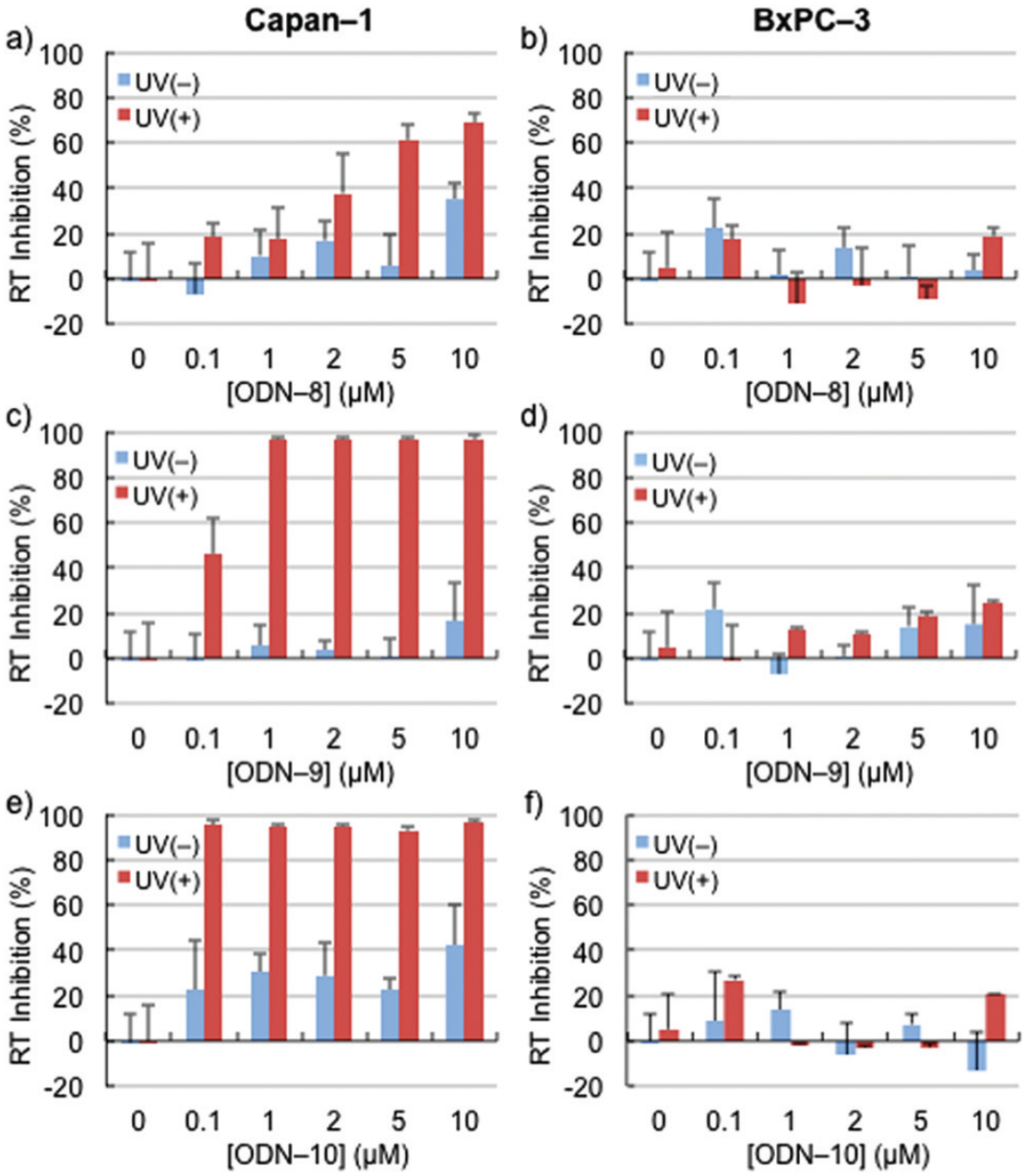

Figure 8. Selective inhibition of reverse transcription activity of K-ras mRNA extracted from Capan-1 (a, c, e) or BxPC-3 (b, d, f) by ODN-8 (a, b), -9 (c, d) and -10 (e, f). Inhibition % was calculated from the C_T values of the amplification curves of real-time PCR. The CT values were normalized with the CT values of the amplification curves of GAPDH in the same mixture of ODN-8 and total RNA. Error bar = standard deviation (n = 3).

The same inhibition effect of the reverse transcription of K-ras mRNA was reported using 2′-Opsoralen modified 15 nt AS-ODNs, and the concentration required for 40% inhibition was 400 nM.[19-21] In our cases, 2 μM of 20 nt AS-ODN (ODN-8) was required for 40% inhibition efficiency, indicating that our ODN requires at least 5-fold high concentrations of AS-ODN to regulate the mRNA function with the same oligonucleotide length of AS-ODN. As the ^{CNV}K does not have hydrogen bonding ability to the nucleobase in the target mRNA, it seems that the relatively low affinity of our AS-ODN leads to the requirement of a high concentration of ODNs. The 100 nM ODN-9 (24 nt) inhibited 50% of the reverse transcription, indicating that the disadvantage mentioned above can easily be overcome by controlling the oligonucleotide length of the AS-ODNs. The photoirradiation time for the regulation of reverse transcription was shorter, only 1 s, compared with 2′-Opsoralen modified AS-ODNs that required 10 min photoirradiation for 40% inhibition of the reverse transcription, indicating that AS-ODNs containing CNVK can much more quickly photocrosslink to RNAs compared with 2′-O-psoralen modified AS-ODNs. These results also suggest that the photocrosslinking reaction occurs not only in the case of ORN but also in the case of mRNA. Compared with some other crosslinkable ODNs, such as ODNs containing 2-amino-6-vinylpurine nucleoside,[28-29] it takes hours of incubation for 50% conversion of the crosslinking reaction, our photocrosslinkable ODNs are superior for the quick regulation of the mRNA functions. The same photoinduced inhibition of reverse transcription using our photocrosslinkable ODN was also observed in the case of the vascular endothelial growth factor receptor (VEGFR) mRNA and its complementary ODN containing ^{CNV}K (ODN-11), indicating that the photocrosslinking strategy is effective not only in the case of K-ras mRNA but also other mRNA (Fig. 9).

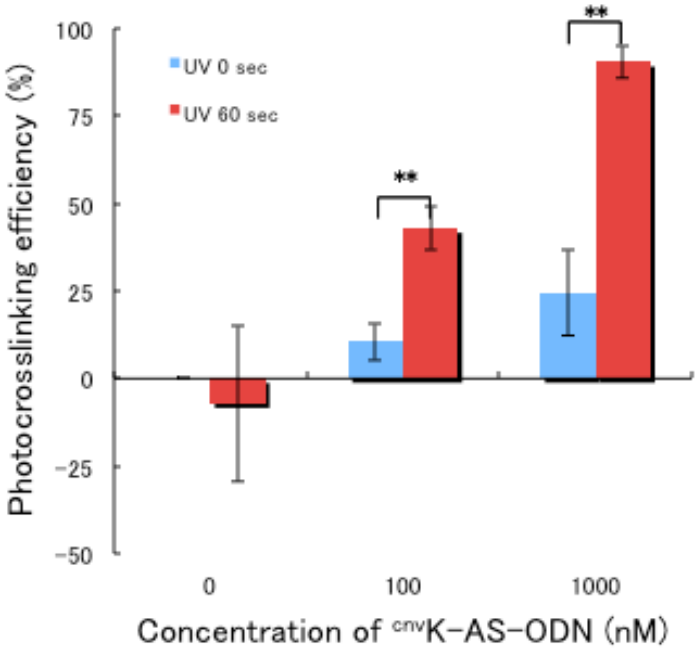

Figure 9. Photocrosslinking efficiency of ODN-11 with VEGF mRNA estimated by inhibition of reverse transcription of VEGF mRNA.

Quick and selective photo-regulation of translation activity of G12V point mutated K-ras mRNA extracted from pancreatic cancer cell lines.

To assess the feasibility of ODN having ^{CNV}K for the regulation of K-ras protein expression, an in vitro translation study was performed using the rabbit reticulocyte lysate system. Total RNA from Capan-1 or BxPC-3 was irradiated with ODN-8 and subjected to the in vitro translation system. Then translated K-ras protein was quantified by the ELISA system. As shown in Fig. 10, UV irradiation in the presence of ODN-8 clearly decreases the amount of translated K-ras protein when using the total RNA from Capan-1 that has G12V point mutation on the codon 12 of K-ras gene. Such a decrease was not observed without the UV irradiation, indicating that the photocrosslinking reaction between ODN-8 and K-ras mRNA is a key factor in this down regulation. Such a photo-induced down regulation was not observed in

the case of the total RNA from BxPC-3 that has an unmutated K-ras gene, indicating that the ODN-8 selectively photocrosslinks to mutated K-ras mRNA, and inhibits the translation as expected. The strategy, that targeted the mutated uridine base at the center of codon 12 of K-ras mRNA as a photocrosslinking site of the photoreactive ODNs containing trioxalen as a photoreactive moiety, was previously reported by Higuchi et al.[19-21] They successfully regulated the expression of the K-ras gene in cells with the photoirradiation, however, the photoreactivity of their ODNs is much lower than that of our photoreactive ODNs containing ^{CNV}K. This suggests that the ODNs containing ^{CNV}K enable the effective photodynamic antisense therapy with quicker UV treatment compared with that of the reported photoreactive ODNs.

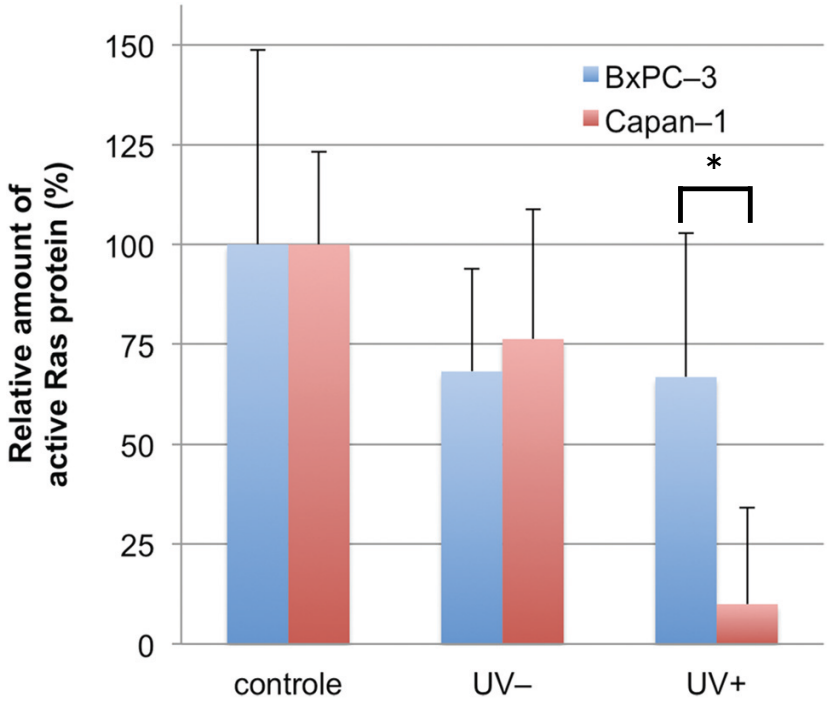

Figure 10. Photo-regulation of the in vitro translation of active K-ras proteins using ODN-8. The error bars indicate the standard error of the mean. * $P < 0.05$.

Selective inhibition of growth of pancreatic cancer cell lines by ^{cnv}K-AS

Using BxPC-3 cells (K-ras wild type) and Capan-1 (K-ras mutant type) cells, the possible selective anti-proliferative of ^{cnv}K-AS was examined. Twenty-four hours after transfection, phosphorothioate modified ODN 9 (ODN 9) significantly inhibited the growth of Capan-1 cells by only after UV irradiation ($P < 0.05$). When compared to BxPC-3 cells, the cytostatic activity of phosphorothioate modified ODN 9 on Capan-1 cells was higher (Fig 11). Therefore, I achieved sequence selective photo-regulation of cancer cell growth by using ODN containing ^{CNV}K.

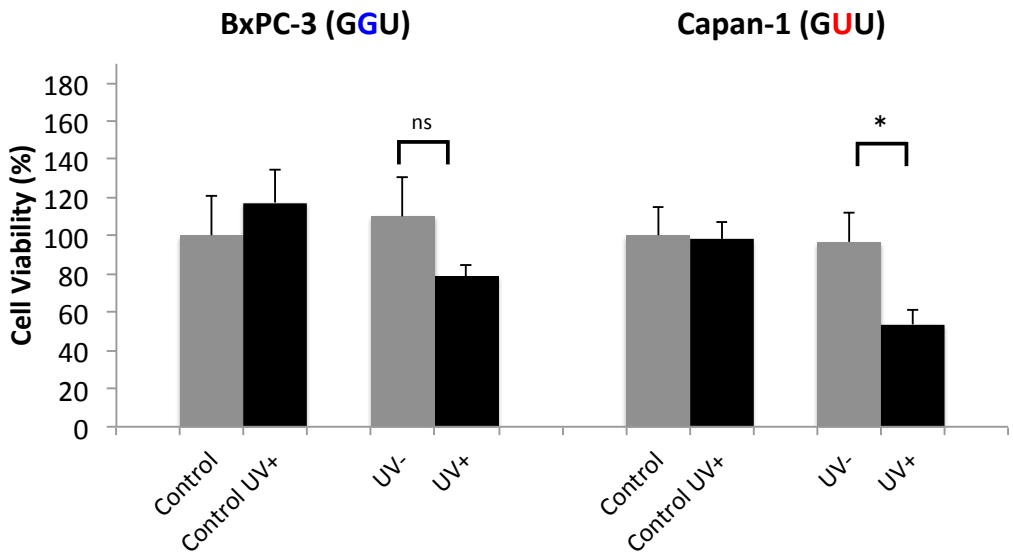

Figure 11. Selective cytostatic activity of ^{cnv}K-AS (nucleoside phosphorothioate)s on the proliferation of human pancreatic cell line. ODN9 (phosphorothioate modified) was 100 nM. Error bar = standard deviation (n = 3). (ns=not significant, *P < 0.05)

1.4. Conclusions

In this study, I demonstrated that the ODNs containing ^{CNV}K are quickly and selectively photocrosslinked to ORNs having mutated K-ras sequences by a few seconds of photoirradiation and that the selectivity can be enhanced by adopting the mutated pyrimidine base as the photocrosslinking site of ^{CNV}K. RT-PCR experiments revealed that the ODN having ^{CNV}K clearly photocrosslinks to its target mRNA in a sequence selective manner and then the function of mRNA as the substrate of reverse transcriptase is clearly regulated with only 1 s photoirradiation. In addition, the translation activity of target mRNA is clearly inhibited by photoirradiation, suggesting that ODNs having ^{CNV}K have the potential to be effective photodynamic antisense drugs that act at desired locations around the body with a few seconds of photoirradiation.

1.5. References

1. Miller, P. S. , Braiterman L. T., and Ts'o, P. O. Effects of a trinucleotide ethyl phosphotriester, Gmp(Et)Gmp(Et)U, on mammalian cells in culture. *Biochemistry*. **1977**, 16, 1988-1996.
2. Zamecnik, P. C., and Stephenson, M. L. Inhibition of Rous sarcoma viral RNA translation by a specific oligodeoxyribonucleotide. *Proc. Natl. Acad. Sci. U. S. A.* **1978**, 75, 285-288.
3. Marcus-Sekura, C., Woerner, A. M., Shinozuka, K., Zon G., and. Quinnan, G.V.Jr. Comparative inhibition of chloramphenicol acetyltransferase gene expression by antisense oligonucleotide analogues having alkyl phosphotriester, methylphosphonate and phosphorothioate linkages. *Nucleic Acids Res.* **1987**, 15, 5749-5763.
4. Cazenave, C., *et al.* Comparative inhibition of rabbit globin mRNA translation by modified antisense oligodeoxynucleotides. *Nucleic Acids Res.* **1989**, 17, 4255-4273.
5. Nielsen, P. E., Egholm, M., Berg R. H., and Buchardt, O. Sequence-selective recognition of DNA by strand displacement with a thymine-substituted polyamide. *Science.* **1991**, 254, 1497-1500.
6. Kaihatsu, K. Huffman K. and Corey, D. R. Intracellular uptake and inhibition of gene expression by PNAs and PNA-peptide conjugates. *Biochemistry*, **2004**, 43, 14340-14347.
7. Shiraishi T., and Nielsen, P. E., Nanomolar cellular antisense activity of peptide nucleic acid (PNA) cholic acid ("umbrella") and cholesterol conjugates delivered by cationic lipids. *Bioconjugate Chem*. **2012**, 23, 196-202.
8. Koshikin, A.A., et al. LNA (Locked Nucleic Acids): Synthesis of the Adenine, Cytosine, Guanine, 5-Methylcytosine, Thymine and Uracil Bicyclonucleoside Monomers, Oligomerisation, and Unprecedented Nucleic Acid Recognition. *Tetrahedron*, **1998**, 54, 3607-3630.
9. S. Obika, D. Nanbu, Y. Hari, J. Andoh and K. Morio, Stability and Structural Features of the Duplexes Containing Nucleoside Analogues with a Fixed N-type Conformation, 2'-O,4'-C-Methyleneribonucleosides. *Tetrahedron Lett.* **1998**, 39, 5401-5404.

10. Singh, S.K., Kumar, R., and Wengel, J. Synthesis of 2-amino-LNA: a novel conformationally restricted high-affinity oligonucleotide analogue with a handle. *J. Org. Chem.* **1998**, 63, 10035-10039.
11. Kurnar, R., Singh, S.K., Koshkin, A.A., Rajwanshi V.K., and Meldgaard, M. The first analogues of LNA (locked nucleic acids): Phosphorothioate-LNA and 2'-thio-LNA. *Bioorg. Med. Chem. Lett.* **1998**, 8, 2219-2222.
12. Wahlestedt, C., *et al.* Potent and nontoxic antisense oligonucleotides containing locked nucleic acids. *Proc. Natl. Acad. Sci. U. S. A.* **2000**, 97, 5633-5638.
13. Monia, B. P., Johnston, J. F., Geiger, T., Muller M., and Fabbro, D. Antitumor activity of a phosphorothioate antisense oligodeoxynucleotide targeted against C-*raf* kinase. *Nat. Med.* **1996**, 2, 668-675.
14. Yin, H., Betts, C., Saleh, A.F., Ivanova, G.D., Lee, H., Seow, Y., Kim, D., Gait M.J., and Wood, M. J. Optimization of peptide nucleic acid antisense oligonucleotides for local and systemic dystrophin splice correction in the mdx mouse. *Mol. Ther.* **2010**, 18, 819-827.
15. Straarup, E. M., et al. Short locked nucleic acid antisense oligonucleotides potently reduce apolipoprotein B mRNA and serum cholesterol in mice and non-human primates. *Nucleic Acids Res.* **2010**, 38, 7100-7111.
16. Tallafuss, A., Gibson, D., Morcos, P., Li, Y., Seredick, S., Eisen J., and Washbourne, P. Turning gene function ON and OFF using sense and antisense photo-morpholinos in zebrafish. *Development.* **2012**, 139, 1691-1699.
17. Matsunaga, D., Asanuma H., and Komiyama, M. Photoregulation of RNA digestion by RNase H with azobenzene-tethered DNA. *J. Am. Chem. Soc.* **2004**, 126, 11452-11453.
18. Asanuma, H., Liang, X., Nishioka, H., Matsunaga, D., Liu M., and Komiyama, M. Synthesis of azobenzene-tethered DNA for reversible photo-regulation of DNA functions: hybridization and transcription. *Nat. Protoc.* **2007**, 2, 203-312.
19. Higuchi, M., Yamayoshi, A., Yamaguchi, T., Iwase, R., Yamaoka, T., Kobori A., and Murakami, A. Selective Photo-Cross-Linking of 2'-O-Psoralen-Conjugated Oligonucleotide with Rnas Having Point Mutations. *Nucleosides, Nucleotides Nucleic Acids.* **2007**, 26, 277-290.
20. Higuchi, M., Kobori, A., Yamayoshi A., and Murakami, A. Synthesis of antisense oligonucleotides containing 2'-O-psoralenylmethoxyalkyladenosine

for photodynamic regulation of point mutations in RNA. *Bioorg. Med. Chem*. **2009**, 17, 475-483.

21. Higuchi, M., Yamayoshi, A., Kato, K., Kobori, A., Wake N., and Murakami, A. Specific regulation of point-mutated K-ras-immortalized cell proliferation by a photo-dynamic antisense strategy. *Oligonucleotides.* **2010**, 20, 37-44.
22. Yoshimura, Y. and Fujimoto, K. Ultrafast reversible photo-cross-linking reaction: toward in situ DNA manipulation. *Org. Lett.* **2008**, 10, 3227-3230
23. Fujimoto, K., Hiratsuka-Konishi, K., Sakamoto T., and Yoshimura, Y. Site-specific cytosine to uracil transition by using reversible DNA photo-crosslinking. *ChemBioChem*. **2010**, 11, 1661-1664.
24. Fujimoto, K., Hiratsuka-Konishi, K., Sakamoto, T., Ohtake, T., Shinohara K., and Yoshimura, Y. Specific and reversible photochemical labeling of plasmid DNA using photoresponsive oligonucleotides containing 3-cyanovinylcarbazole. Mol. Biosyst. **2012**, 8, 491-494.
25. Yoshimura, Y. Ohtake, T. Okada H. and Fujimoto, K. A new approach for reversible RNA photocrosslinking reaction: application to sequence-specific RNA selection.*ChemBioChem,* **2009**, 10, 1473-1476.
26. Fujimoto, K., Hiratsuka-Konishi, K., Sakamoto T., and Yoshimura, Y. Quick, Selective and Reversible Photocrosslinking Reaction between 5-Methylcytosine and 3-Cyanovinylcarbazole in DNA Double Strand. *Chem. Commun*. **2010**, 40, 7545-7547.
27. Watanabe, M., Nobuta, A., Tanaka J., and Asaka, M. An effect of K-*ras* gene mutation on epidermal growth factor receptor signal transduction in PANC-1 pancreatic carcinoma cells. *Int. J. Cancer*. **1996**, 67, 264-268.
28. Winder, T., et al. Different types of K-Ras mutations are conversely associated with overall survival in patients with colorectal cancer. *Oncol. Rep.* **2009**, 21, 1283-1287.
29. Taniguchi, Y., Kurose, Y., Nishioka, T., Nagatsugi F., and Sasaki, S. The alkyl-connected 2-amino-6-vinylpurine (AVP) cross-linking agent for improved selectivity to the cytosine. *Bioorg. Med. Chem.* **2010**, 18, 2894-2901.

30. Imoto, S., Hori, T., Hagihara, S., Taniguchi, Y., Sasaki S., and Nagatsugi, F. Bioorg. Alteration of Cross-linking Selectivity with the 2'-OMe Analogue of 2-Amino-6-Vinylpurine and Evaluation of Antisense Effect. *Bioorg. Med. Chem. Lett.* **2010**, 20, 6121-1624.

Chapter 2

Photochemical regulation of RNA functions in cell by cyanovinyl-carbazole mediated photocrosslinking

2.1. Introduction

3-Cyanovinylcarbazole nucleoside contained in oligonucleotide can be effectively photocrosslinked to the pyrimidine base in complementary RNA strands by a few seconds of photo irradiation. Here I report the potential of the photocrosslinkable antisense oligonucleotide containing 3-Cyanovinylcarbazole nucleoside (^{cnv}K-AS) for gene regulation in cells. I demonstrate that a ^{cnv}K-AS that targets GFP mRNA disrupts GFP in transfected cells by a few seconds of photoirradiation.

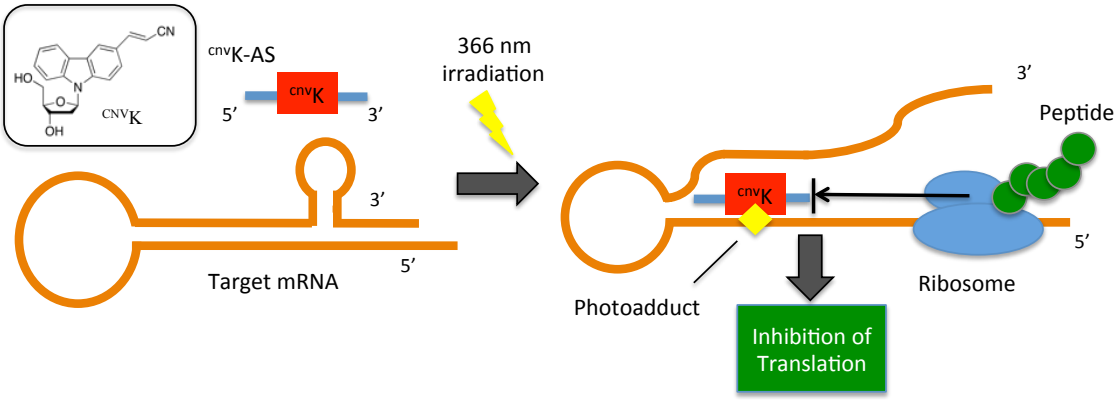

Figure 1. Schematic drawing of GFP gene regulation by photoreaction

In the antisense method, the antisense oligonucleotide (AS-ODN) is required to have high affinity and specificity for the target mRNA[1]. Hence, a number of studies have reported on chemically modified antisense oligonucleotides, such as phosphorothioates,[2] peptide nucleic acids[3] and bridged (locked) nucleic acids[4,5]. Besides, several photoresponsive AS-ODNs have been reported, as exemplified by photo caged AS-ODNs that hybridized with complementary caging ODN (ccODN) having a photocleavable temporary block of the binding capability[6] or an azobenzene moiety that can control the stability of the AS-ODN/ccODN duplex by photoisomerization[7]. Moreover, photocrosslinkable antisense oligonucleotides containing psoralen have been reported by Higuchi *et al*[8]. Because of the specific and irreversible complexation between psoralen-conjugated oligodeoxy nucleotides

and the target mRNA, the regulation of gene expression was achieved with a low concentration of AS-ODN (IC_{50} = 50 nM) and UV irradiation. However, this method requires relatively long photoirradiation because the low photoreactivity of AS-ODN may cause undesired toxicity to healthy cells. On the other hand, we previously reported on photoresponsive synthetic oligonucleotides containing 3-Cyanovinylcarbazole nucleoside (^{cnv}K), which can photocrosslink to complementary DNA or RNA strand via [2+2] photocycloaddition between the ^{cnv}K and pyrimidine base in the complementary strand with a few second of 366 nm irradiation[9] . We reported that the ODN having ^{CNV}K clearly photocrosslinks to the target mRNA extracted from cells in a sequence selective manner and then the function of mRNA as the substrate of reverse transcriptase is clearly regulated with only 1 second of photoirradiation. In addition, the translation activity of the target mRNA is clearly inhibited by photoirradiation[10]. However, the efficiency of ^{CNV}K-AS in cell culture models remains to be investigated. Therefore, in this study, I evaluated the effect of regulating the gene expression of GFP stably expressed in HeLa cells by ^{CNV}K-AS.

2.2. Materials and methods

General methods

Mass spectra were recorded on a Voyager-DE PRO-SF, Applied Biosystems. Irradiation was performed by UV-LED (366 nm, 1600 mW cm^{-2}; ZUV, OMRON, Japan). HPLC was performed on a Chemcobond 5-ODS-H column (10 x 150 mm, 4.6 x 150 mm) or a Chemcosorb 5-ODS-H column (4.6 x 150 mm) with a JASCO PU-980, HG-980-31, DG-980-50 system equipped with a JASCO UV 970 detector at 260 nm. Reagentsfor the DNA synthesizer such as A, G, C, T-β-cyanoethyl phosphoramidite,and CPG support were purchased from Glen Research. Oligo RNAs were purchased from Fasmac (Japan) and used without further purification.

Denaturing polyacrylamide gel electrophoresis

For analysis of the sizes of DNA nanostructures by gel electrophoresis, sample solutions were diluted by 7 M Urea in formamide. Loading samples were prepared with an appropriate amount of 6x loading buffer [36% (v/v) glycerol, 30 mM EDTA and 0.05% (w/v) each of bromophenol blue and xylene cyanol] and loaded onto gels prepared with 15% polyacrylamide (29:1, polyacrylamide: bisacrylamide) containing 7 M Urea and running buffer (1 x TBE). The gels were run at 180 V on a gel electrophoresis apparatus (Bio-RAD). After electrophoresis, the gels were stained with SYBRgold (Molecular Probe) and imaged on an Imaging System LAS-3000 (FUJIFILM Inc.).

Preparation of ODNs

ODN sequences were synthesized by the conventional phosphoramidite method using an automated DNA synthesizer (3400 DNA synthesizer, Applied Biosystems, CA). The coupling efficiency was monitored with a trityl monitor. The coupling efficiency of a crude mixture of ^{CNV}K showed a 97% yield. The coupling time of a

crude mixture of ^{CNV}K was 999 s. They were deprotected by incubation with 28% ammonia for 5 h at 65 °C and purified on a Chemcobond 5-ODS-H column (10 x 150 mm) by reverse phase HPLC; elution was with 0.05 M ammonium formate containing 1–25% CH_3CN, linear gradient (40 min) at a flow rate of 3 mL min^{-1}. Preparation of ODNs was confirmed by MALDI-TOF-MS analysis. MALDI-TOF-MS: calcd 8020.77 for ^{cnv}K-AS (a-2) [$(M + H)^+$], found 8020.51; calcd 7996.76 for ^{cnv}K-AS (a-14) [$(M + H)^+$], found 7997.45; calcd 7913.73 for AS (a-con) [$(M + H)^+$], found 7913.48; calcd 8020.77 for ^{cnv}K-AS (a-invert) [$(M + H)^+$], found 8018.87; calcd 8037.74 for ^{cnv}K-AS (b-2) [$(M + H)^+$], found 8037.41; calcd 7995.72 for AS (b-con) [$(M + H)^+$], found 7996.88; calcd 8247.78 for ^{cnv}K-AS (c-2) [$(M + H)^+$], found 8247.92; calcd 8140.74 for ^{cnv}K-AS (c-con) [$(M + H)^+$], found 8303.78. ^{cnv}K-AS (d-2) [$(M + H)^+$], found 8300.48; calcd 8211.74 for ^{cnv}K-AS (d-con) [$(M + H)^+$], found 8216.00.

Cell culture and Cell treatment with ^{cnv}K-AS

HeLa-GEP cell lines were purchased from Cell Biolabs, Inc. HeLa-GFP cells were grown in Dulbecco'MEM (Life technologies) containing 10% fetal bovine serum (FBS), 100 U/ml penicillin, and 100 μg/ml streptomycin at 37 ºC, 5%CO_2 in a moist atmosphere. Cells were trypsinized and resuspended in Opti-MEM medium without antibiotics and transferred to 96-well plate at a density of 2×10^4 cells per well in a volume of 100 μl and incubate for 24 h (37 ºC, 5%CO_2). Transfection of ^{cnv}K-ASs was carried our using Lipofectamine RNAi MAX (Invitrogen) according to the manufacture's protocol.

Real-time RT-PCR analysis.

Total RNA was extracted using CellAmp^{TM} Direct RNA Prep Kit (Takara) and Reverse transcription was performed by the PrimeScript® RT reagent Kit (Takara, Japan) according to the manufacturer's instructions. Resulting cDNA was subjected

to Real-time PCR using an automated real-time PCR system (Smart Cycler®, Takara, Japan) with SYBR Premix Ex Taq II perfect real time (Takara, Japan) and 0.4 μM of primers (Sequences of the primers used for PCR are listed in Table 1). Inhibition efficiency was estimated from the change in C_T values with the normalization using the amounts of GAPDH mRNA estimated from RT-PCR with a GAPDH primer set.

Table 1. Primers were used in the study for qRT-PCR

Name	Direction	Primer (5'-3')	Used for
GFP a (f)	Forward	ATGGTGAGCAAGGGCGAG	Amplification for target site A
GFP a (r)	Reverse	GTGGTGCAGATGAACTTC	
GFP b,c,d (f)	Forward	CAACAGCCACAACGTCTATATC	Amplification for target site B
GFP b,c,d (r)	Reverse	AACTCCAGCAGGACCATGTGAT	or target site C or target site D
GAPDH (f)	Forward	CATGCCAGTGAGCTTCCCGTT	
GAPDH (r)	Reverse	GTGGAGTCTACTGGCGTCTTC	

Confocal microscopy

Confocal microscopy was carried out using a Nikon confocal laser scanning microscope (C2Si). All images were taken using a x10 objective lens. GFP fluorescence was excited at a wavelength of 488 nm and detected at 525 nm, pinhole radius of 30.00 μm. For fluorescence images, identical operation Monochrome images generated with charge-couple device (CCD) camera were pseudocolored to the appropriate color. Following confocal microscopy, image analysis was performed using NIS-Elements AR 3.2. The mean fluorescence intensity of equally divided squares for each channel was calculated.

2.3. Results and discussion

Photocrosslinking properties of ^{cnv}K-ASs

In this study, I adopted a phosphorothioate backbone modification to protect ^{CNV}K-AS from cellular nucleases degradation. Before evaluation in cells, to evaluate the photoreactivity of phosphorothioate ^{CNV}K-AS, I performed denaturing PAGE analysis of the 1 : 1 mixture of ^{CNV}K-ASs and complementary oligo RNA (ORN)s after the UV irradiation. ^{CNV}K-ASs that have complementary sequences for 4 different GFP mRNA target sites (Fig. 2) were prepared (Table 2). ^{cnv}K-ASs is low identity (76% or less) sequence relative to other mRNA.

Table 2. Oligonucleotides used in this study

Name	Sequence[a]	Target	T_M With Target ORN (ºC)
AS (a-con)	ACCACCCCGGTGACCAGCTCCTCGC	ORN-a	69.4±0.6
^{cnv}K-AS (a-2)	AXCACCCCGGTGAACAGCTCCTCGC	ORN-a	67.0±0.5
^{cnv}K-AS (a-14)	ACCACCCCGGTGAXCAGCTCCTCGC	ORN-a	64.5±0.5
^{cnv}K-AS (a-6-G)	ACCACXCCGGTGAACAGCTCCTCGC	ORN-a	65.8±0.8
^{cnv}K-AS (a-2-invert)	CGCTCCTCGACAAGTGGCCCCACXA	-	n.d.[b]
AS (b-con)	AGTTCACCTTGATGCCGTTCTTCTG	ORN-b	55.6±0.6
^{cnv}K-AS (b-2)	AXTTCACCTTGATGCCGTTCTTCTG	ORN-b	52.3±0.4
AS (c-con)	ACTGGGTGCTCAGGTAGTGGTTGTC	ORN-c	59.3±0.6
^{cnv}K-AS (c-2)	AXTGGGTGCTCAGGTAGTGGTTGTC	ORN-c	57.6±0.6
AS (d-con)	ATGGGGGTGTTCTGCTGGTAGTGGT	ORN-d	67.3±0.0
^{cnv}K-AS (d-2)	AXGGGGGTGTTCTGCTGGTAGTGGT	ORN-d	65.4±0.3
ORN-a	GCGAGGAGCUGUUCACCGGGGUGGU		
ORN-b	CAGAAGAACGGCAUCAAGGUGAACU		
ORN-c	GACAACCACUACCUGAGCACCCAGU		
ORN-d	UGACCCACGAGUCCAUCACCAACAG		

[a] X indicates ^{cnv}K

[a] T_M values were determined from UV melting curves of the duplex ([Duplex] = 0.5 μM in 50 mM soduim cacodylate (pH 7.4) containing 100 mM NaCl). [b] Not determined.

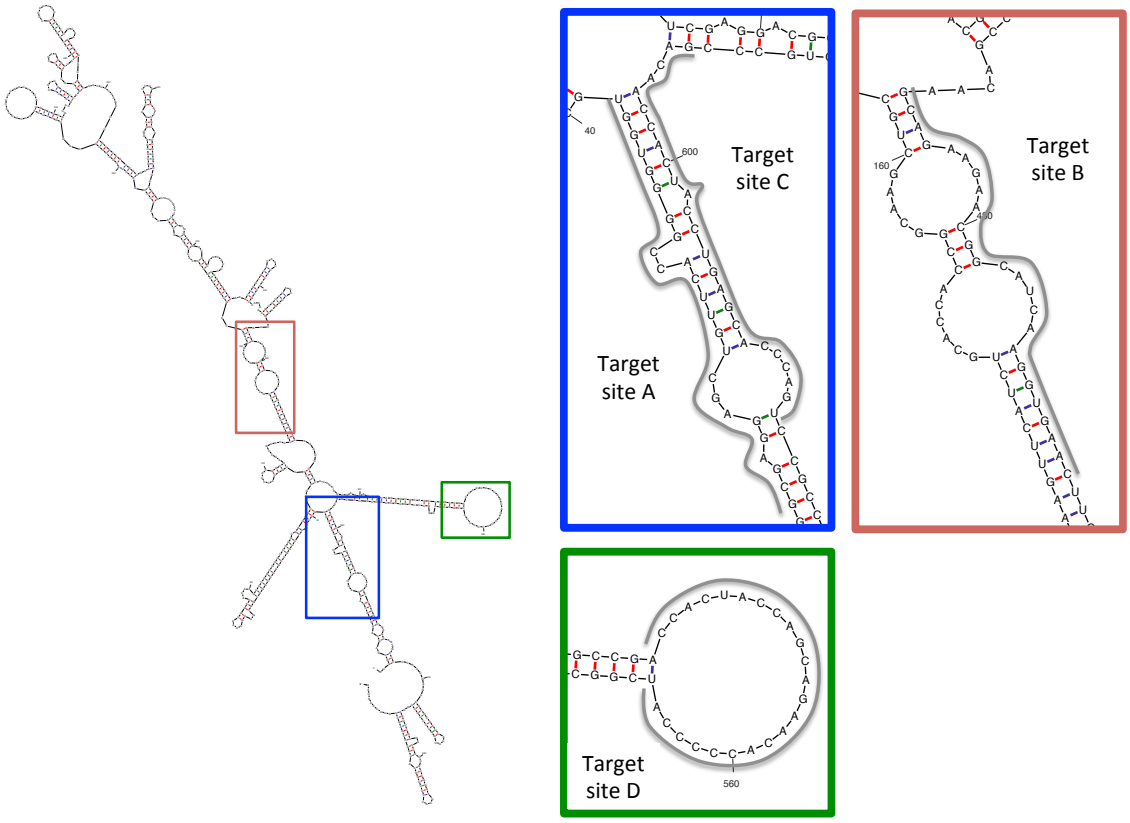

Figure 2. GFP mRNA secondary structure

^{CNV}K-AS (a-2), ^{CNV}K-AS (a-14) and ^{CNV}K-AS (a-6-G) were complementary to 14 nt~38 nt (Target Site A). ^{CNV}K-AS (a-2) and ^{CNV}K-AS (a-14) was including ^{CNV}K in the second-base position and the fourteenth-base position from 5', respectively. As a result of PAGE analysis, ORN-a and ^{CNV}K-AS (^{CNV}K-AS (a-2) or ^{CNV}K-AS (a-14)) clearly disappeared and a band having mobility of about 40 nt appeared after UV irradiation (Fig. 3a,b). In addition, after the UV irradiation for 5 seconds, conversion of ORN-a did not confirm the remarkable difference in case of comparing ^{CNV}K-AS (a-2) with ^{CNV}K-AS (a-14) (Fig. 3e). On the other hand, these phenomena were not observed in the case of ^{CNV}K-AS (a-6-G) and ^{CNV}K-AS (a-2-invert) (Fig 3c,d). ^{CNV}K-AS (a-6-G) was included ^{CNV}K in sixth-base position from 5'. This ^{CNV}K-AS has no crosslinking ability to the complementary sequence because ^{CNV}K cannot crosslink to guanine. ^{CNV}K-AS (a-2-invert) is inverted control of ^{CNV}K-AS (a-2).

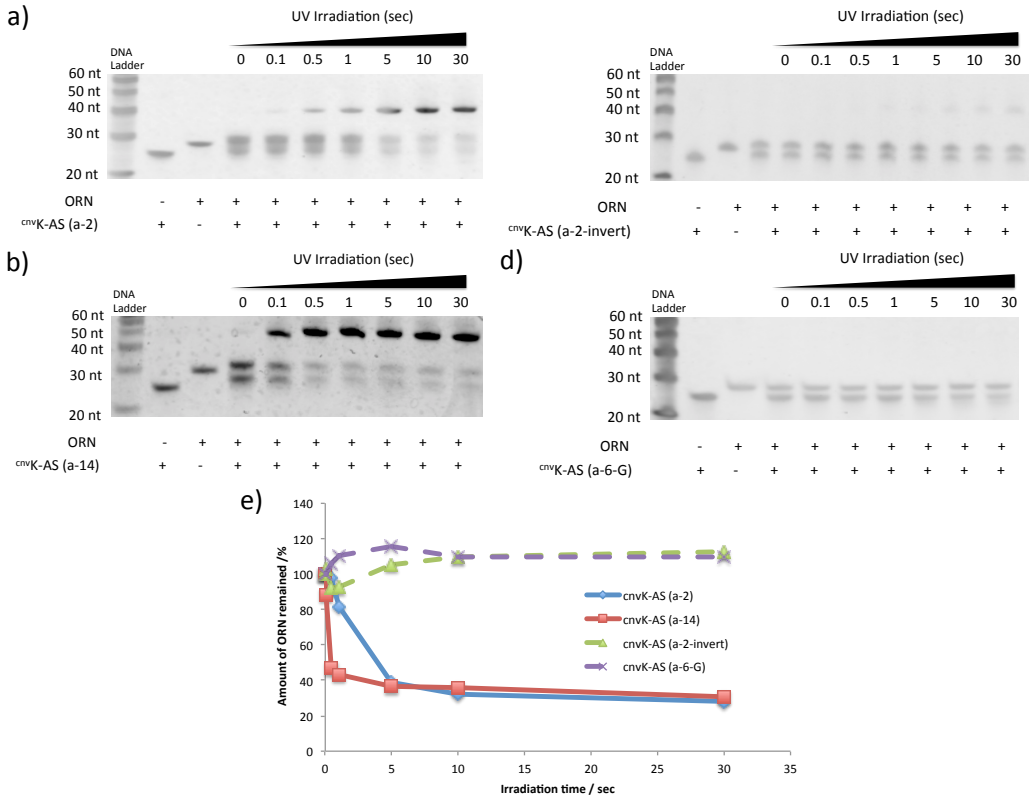

Figure 3. photocrosslinking between ^{CNV}K-AS and its complementary ORNs. PAGE analysis of the mixture of ORN-a and ^{CNV}K-AS (a-2) (a) , ^{CNV}K-AS (a-14) (b), ^{NV}K-AS (a-2-invert) (c) or ^{CNV}K-AS (a-6) (d) after UV irradiation. (e) Time course of the remaining ORNs during the photocrosslinking reaction. Photoreactions were performed with a 1 : 1 mixture of ^{CNV}K-AS and ORN ([^{CNV}K-AS] = [ORN] = 2 μM in PBS (-), 37 °C). Error bar = standard deviation.

This result shows that ^{cnv}K-ASs can photocrosslinke to complementary ORN sequence selectively at the single base level with a few seconds of UV irradiation. Furthermore, we evaluated the photoreactivity other ^{CNV}K-AS that have different target sites. ^{CNV}K-AS (b-2), ^{CNV}K-AS (c-2), ^{CNV}K-AS (d-2) was complementary to 471 nt~495 nt (Target Site B), 592 nt~616 nt (Target Site C), 542 nt~566 nt (Target Site D). These ^{CNV}K-ASs also photocrosslinked to complementary ORNs.

Photo-regulation of reverse-transcription of GFP mRNA in GFP-HeLa cells

A major difficulty with the phosphorothioate-antisense approach is that most phosphorothioate antisense oligonucleotides are ineffective against their targeted RNA because their low affinity for complementary RNA substantially limits their ability to invade RNA secondary structures. ^{cnv}K-AS's target mRNA sites (Target Site A, B or C) form two types of structure. Target Site A and Target Site B form a long base-paired structure, whereas Target Site C consists of two internal loops (Fig. 2). To evaluate the photoreactivity of ^{cnv}K-ASs that have different target mRNA sites, it is necessary to quantitate the GFP-mRNA of ^{cnv}K-ASs treated cells. In this study, real-time reverse transcription polymerase chain reaction (qRT-PCR) protocol was adopted.

Total mRNAs were extracted from cells 2 hours after ^{cnv}K-ASs treatment with UV irradiation. They were transcribed by reverse transcriptase in the presence of oligo (dT) primer, followed by PCR reactions. If a photocrosslinking reaction occurred, the reverse transcription was completely inhibited by the steric hindrance caused by the formation of an irreversible photoadduct. As shown in Fig. 3a, 100 nM ^{cnv}K-AS (a-2) and ^{cnv}K-AS (a-14) caused 57 % and 42% inhibition of reverse transcription respectively with 10 seconds of UV irradiation. The inhibition rate of reverse transcription of ^{cnv}K-AS (a-2) containing ^{cnv}K in the second-base position from 5' was 15% higher compared with ^{cnv}K-AS (a-14) containing ^{cnv}K in the fourteenth-base position from 5'. On the other hand, AS (a-con), ^{cnv}K-AS (a-6-G) and ^{cnv}K-AS (a-2-invert) did not inhibit reverse transcription regardless of whether receiving UV irradiation or not (Fig 4a). This result shows that ^{cnv}K-AS can photocrosslink to target mRNA site sequences selectively at the single base level with a few seconds of UV irradiation. Furthermore, we evaluated ^{cnv}K-AS (b-2) and ^{cnv}K-AS (c-2) against different target sites of GFP mRNA. As a result, ^{cnv}K-AS (b-2) and ^{cnv}K-AS (c-2) were found to cause 47 % and 39% inhibition of reverse

transcription respectively with 10 seconds of UV irradiation. In addition, ^{cnv}K-AS (d-2) was found to cause 44 inhibition of reverse transcription respectively with 10 seconds of UV irradiation. ^{cnv}K-ASs targeting other regions of GFP mRNA (^{cnv}K-AS (b-2, c-2, d-2)) show the same levels of gene silencing effect as ^{cnv}K-AS (a-2) (Fig 4b), although the secondary structure of these target regions would be different from each other (Fig. 2), suggesting the possibility that the K-AS invade the intramolecular duplex of the target region.

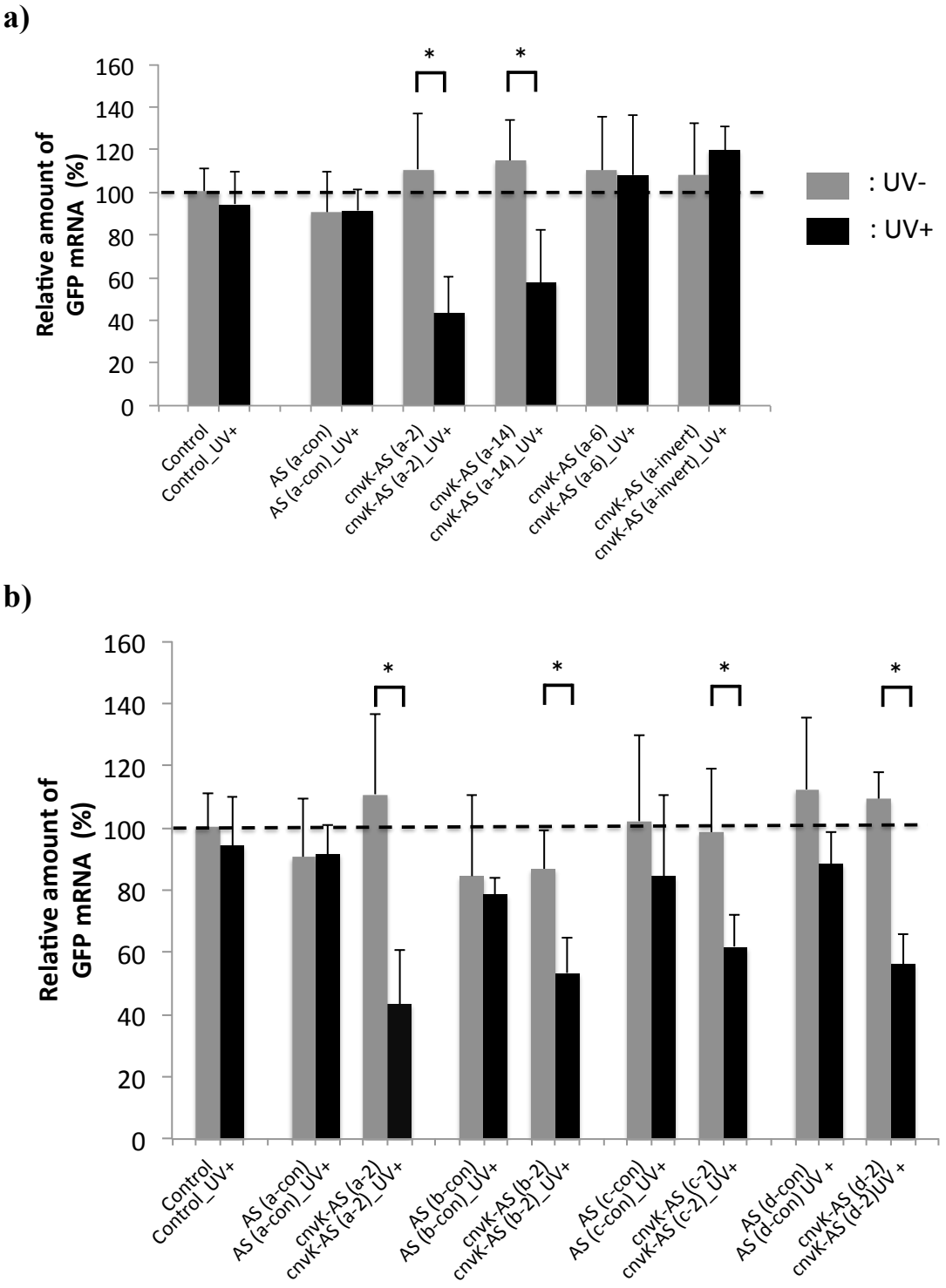

Figure 4. Down regulation of GFP expression in GFP-HeLa cells caused by photoirradiation with ^{cnv}K-ASs treatment.^{cnv}K-ASs were 100 nM. Relative amount % was calculated from the C_T values of the amplification curves of real-time PCR. The C_T values were normalized with the C_T values of the amplification curves of GAPDH in the same total RNA. Error bar = standard deviation (n = 3). The error bars indicate standard deviation of the mean. $*P < 0.05$.

This result shows that ^{cnv}K-ASs can bind to the target mRNA regardless of the different target site and difference in Tm value. The reason for this is thought to be because the ^{cnv}K-ASs and target site crosslink by forming a covalent bond between ^{cnv}K and the target pyrimidine base. Therefore, it is easier to design the antisense sequence with ^{cnv}K-AS than with normal phosphorothioate-antisense. As shown in Fig. 5, the photo-regulation efficiency of ^{cnv}K-AS (a-2) has a dose dependent manner, and the 50% inhibition concentration (IC_{50}) was 75 nM. The IC_{50} was 2- to 3-fold smaller than that of standard phosphorothioate antisense ODNs for endogenous GFP,[6,11] suggesting that the irreversible covalent bond formation between K- AS ODNs and target mRNA enhances the antisense effect.

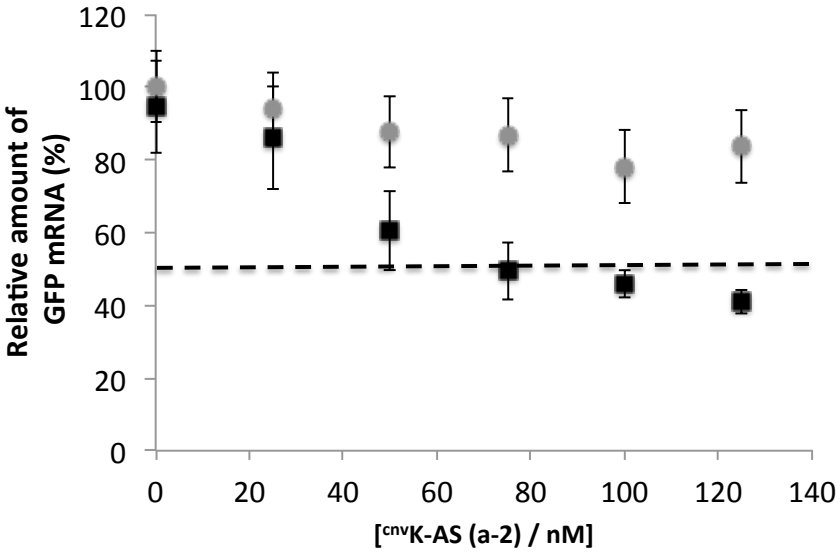

Figure 5. Dose dependency of ^{cnv}K-AS (a-2) for the down regulation of GFP gene expression. The error bars = standard deviation (n=3)

UV irradiation timing dependent regulation of reverse-transcription of GFP mRNA in GFP-HeLa cells

Next, I examined the correlation between UV irradiation timing and the amount of intact GFP mRNA in ^{cnv}K-AS (a-2) transfected cells. In the experiment shown in Fig. 6a, media were changed to fresh media containing 0.5 % FBS after 5 hours transfection and cells were allowed to culture for another 2, 26, 50 hours. After that time total mRNAs were extracted from cells. To evaluate the amount of intact GFP mRNA, the total RNAs were subjected to qRT-PCR protocol. The result shows that remarkable inhibition of reverse transcription was not confirmed. By contrast, in the experiment shown in Fig. 6b, cells were washed with PBS buffer and UV irradiated for 10 seconds after 5 hours transfection. After 10 seconds UV irradiation, fresh media were applied and cells were allowed to culture for another 2, 26, 50 hours. The result shows that 57 % inhibition of reverse transcription was confirmed after 2 hours of UV irradiation. Additionally, after 26 and 50 hours from 10 seconds of UV irradiation, 36%, 22% inhibition of reverse transcription was confirmed. This phenomena seems to be due to the constant production of mRNA by transfection from the gene. In the experiment shown in Fig 6c, cells were UV irradiated for 10 seconds after 24 hours transfection. The result shows that inhibition of reverse transcription was not confirmed before UV irradiation for 10 seconds, 58% inhibition was confirmed after UV irradiation. In the experiment shown in Fig. 6d cells were UV irradiated for 10 seconds twice after 5 hours transfection and 24 hours incubation. The result shows that 87% inhibition of reverse transcription was confirmed after a second course of UV irradiation for 10 seconds. After 24 hours from the second course of UV irradiation for 10 seconds, 78% inhibition of reverse transcription was confirmed. These results showed that ^{cnv}K-AS (a-2) clearly causes inhibition of reverse transcription by UV irradiation in a time dependent fashion. The ability to control gene expression by UV irradiation at desired timing would be useful in biotechnology, molecular biology and other applications.

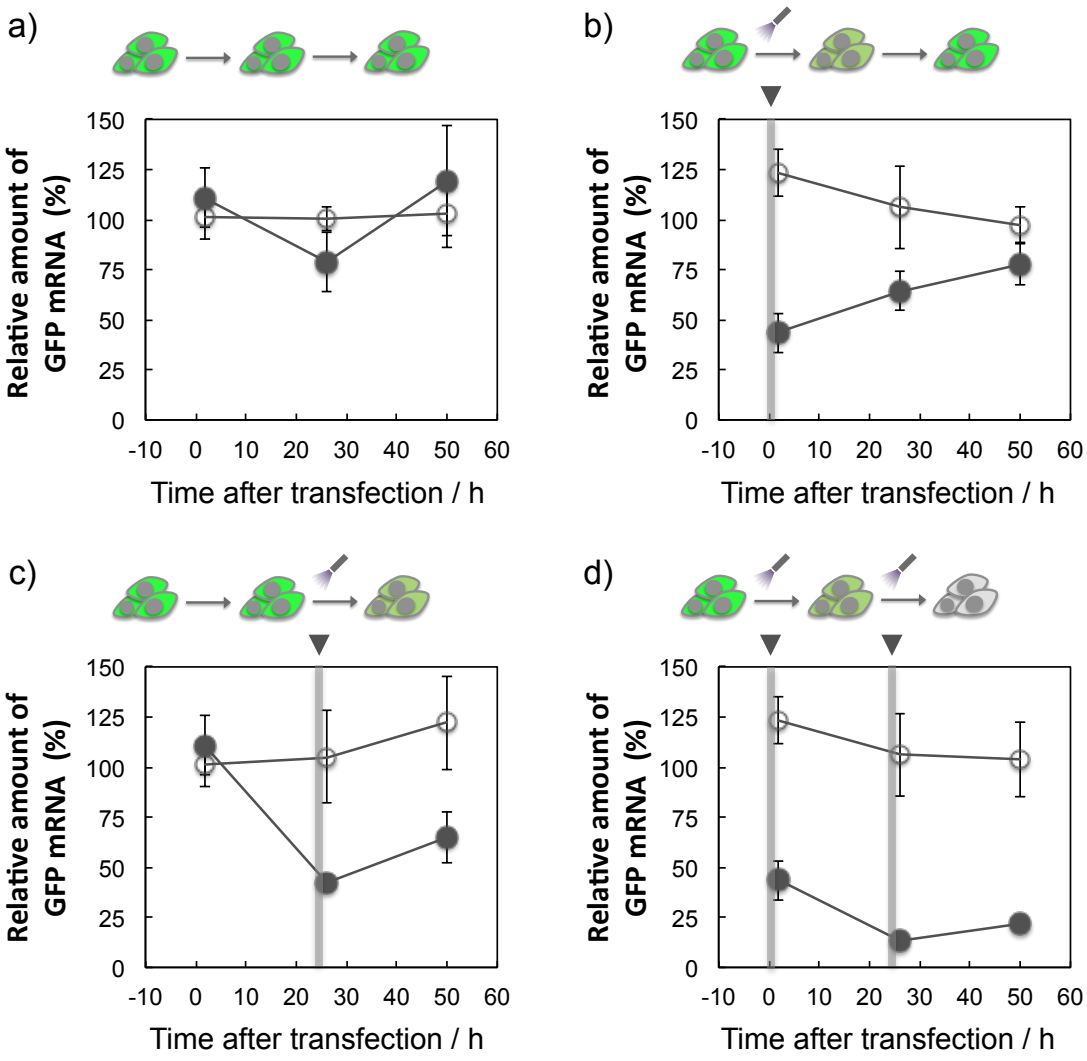

Figure 6. Inhibition of reverse transcription of GFP mRNA by ^{cnv}K-AS (a-2) ^{cnv}K-AS (a-2) was 100 nM. Relative amount % was calculated from the C_T values of the amplification curves of real-time PCR. The C_T values were normalized with the C_T values of the amplification curves of GAPDH in the same total RNA. Error bar = standard deviation (n = 3).

Photo-regulation of GFP expression in GFP-HeLa cells

To determine the efficacy of ^{cnv}K-ASs at regulating GFP knockdown by UV irradiation, GFP-HeLa cells were transfected with ^{cnv}K-AS (a-2). Cells in one group of experiments were washed with PBS buffer and UV irradiated after 5 hours transfection. After 10 seconds of UV irradiation, fresh media were applied and cells were allowed to culture for another 24 hours. In the other group, cells were treated in the same way but with no UV irradiation. The GFP signals of the cells were examined by confocal laser scanning microscopy. All images were taken under the identical imaging conditions for all experimental groups. Fig. 7 shows the result of photoregulation of GFP expression with ^{cnv}K-AS (a-2). ^{cnv}K-AS (a-2) inhibited GFP translation only in the case of UV irradiation for 10 seconds. This loss of GFP is not the result of UV quenching, since no transfected cells not conformed loss of GFP after UV irradiation (Fig. 7f).

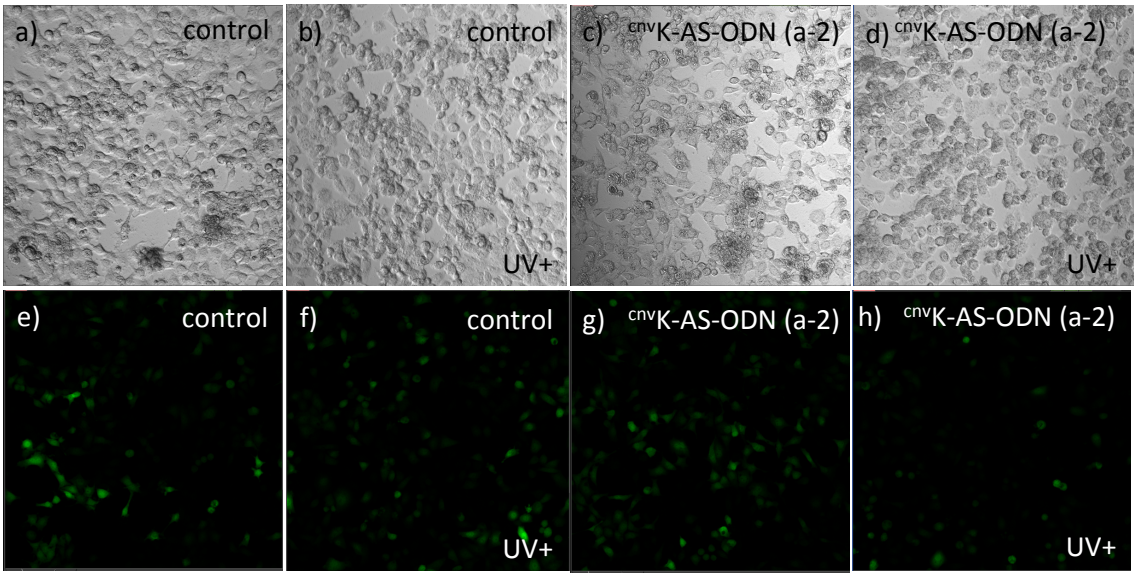

Figure 7. Photomodulation of GFP expression in GFP-HeLa cells.
In a 96-well plate, GFP-HeLa cells were transfected with ^{cnv}K-AS (a-2) using Lipofectamine® RNAiMAX Reagent. (a,e) GFP-HeLa cells . (b,f) GFP-HeLa cells were UV irradiation [366 nm (1600 mW/cm^2), 10 sec].(c,g) GFP-Hela Cells transfected with ^{cnv}K-AS-ODN (GFP) . (d,h) GFP-Hela Cells transfected with ^{cnv}K-AS-ODN (GFP) were UV irradiation [366 nm (1600 mW/cm^2), 10 sec].

As shown in Fig. 8, the fluorescence intensity of GFP in cells was clearly decreased 40% by the photoirradiation with the treatment of K-AS-a1, suggesting that the K-AS-a1 can down regulate the cellular synthesis of GFP by 10 sec of photoirradiation.

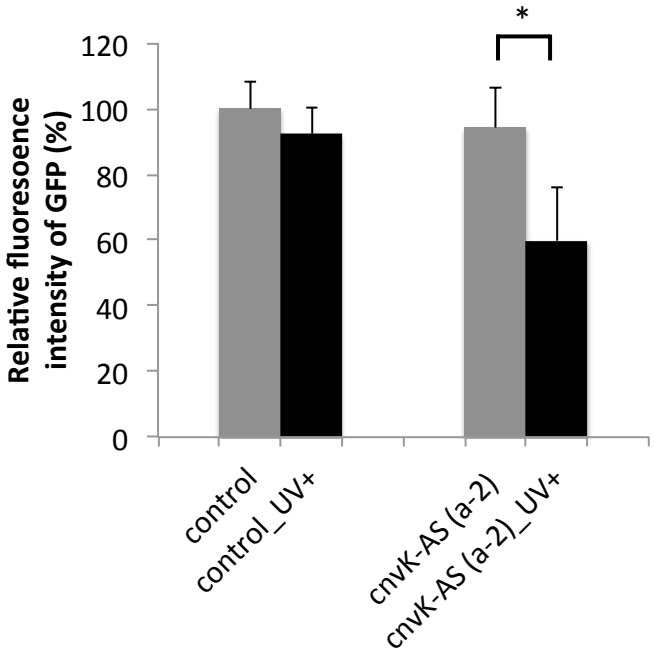

Figure 8. Fluorescence intensity of GFP in cells before and after the treatment of antisense (K-AS-a1) and 10 sec of 366 nm irradiation. The error bars indicate the standard error of the mean. * $P < 0.05$.

Comparison of lipofection reagent

I compared the antisense effects of ^{cnv}K-AS (a-2) transfected in GFP-HeLa cells by Lipofectamine 2000 transfection reagent (Invitrogen) with antisense effects of ^{cnv}K-AS (a-2) transfected in GFP-HeLa cells by Lipofectamine RNAiMAX transfection reagent (Invitrogen). As shown in Fig. 9, in the case of ^{cnv}K-AS (a-2) transfected by Lipofectamine 2000 transfection reagent, significant down regulation of GFP mRNA was induced by 366 nm photoirradiation as well as in the case of ^{cnv}K-AS (a-2) transfected by Lipofectamine RNAiMAX.

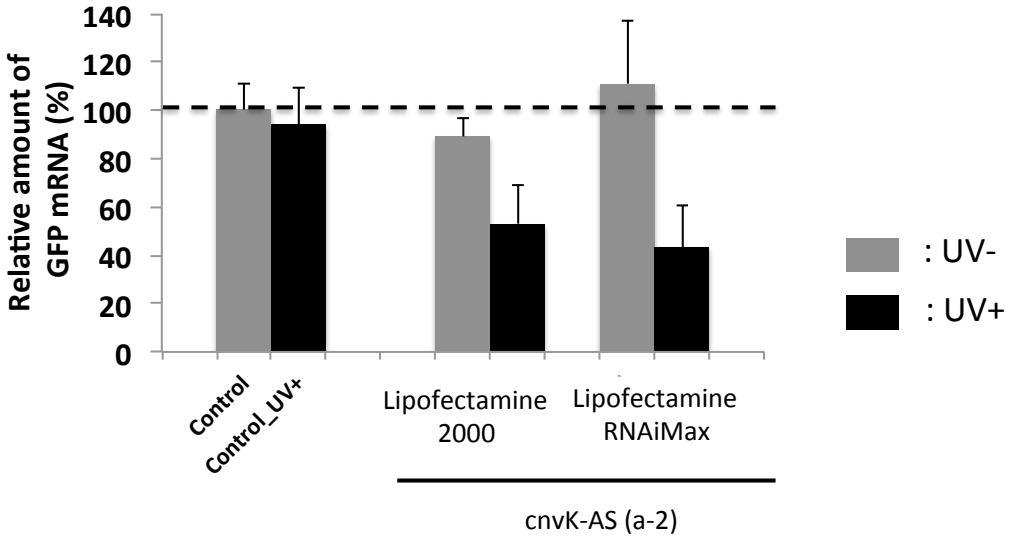

Figure 9. Comparison of lipofection reagent.^{cnv}K-ASs were 100 nM. Relative amount % was calculated from the C_T values of the amplification curves of real-time PCR. The C_T values were normalized with the C_T values of the amplification curves of GAPDH in the same total RNA. GFP mRNA wasquantified by real-time RT-PCR at 2 h after the photoirradiation. Error bar = standard deviation (n = 3). The error bars indicate standard deviation of the mean. *P < 0.05.

2.4. Conclusion

In this study, I demonstrated that ^{cnv}K-ASs that targets GFP mRNA disrupts GFP in transfected cells by 10 seconds of UV irradiation. qRT-PCR experiments revealed that the ^{cnv}K-ASs clearly photocrosslinks to its target mRNA in a sequence selective manner. Further, in spite of difference of Tm value and difference of target site, all active ^{cnv}K-ASs caused inhibition of reverse transcription by 10 seconds UV irradiation. Furthermore, ^{cnv}K-AS (a-2) clearly caused inhibition of reverse transcription by 10 seconds UV irradiation timing dependent. In addition, the translation of target GFP mRNA is inhibited by 10 seconds UV irradiation. ^{cnv}K-AS have the potential to be applications to spatiotemporal photoregulation of gene expression or effective photodynamic antisense drugs that act at desired locations around the body with a few seconds of 10 seconds UV irradiation.

2.5. References

1. Moody,H.M., van Genderen,M.H., Koole,L.H., Kocken,H.J., Meijer,E.M., and Buck,H.M. Regiospecific inhibition of DNA duplication by antisense phosphate-methylated oligodeoxynucleotides. *Nucleic Acids Res.* **1989**, 17, 4769–4782.
2. De Clercq, E., Eckstein, F., and Merigan, T.C. Interferoninduction increased through chemical modification of a synthetic polyribonucleotide. *Science.* **1969**, 165, 1137-1139.
3. Jensen, K.K., Orum, H., Nielsen, P.E., and Norden, B. Kinetics for hybridization of peptide nucleic acids (PNA) with DNA and RNA studied with the BIAcore technique. *Biochemistry.* **1997**, 36, 5072-5077.
4. Obika, S., Nanbu, D., Hari, Y., Morio, K., In, Y., Ishida T., and Imanishi, T. Synthesis of 2'-O,4'-C-Methyleneuridine and -cytidine. Novel Bicyclic Nucleosides Having a Fixed C3'-endo Sugar Puckering. *Tetrahedron Lett.* **1997**, 38, 8735-8738.
5. Koshkin, A.A., Singh, S.K., Nielsen, P., Rajwanshi, V.K., Kumar, R., Meldgaard, M., Olsen, C.E., and Wengel, J. LNA (Locked Nucleic Acids): Synthesis of the Adenine, Cytosine, Guanine, 5-Methylcytosine, Thymine and Uracil Bicyclonucleoside Monomers, Oligomerisation, and Unprecedented Nucleic Acid Recognition. *Tetrahedron.* **1998**, 54, 3607-3630.
6. Deiters, A., Garner, R.A., Lusic, H., Govan, J.M., Dush, M., Nascone-Yoder, N. M., and Yoder, J. A. Photocaged morpholino oligomers for the lightregulation of gene function in zebrafish and Xenopus embryos. *J. Am. Chem.Soc.* **2010**, 132, 15644-15650.
7. Asanuma, H., Liang, X., Yoshida, T., and Komiyama, M., Photocontrol of DNA Duplex Formation by Using Azobenzene-Bearing Oligonucleotides. *ChemBioChem.* **2001**, 2, 39-44.

8. Higuchi. M., Yamayoshi, A., Kato, K., Kobori, A., Wake, N., and Murakami, A. Specific Regulation of Point-Mutated K-ras-Immortalized Cell Proliferation by a Photodynamic Antisense Strategy. *Oligonucleotides*. **2010**, 20, 37-44.
9. Fujimoto, K., Hiratsuka-Konishi, K., Sakamoto, T., Ohtake, T. Shinohara K., and Yoshimura, Y. Specific and reversible photochemical labeling of plasmid DNA using photoresponsive oligonucleotides containing 3-cyanovinylcarbazole *Molecular BioSystems.* **2012**, 8 (2), 491-494.
10. Yoshimura, Y., and Fujimoto, K. Ultrafast Reversible Photo-Cross-Linking Reaction: Toward in Situ DNA Manipulation. *Org. Lett*. **2008**, 10, 3227-3230.
11. Shigeno, A., Sakamoto, T., Yoshimura, Y., and Fujimoto, K. Quick Regulation of mRNA Functions by a Few Seconds of Photoirradiation. *Organic & Biomolecular Chemistry*. **2012**, 10(38), 7820-7825.
12. Govan, J. M., Uprety, R., Thomas, M., Lusic, H., Lively, M. O., and Deiters. A. Cellular delivery and photochemical activation of antisense agents through a nucleobase caging strategy. *ACS Chem. Biol.* **2013**, 8, 2272–2282.

Chapter 3

Synthesis of disulfide crosslinking tethered CpG oligonucleotide for immune activation by radiation

3.1. Introduction

Microbial and bacterial DNA are potent immunostimulants [1] and research has found that the abundance of CpG dinucleotides (CpGs) in genomes of prokaryotes is a major factor contributing to their immunostimulatory properties[2]. Toll-like receptor 9 (TLR9) belongs to the innate immune system and recognizes microbial and vertebrate DNA. This receptor is located intracellularly within the endosomal compartments and functions to alert the immune system of viral and bacterial infections by binding to DNA rich in CpG motifs. CpG-motifs activate the TLR9-mediated MyD88 dependent NF-κB signaling pathway and interferin regulatory factor 3 (IRF3)[3]. TLR9 have attracted attention for application of the microbial recognition mechanism mediated activation of the innate immune system to therapy for infectious diseases and cancer. In recent years, a synthetic oligodeoxynucleotide that contains unmethylated CpG motifs (CpG-ODN) has been demonstrated to activate TLR9 [4,5], improve cell survival and prevent cell apoptosis [6]. However, the clinical use of CpG ODN is limited to one phase I trial of 23 patients with non-Hodgkin lymphoma (diverse group of blood cancers that include any kind of lymphoma except Hodgkin's lymphomas) who had progressed through at least one round of therapy[7]. Patients were given two infusions of increasing doses of a CpG ODN. The safety analysis demonstrated serious adverse events including anemia, thrombocytopenia and neutropenia that were attributed to the disease; however, given more recent data, these events may also have been at least partly due to the CpG ODN[8,9]. No clinical effects were seen with this infusion and the immunological effects were limited to mild increases in NK cell number, anecdotal improvement in NK cell activity and the transient increases in circulating IL-6. The lack of effects seen in this phase I trial is unlikely to reflect underdosing as the rate of serious side effects is troubling and reminiscent of the trial of subcutaneously injected CpG ODN in patients with non-small-cell lung cancer (NSCLC), which was stopped early owing to a combination of serious adverse events and poor efficacy[8,9].

Therefore development of new immune activators with fewer side effects and high efficacy is urgently required.

In this study I designed and synthesized an original immune activator which containing the CpG motif. CpG ODN can stimulate the immune system via interaction with the TLR9, but the direct interaction of the receptor and ligand is unclear[2,3]. Recent investigations have suggested that CpG ODN have two types of secondary structure, because of the palindromic sequence[10] (Figure 1). We hypothesized that TLR9 recognizes the secondary structures of CpG DNA.

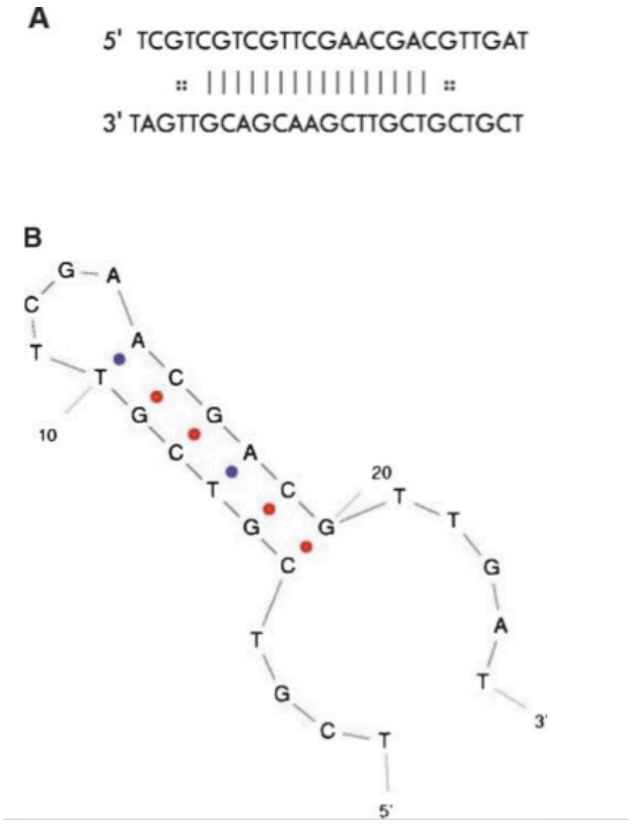

Figure 1. Modifications in the stem-loop structure affect CpG induced invasion.
Homopolymeric duplex (A) and hairpin stem-loop structure (B) of the CpG ODN molecule.
(Mol Cancer Res 2008;6:1534–43.)

Therefore, we designed disulfide crosslink CpG ODN (S-S CpG) (Fig. 2.).

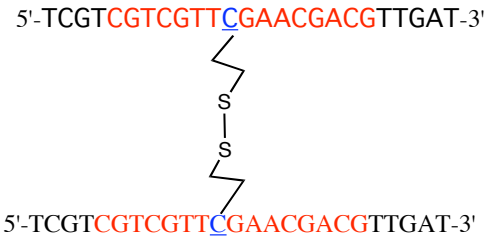

Figure 2. S-S CpG synthesized in this study

S-S CpG DNA were obstructed the formation of the original structure of CpG ODN by disulfide crosslinking. X-irradiation, which triggered selective reduction at the disulfide bond in the S-S CpG ODN, induced an exchange reaction, resulting in dissociation of the disulfide crosslinking and S CpG conforming to the original structure of CpG ODN as shown in Fig. 1. Mechanistic studies revealed that reducing species such as hydrogen atoms and/or hydrated electrons (e_{aq}^{-}) generated from radiolysis of water molecules are most likely to be a key active species for the exchange reaction. Therefore, I tried to develop spatiotemporal radiation trigger immuno drugs using these unique properties of S-S CpG DNA and the reaction of the disulfide bond.

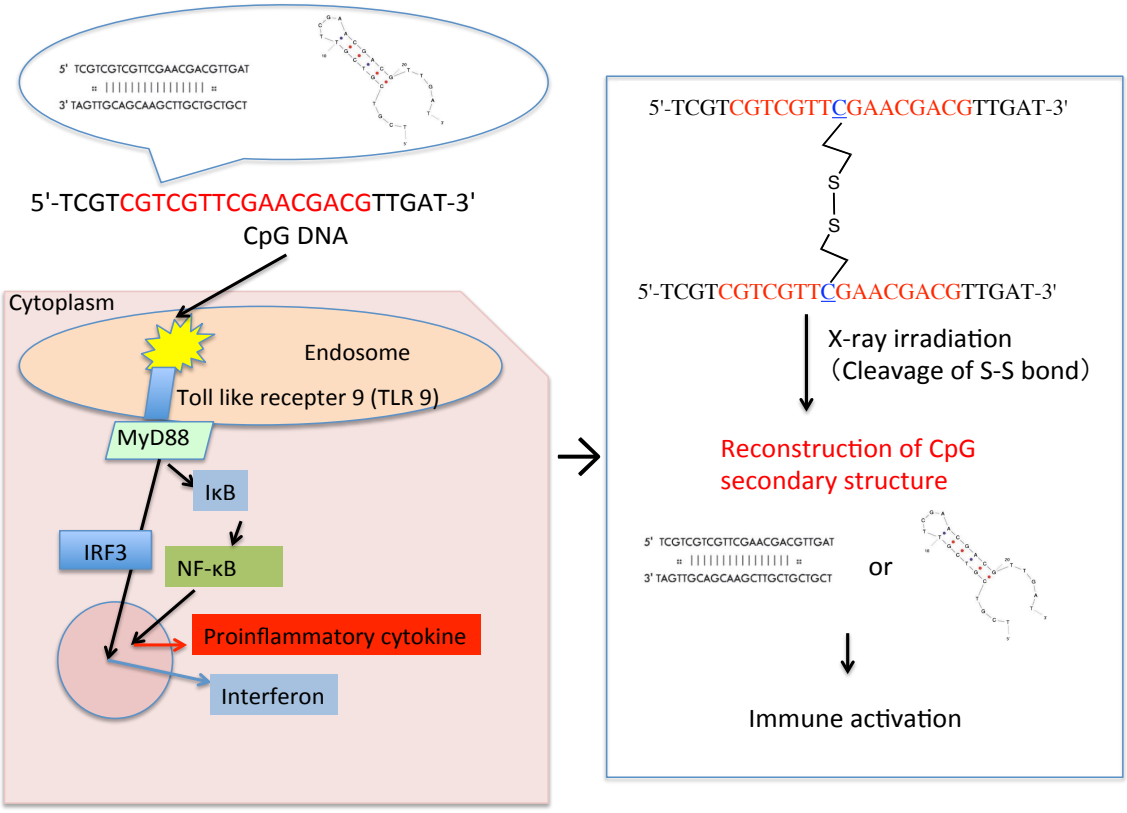

Figure 3. Schematic drawing of radiation trigger artificial CpG oligonucleotide (S-S CpG)

3.2. Materials and methods

General methods

1H-NMR spectra were measured with AVANCE III NMR 400 (Bruker, 400 MHz) spectrometer. Coupling constant (J value) are reported in hertz. The chemical shifts are expressed in ppm downfield from tetramethylsilane, using residual chloroform (δ = 7.24 in ^{1}H-NMR) and DMSO (δ = 2.49 in ^{1}H-NMR) as an internal standard.Mass spectra were recorded on a Voyager-DE PRO-SF, Applied Biosystems. HPLC was performed on a Chemcobond 5-ODS-H column (10 x 150 mm, 4.6 x 150 mm) or a Chemcosorb 5-ODS-H column (4.6 x 150 mm) with a JASCO PU-980, HG-980-31, DG-980-50 system equipped with a JASCO UV 970 detector at 260 nm. Reagentsfor the DNA synthesizer such as A, G, C, T-β-cyanoethyl phosphoramidite,and CPG support were purchased from Glen Research. Oligo RNAs were purchased from Fasmac (Japan) and used without further purification.

Gel Electrophoresis

Oligonucleotides were electrophoresed in 15 % (29:l, polyacrylamide: bisacrylamide) containing (7 M urea) polyacrylamide gels. Samples were prepared by adding an equal volume of loading dye to the reaction mixture (36% (v/v) glycerol, 30 mM EDTA and 0.05% (w/v) each of bromophenol blue and xylene cyanol). Gels were prerun for 20 min prior to loading the DNA. Analytical samples were visualized by staining with SYBR gold (Molecular Probe), and imaged on an Imaging System LAS-3000. The samples were viewed under UV light, cut out, crushed, and soaked overnight in 1 M triethylammonium bicarbonate (TEAB), pH 7.5, at room temperature. After this time, the supernatant was removed and the DNA was further extracted once with 1 M TEAB and three times with 25 mM TEAB. This solution of DNA was loaded onto a C_{l8} Sep-Pak cartridge (Waters), which was washed with 20 mL of 25 mM TEAB. The DNA was then eluted in 6 mL of 30% CH_3CN in 100 mM TEAB. The resulting fractions were lyophilized.

5′-O-(4,4′-Dimethoxytriryl) -2′-deoxyuridine (4).

2′-deoxyuridine (1.0 g, 4.4 mmol) was dissolved in dry pridine and coevaporated three times. 4,4′-Dimethoxytrityl chloride (1.4 g, 4.2 mmol), N,N-dimethylaminopyridine (51 mg, 0.42 mmol) and triethylamine (0.375 mL, 2.69 mmol) was added to a solution of 2′-deoxyuridine in dry pyridine (6 mL) The solution was stirred at ambient temperature under nitrogen atmosphere 18 h. The TLC analysis $CHCl_3$/MeOH (9:1) showed the presence of starting material, but the reaction mixture was evaporated to dryness in vacuo. The residue was extracted with $CHCl_3$ (20 mL x 3) and water (20 mL), and the organic layer was collected, dried over Na_2SO_4, filtered, and evapolated to dryness under reduced pressure. The crude product was purified by silica gel column chromatography with CHCl3/MeOH (9:1) and 5′-O-(4,4′-dimethoxytrityl)- 2′-deoxyuridine (1.3 g) was isolated in 56.0% yield as a white solid. ^{1}H NMR(400 MHz DMSO): δ _11.30 (s, 1H, NH uracil), 7.64 (d, 1H, J=8.0 Hz, H-6), 7.38 (d, 2H, trityl), 7.31 (t, 2H, J=7.2, 7.8 Hz, trytyl), 7.25 (dd, 5H, J=2.4, 9.0, trityl), 6.90 (d, 2H, J=1.1, trityl), 6.88 (d, 2H, J=1.1 Hz, trityl), 6.15 (t, 1H, J=6.5, 6.4 Hz,H-1', 5.38 (d, 1H, J=8.0 Hz, H-5 uracil), 5.32 (d, 1H, J=4.7 Hz,H-4') 4.30 (m, 1H, H-3') , 3.87(m, 1H, OH-3') , 3.73 (s, 6H, OCH_3 x 2), 3.22 (m, 1H, H-5') , 3.18 (m, 1H, H-5'), 2.19 (t, 2H, J=5.9, 6.3 Hz, H-2' x 2)

5′-O-(4,4′-Dimethoxytrityl)-3′-O-[2-cyanoethoxy-(N,N-diisopropylamino)-phosphino] -2′- deoxyuridine (5).

5′-O-(4,4′-Dimethoxytriryl)- 2′-deoxyuridine (300 mg, 0.57 mmol) in a sealed bottle with septum was dissolved in dry acetonitrile and coevaporated three times in vacuo. After substitution with argon, 2-cyanoethyl-N,N,N′,N′-tetraisopropylphosphoroamidite (180 μL, 0.57 mmol) in dry acetonitrile (2.0 mL), and 0.25 M tetrazole in dry acetonitrile (3.0 ml, 0.73 mmol) were stirred for 1.0 h. After the completion of the reaction as evidence by

TLC, the reaction mixture was extracted with ethyl acetate (20 mL x 2), which was washed with saturated sodium bicarbonate aqueous solution and water (15 mL). The organic layer was collected, dried over anhydrous sodium sulfate, filtered, and evaporated to dryness under reduced pressure. Then, the crude product 5′-O-(4,4′-Dimethoxytrityl)-3′-O-[2-cyanoethoxy-(N,N-diisopropylamino)-phosphin o]- 2′-deoxyuridine (0.34 g, 81 %) in a sealed bottle with septum was dissolved in dry acetonitrile and coevaporated three times.

5′-O-(4,4′-Dimethoxytrityl)-N4-1,2,4-triazolyl-3′-O-[2-cyanoethoxy-(N, N-diisopropylamino)-phosphino] -2′-deoxyuridine (6).

To an ice cooled stirred suspension of 1,2,4-triazole (1.52 g, 22.0 mmol) in dry acetonitrile (28 mL) was added slowly $POCl_3$ (0.44 mL, 4.72 mmol) followed by dry triethylamine (3.33 mL, 23.9 mmol). After 30 min a solution of 5′-O-(4,4′-dimethoxytrityl)-3′-O-(2-cyanoethoxy- (N,N-diisopropylamino)-phosphin o)-5 -2′-deoxyuridine (0.38 mg, 0.53 mmol), in dry acetonitrile (3 mL) was added over a period of 5 min. Ice-cooled stirring was continued for 20 min followed by 40 min at room temperature. The reaction solution was diluted with EtOAc (50 mL) and extracted with saturated $NaHCO_3$ solution (50 mL). The organic layer was collected, dried over anhydrous sodium sulfate, filtered, and evaporated to dryness to yield 5′-O-(4,4′-dimethoxytrityl)-N4-1,2,4-triazolyl-3′-O- [2-cyanoethoxy-(N,N-diisopropylamino)-phosphino]-2′-deoxyuridine (276 mg, 0.341 mmol, 95%), which was directly used in an automated DNA synthesizer without further purification.

Cystamine modified Oligonucleotide [Synthesis and Purification]

Oligonucleotides were prepared by β-(cyanoethyl) phosphoramidite method on controlled pore glass supports (1 μmol) by using Applied Biosystems Model ABI3400 DNA synthesizer. Cyanoethylphosphoramidite of elaborated compounds was prepared as described above. After automated synthesis, the oligomer was detached from the support by soaking in conc. aqueous ammonia for 1 h at room temperature.5′-O-(4,4′-Dimethoxytrityl)-N4-1,2,4-triazolyl-3′-O-[2-cyanoethoxy-(N,

N-diisopropylamino)-phosphino] -2′-deoxyuridine was used as a 0.1 M solution in acetonitrile, and the 1 μmol synthesis cycle was modified to add an extra 2 min to the coupling time for this base. With this modification, there is no notable difference between the efficiency of coupling for this amidite and for commercially available ones. After automated synthesis, Oligonucleotides were detached from the support by 1 M amine (cystamine), 1 mL per μmol of DNA. Mixtures were incubated at 65 ºC for 18 h. CPG support was then removed by filterting, and the crude oligomer was purified by reverse phase HPLC and lyophilized.

Preparation of Disulfide Cross-Linked Oligomers.

Cystamine modified Oligonucleotide (1 μmol per mL of solution) were incubated in 10 mM dithiothreitol (DTT) in 10 xTE (100 mM TrisCI and 10 mM EDTA, pH 8.0, degassed) under nitrogen at 37 ºC for 10-12 h. The reducing agent was removed by dialysis CIS Sep-Pak cartridge under aerobic conditions so as to allow air oxidation to the disulfide cross-link. The oligomers were purified by Gel Electrophoresis (as described above).

Radiation-induced imume activation of S-S CpG.

Raw264.7 cells were seeded into 12-well plates ($1x10^5$ cells/well) and incubated at 37 °C for 24. The cells were then added the CpG DNAs and X ray irradiate (30 Gy). The cells were incubated for 3 h. After incubation, the qRT-PCR assay was performed as described above.

Real-time RT-PCR

Reverse transcription was performed by the PrimeScript® RT reagent Kit (Takara, Japan) with 0.2 μg of total RNA from cells. Resulting cDNA was subjected to Real-time PCR using an automated real-time PCR system (Step One Plus: Applied Biosystems) with SYBR Premix Ex Taq II perfect real time (Takara, Japan) and 0.4 μM of primers (Ifnb, forward; GAGCTCCAAGAAAGGACGAAC, reverse; GGCAGTGTAACTCTTCTGCAT, GAPDH, forward; AGGTCGGTGTGAACGGATTTG, reverse; TGTAGACCATGTAGTTGAGGTCA). Inhibition efficiency was estimated from the change in C_T values with the normalization using the amounts of GAPDH mRNA estimated from RT-PCR with a GAPDH primer set.

3.3 Results and discussion

In this study, I have used the convertible nucleoside 4-triazolyl-2′-deoxyuridine (Tri-dU) to insert disulfide-containing tethers into DNA at the C4 position of Cytosine. AM E. Ferentz et.al. reported that these tethers, when introduced as pairs into duplex DNA, can undergo efficient redox chemistry resulting in the formation of an interstrand disulfide cross-link[11]. I synthesized the one modified version of the CpG DNA sequence 5'-d(TCGTCGTCGTTCGAACGACGTTGAT)-3' by this approach (Fig. 2).

The Tri-dU moiety was then converted to dU bearing a tether at C4 by an addition-elimination reaction using a primary amine (Scheme 1).

Scheme 1. Synthesis of the Cystamine CpG

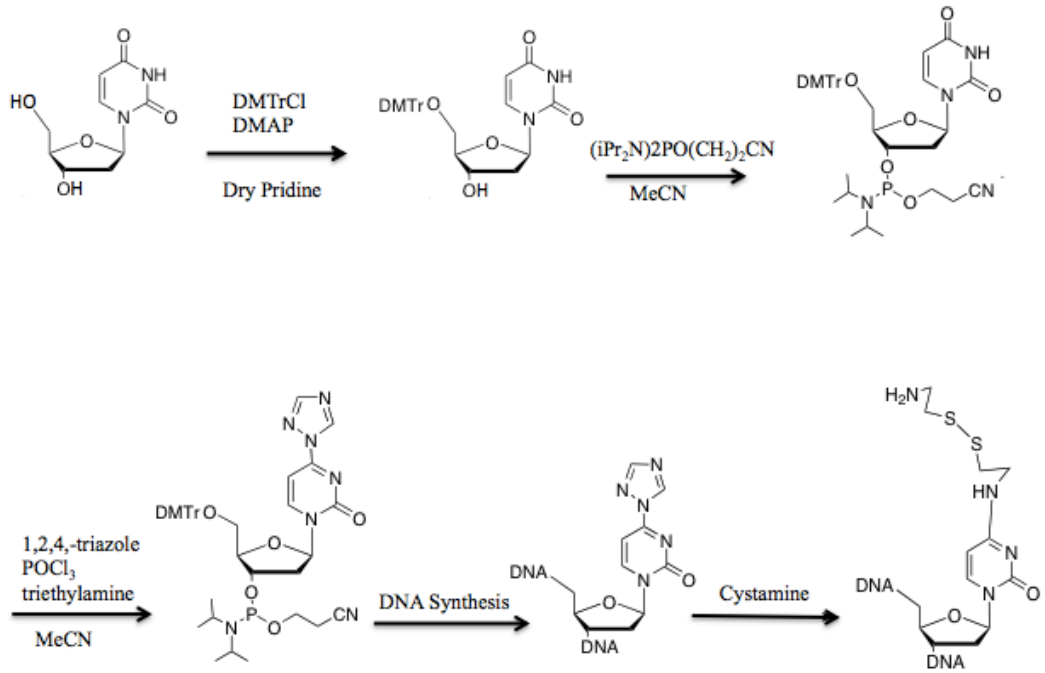

Scheme 2. Synthesis of the S-S CpG

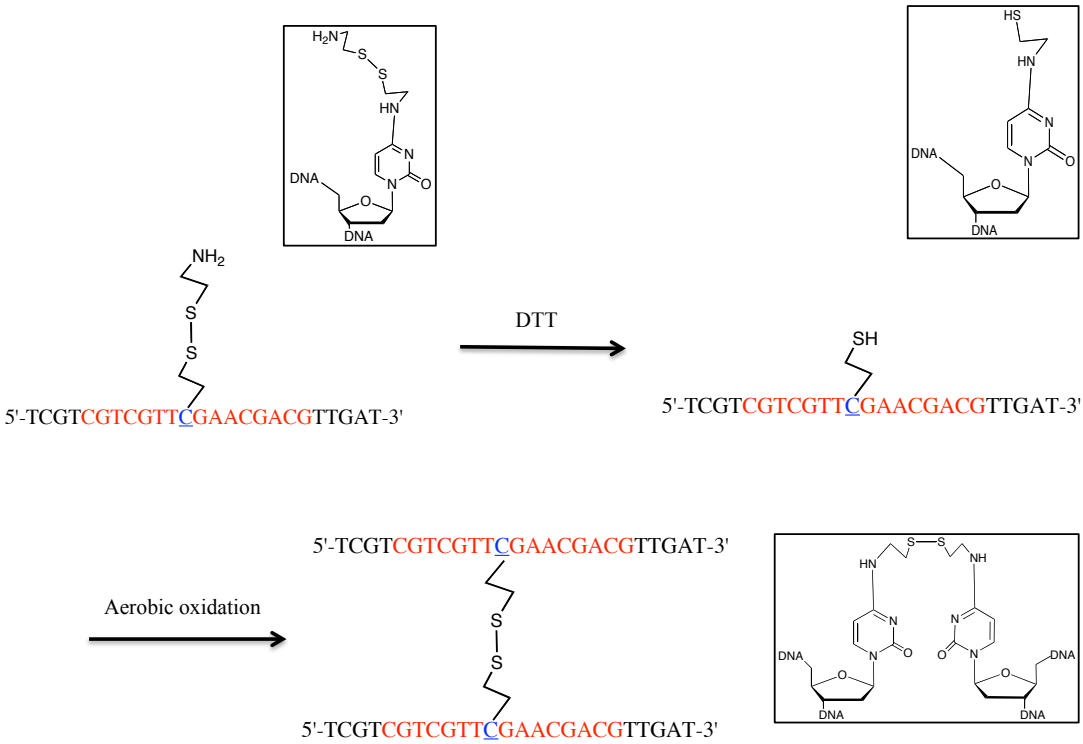

Reactions with cystamine resulted in high conversion to the desired tethered cytosine without significant quantities of side products, as assayed by HPLC analysis. The excess amine was removed, and the DNA mixed disulfides S-S CpG was cross-linked (Scheme 2).

Table 2. Oligonucleotides used in this study

Name	Sequence	
S-S CpG	5'-tcgtcgtcgttCgaacgacgttgat-3' (25mer×2)	C : Disulfide crosslink
S CpG	5'-tcgtcgtcgttCgaacgacgttgat-3' (25mer)	C : Thioethyl tethered C
CpG DNA	5'-tcgtcgtcgttcgaacgacgttgat-3' (25mer)	

Reductive cleavege of S-S CpG

The cross-linked DNA was purified by denaturing polyacrylamide gel electrophoresis (PAGE) at the end of the synthesis. The ability to form cross-linked duplexes was examined by denaturing PAGE using oligonucleotides S-S CpG, the tethers of which contained a mixed disulfide function. Brief treatment of the S-S CpG with 10 mM dithiothreitol (DTT), a disulfide reducing agent, led to a marked increase in mobility (band lower in gel; Fig. 4, compare Lanes 1 with 2). Removal of the reducing agent resulted in virtually quantitative conversion of the DTT-treated S-S CpG to the retarded species (lanes 1, which had the mobility of a linear about 25-mer (lane 3).

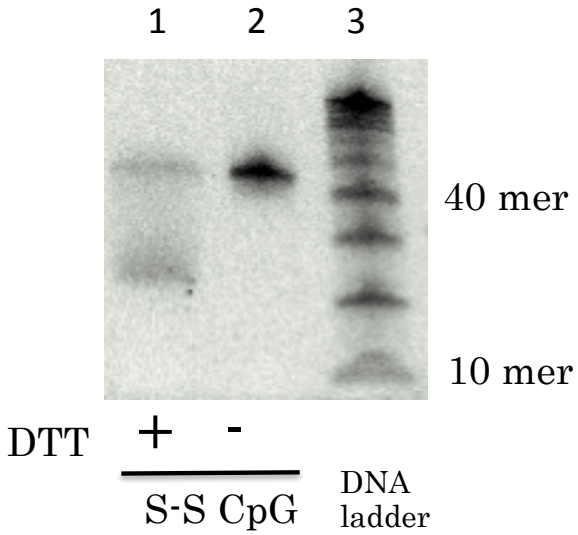

Figure 4. Denaturing polyacrylamide gel of cross-linking reactions. Lanes 1 show the S-S CpG contain the products of reduction of cross-links S-S CpG with 10 mM DTT. containing C2 mixed disulfide tethers, respectively; in lanes 2 are the disulfide cross-linked products. Lanes 3 are 10 bp DNA step ladder

S-S CpG induced *Ifnb* gene expression

Even though the disulfide cross-linked molecules possess 50 nucleotide units, their mobility is more like that of a linear 50-mer. This behavior, which probably arises from their inherently higher compactness relative to that of linear molecules of the same size or their propensity to form transient duplex species even under the denaturing conditions of gel electrophoresis.

I subsequently investigated the radiation-dependent immune activation effect of S-S CpG. After administration of S-S CpG to Raw cells and exposed Raw cells to X-radiolysis (30 Gy). After incubation for 3 h, I extract total RNA from Raw cells. RT-PCR experiments revealed that the S-S CpG slightly-induced Ifnb gene expression (Fig. 4).

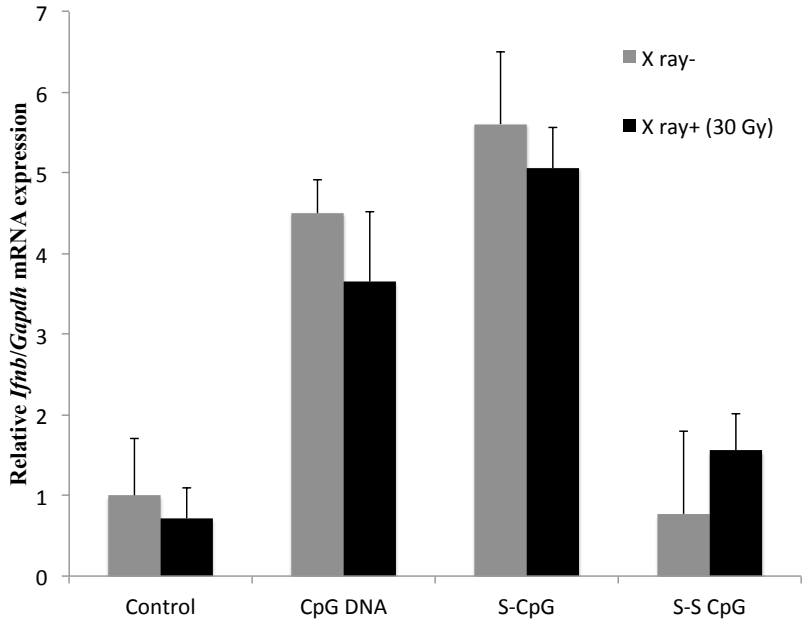

Figure 5. Ifnb mRNA expression in Raw cells. measured by qRT-PCR after stimulation in cell with non-CpG control, CpG (1 μM), S-CpG (1 μM) and S-S CpG (500 nM) for 3 h. The mRNA levels were normalized against GAPDH expression.

Anticipation of the secondary structure of CpG DNAs

In order to anticipate the CpG DNA's secondary structures, the CpG DNAs were analyzed by Tm analysis and 16% native PAGE analysis. As shown in Fig. 6, the reciprocal CpG DNA's melting temperature, Tm^{-1} is linearly-related the log of the CpG DNA's concentration, C_T. Furthermore, a dimer band was observed in Lane1, Lane 2 and Lane 3, and high mobility band was distantly observed in addition to the dimer band in Lane 1 and Lane 3. These results suggest that CpG DNA and S CpG forms a duplex structure mainly, and monomeric ODN is in the minor state in medium. However, an intramolecular hydrogen bond is thought of as the dominant bond at low concentration CpG ODN. Moreover, disulfide crosslinked S-S CpG has no immunostimulatory activity. Therefore, I speculate that monomeric ODN play an important role in TLR9 mediated immunostimulatory activity within the cell.

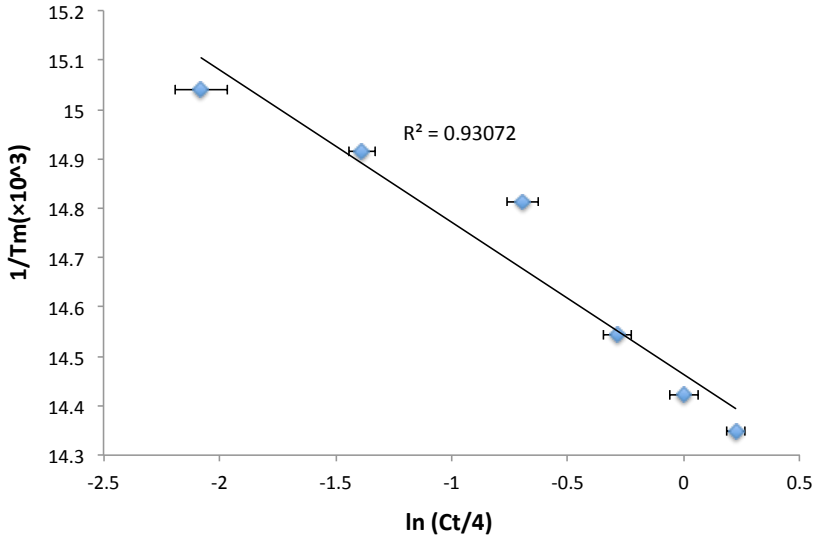

Figure 6. Plots of T_M^{-1} vs. ln (C_T/4) .

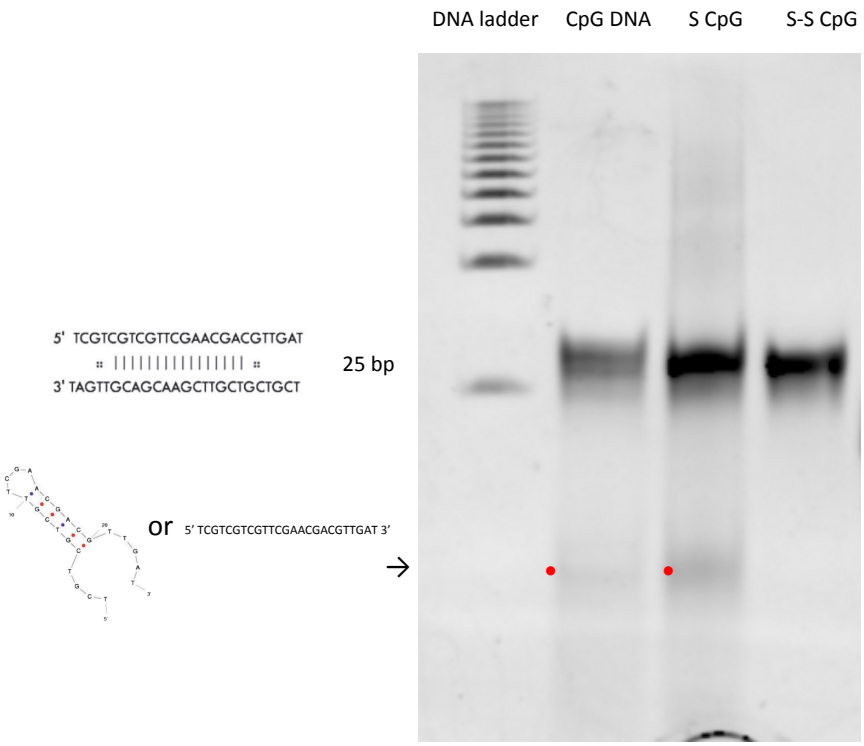

Lane 1 2 3 4

Figure 7. 16 %Native polyacrylamide gel electrophoresis of CpG DNA. [ODN] = 1 µM in PBS buffer. Lane 1, which is 25 bp DNA step ladder Lane 2 is 1 µM CpG DNA Lane 3 is 1 µM S CpG Lane 3 is 500 nM S-S CpG DNA.ODN= 1 µM in PBS buffer.

3.4. Conclusions

In conclusion, the author has synthesized disulfide crosslinking tethered CpG oligonucleotide (S-S CpG) as radiation-trigger immune activater. The S-S CpG had an alkyl chain and two CpG DNA units were connected by an X-ray-sensitive disulfide bond. X-irradiation of Raw cells, to which S-S CpG were administered, resulted in an Induced Ifnb because of the reductively- cleaved CpG immune activation. Thus, S-S CpG are promising as radiation-trigger immune activater that are applicable to drug.

3.5. References

1. Yamamoto, S., Kuramoto, E., Shimada. S., and Tokunaga, T. In vitro augmentation of natural killer cell activity and production of interferon-alpha/beta and gamma with deoxyribonucleic acid fraction from Mycobacterium bovis BCG. *Jpn J Cancer Res.* **1988**, 79(7), 866-873.
2. Krieg, A.M. CpG motifs in bacterial DNA and their immune effects. *Annu Rev Immunol.* **2002**, 20, 709-760.
3. Kumagai, Y., Takeuchi, O., and Akira, S. TLR9 as a key receptor for the recognition of DNA, *Adv. Drug Deliv. Rev.* **2008**, 60, 795-804.
4. Krieg, A.M. Therapeutic potential of Toll-like receptor 9 activation, *Nat. Rev. Drug Discov.* **2006**, 5, 471-484.
5. Kumagai, Y., Takeuchi, O., and Akira, S. TLR9 as a key receptor for the recognition of DNA, *Adv. Drug Deliv. Rev.* **2008**, 60, 795–804.
6. Sester, D.P., *et al.* CpG DNA activates survival in murine macrophages through TLR9 and the phosphatidylinositol 3-kinase-Akt pathway, J. Immunol. **2006**, 177, 4473–4480.
7. Link, B.K., *et al.* Oligodeoxynucleotide CpG 7909 delivered as intravenous infusion demonstrates immunologic modulation in patients with previously treated non-Hodgkin lymphoma. *J. Immunother.* **2006**, 29(5), 558-568.
8. Readett, D., Denis, L., Krieg, A., Benner, R., and Hanson, D. PF-3512676 (CPG 7909) a Toll-like receptor 9 agonist-status of development for non-small cell lung cancer (NSCLC). Presented at:12th World Congress on Lung Cancer; Seoul, Korea. 2–6 September **2007**:
9. Engel, A.L., Holt, G.E., and Lu, H., The pharmacokinetics of Toll-like receptor agonists and the impact on the immune system. *Expert Rev. Clin. Pharmacol*. **2011**. 4(2) 275–289.

10. Ilvesaro, J.M., *et al*. Toll-like receptor 9 mediates CpG oligonucleotide-induced cellular invasion. *Mol Cancer Res.* **2008**, 6, 1534–1543.
11. Ferentz, A., Keating, T., Verdine, G., Synthesis and characterization of disulfide cross-linked oligonucleotides. *J. Am. Chem. Soc.* **1993**, 115, 9006-9014

General Conclusion

In Chapter 1, I have shown that ODNs containing ^{CNV}K are quickly and selectively photocrosslinked to ORNs having mutated K-ras sequences by a few seconds of photoirradiation and that the selectivity can be enhanced by adopting the mutated pyrimidine base as the photocrosslinking site of ^{CNV}K. RT-PCR experiments revealed that the ODN having ^{CNV}K clearly photocrosslinks to its target mRNA in a sequence selective manner and then the function of mRNA as the substrate of reverse transcriptase is clearly regulated with only 1 s photoirradiation. In addition, the translation activity of target mRNA is clearly inhibited by photoirradiation, suggesting that ODNs having ^{CNV}K have the potential to be effective photodynamic antisense drugs that act at desired locations around the body with a few seconds of photoirradiation.

In Chapter 2, I have demonstrated that ^{cnv}K-ASs that targets GFP mRNA disrupts GFP in transfected cells with 10 seconds of UV irradiation. qRT-PCR experiments revealed that the ^{cnv}K-ASs clearly photocrosslinks to its target mRNA in a sequence selective manner. Further, in spite of difference of Tm value and difference of target site, all active ^{cnv}K-ASs caused inhibition of reverse transcription by 10 s UV irradiation. Furthermore, ^{cnv}K-AS (a-2) clearly caused inhibition of reverse transcription by 10 s UV irradiation timing dependent. In addition, the translation of target GFP mRNA is inhibited by 10 s UV irradiation. ^{cnv}K-AS have the potential to be applications to spatiotemporal photoregulation of gene expression or effective photodynamic antisense drugs that act at desired locations around the body with a few seconds of 10 s UV irradiation.

In Chapter 3, I have synthesized disulfide crosslinking tethered CpG oligonucleotide (S-S CpG) as radiation-trigger immune activator. The S-S CpG had an alkyl chain and two CpG DNA units were connected by an X-ray-sensitive disulfide bond. X-irradiation of Raw cells, to which S-S CpG were administered, resulted in an induced Ifnb mRNA expression because of the reductively-cleaved CpG immune activation. Thus, S-S CpG are promising as radiation-trigger immune activator that are applicable to drug.

Finally, during this thesis, I demonstrated the regulation of gene expression and immune activation by stimuli responsive artificial oligonucleotides. The stimuli responsive artificial oligonucleotides would not simply be due to low side effects of a drug but also useful in biotechnology, molecular biology and other applications. In future, the stimuli responsive artificial oligonucleotides will contribute to the progress of cancer therapy and biological researches.

Achievements

Publications

1. Atsuo Shigeno, Takashi Sakamoto, Yoshinaga Yoshimura and Kenzo Fujimoto, "Quick Regulation of mRNA Functions by a Few Seconds of Photoirradiation" *Organic & Biomolecular Chemistry*. **2012**, 10(38), 7820-7825. DOI: 10.1039/C2OB25883H

2. Takashi Sakamoto, Atsuo Shigeno, Yuichi Ohtaki and Kenzo Fujimoto, "Photo-regulation of Endogenous Gene Expression in Living Cells by Using of Ultrafast Photo-cross-linking Oligonucleotides." (in preparation)

3. Atsuo Shigeno, Takeshi Kameyama, Akinori Takaoka and Kenzo Fujimoto, "Synthesis of Disulfide Crosslinking Tethered CpG Oligonucleotide Toward for Immune Activation by Radiation" (in preparation)

Presentaions

International Conferences

1. Atsuo Shigeno, Yuichi Ohtaki, Takashi Sakamoto, Kenzo Fujimoto, "Development of cyanovinylcarbazole mediated photocrosslinking reaction toward for regulation of RNA functions in cell." 2013 CRS Annual meeting, July, **2013**

2. Atsuo Shigeno, Takashi Sakamoto, Kenzo Fujimoto, "Regulation of gene expression by photocrosslinking antisense oligonucleotide containing of carbazole derivative" 243rd ACS National Meeting, March, **2012**

3. Kenzo Fujimoto, Kaoru Hiratsuka, Atsuo Shigeno, "Photochemical site specific DNA and RNA transition" Tetrahedron Symposium 2011, June, **2011**

4. Atsuo Shigeno, Takashi Sakamoto, Yoshinaga Yoshimura and Kenzo Fujimoto, “Gene regulation of point mutated K-ras using photo-reactiveoligonucleotide containing cyanovinylcarbazole” pacifichem 2010, December, **2010**

5. Atsuo Shigeno, Takashi Sakamoto, Yoshinaga Yoshimura and Kenzo Fujimoto, “Photoreactive Oligonucleotide Containing Cyanovinylcarbazole For the Regulation of Point Mutated K-ras Gene Expression” 37th International Symposium on Nucleic Acid Chemistry (ISNAC2010), June, **2010**

National Conferences

1. ○滋野敦夫・坂本隆・藤本健造 “光架橋反応による遺伝子発現制御法の開発” 平成 25 年度日本化学会北陸地区講演会と研究発表会, 2013 年 11 月

2. ○滋野敦夫・坂本隆・藤本健造 “カルバゾール誘導体を含む光応答性アンチセンス核酸による内在性遺伝子発現制御”日本化学会第 93 春季年会, 2013 年 3 月

3. ○滋野敦夫・坂本隆・藤本健造“ビニルカルバゾール含有光応答性人工核酸を用いた光化学的遺伝子発現制御”アンチセンス•遺伝子•デリバリーシンポジウム 2012, 2012 年 9 月

4. ○滋野敦夫・坂本隆・藤本健造“カルバゾール誘導体を含む光架橋性アンチセンス核酸による遺伝子発現制御” 第 34 回分子生物学会年会,2 012 年 12 月

5. ○滋野敦夫・坂本隆・藤本健造 “光架橋反応による遺伝子発現制御法の開発” 平成 23 年度日本化学会北陸地区講演会と研究発表会, 2011 年 11 月

6. ○滋野敦夫・坂本隆・藤本健造 “シアノビニルカルバゾール修飾アンチセンス核酸による遺伝子発現制御法の開発” 第 5 回バイオ関連化学シンポ

ジウム,2011 年 9 月

7. ○滋野敦夫・坂本隆・藤本健造 “シアノビニルカルバゾール修飾アンチセンス核酸による遺伝子発現制御法の開発” 日本ケミカルバイオロジー学会年会, 2011 年 5 月

8. ○滋野敦夫・坂本隆・吉村嘉永・藤本健造 “シアノビニルカルバゾールを含む光応答性アンチセンス核酸による遺伝子発現制御法の開発” 日本化学会第 91 春季年会, 2011 年 3 月

9. ○滋野敦夫・坂本隆・藤本健造 “シアノビニルカルバゾール誘導体を含む光架橋性アンチセンス核酸による遺伝子発現制御” 第 4 回バイオ関連化学シンポジウム, 2010 年 9 月

10. ○滋野敦夫・坂本隆・吉村嘉永・藤本健造 “カルバゾール修飾アンチセンスオリゴヌクレオチドによる光遺伝子発現制御” 日本化学会第 90 春季年会, 2010 年 3 月

Acknowledgement

Acknowledgement

This study was carried out at the School of Materials Science, Japan Advanced Institute of Science and Technology (JAIST) under the supervision of Prof. Kenzo Fujimoto since 2010. The author expresses sincere thanks for his kind, proper and long-standing guidance, and encouragement throughout the present study.

The author would like to be gratitude to Assist. Prof. Takashi Sakamoto (JAIST), for his useful advice.

The author thanks Prof. Akinori Takaoka (Hokkaido univesity) for advice on the innate immune system and support to use equipment . The author is grateful to Dr. Takeshi Kameyama for kind guidance.

Thanks are due to the all the lab members Fujimoto Laboratory and Takaoka Laboratory for their kind help to my work.

Finally, The author wishes to express sincere thanks to my parents, Mr. Masaru Shigeno and Mrs. Youko Shigeno and my family for their encouragement.